View metadata, citation and similar papers at core.ac.uk

brought to you by CORE

provided by Loughborough University Institutional Repository

Department of Physics

Loughborough University

# Out of equilibrium many-body quantum systems with respect to adiabatic quantum computing through the lens of the Pechukas-Yukawa framework.

by

Mumnuna Aziz Qureshi

A Doctoral Thesis

Submitted in partial fulfilment of the requirements for the award of

Doctor of Philosophy at Loughborough University

© Mumnuna Qureshi 2018

# Abstract

We investigate the theoretical description of adiabatic quantum computing (AQC) algorithms using the evolution of the Hamiltonian eigenvalues in the framework of the Pechukas-Yukawa formalism, exactly mapping the eigenvalues to the dynamics of a fictitious one-dimensional classical gas with cubic repulsion. We exploit the properties of the Pechukas-Yukawa model to describe the behaviour of quantum algorithms used in AQC.

Specifically, we derive the non-equilibrium nonstationary statistical mechanics of the Pechukas-Yukawa gas based on the Bogoliubov-Born-Green-Kirkwood-Yvon (BBGKY) chain of equations with the goal of increasing the efficiency of direct numerical simulation. We extended our research to consider the impacts of level crossings and avoided crossings to evaluate the compatibility of the Pechukas-Yukawa formalism and the Landau-Zener description of these occurrences. This is valuable to the investigation of decoherence in a quantum system and carries scope for research on the description of state dynamics through the energy level dynamics.

We relate the evolution of a quantum state of a system under external perturbation to that of its energy levels. Using this relationship, we produced a cumulant expansion with improved efficiency compared to traditional methods of approximate quantum state evolution description. It is especially significant for the investigation of decoherence in an evolving quantum system.

# Acknowledgements

My sincerest gratitude to my supervisors Drs Alexandre Zagoskin and Joseph Betouras, for your support and guidance throughout both my academic career and personal development. I am grateful for the opportunities afforded to me, the honest advice you have given me and your encouragement to follow my ambitions. To my collaborators, Drs Peter Mason and Wassilij Kopylov, I am grateful to the time, your efforts and focus you have spent working with me.

I would like to express my gratitude to my family. I am indebted to my mother and father, you are my inspiration. I appreciate you being there for me whenever I needed you. Thank you for all your understanding, patience and support throughout my life. My sister Jun, thank you for helping me in all the ways you have. You have been there for me always, I am grateful to that.

I express my gratitude to Johnny Zhong, thank you for challenging me and for taking a chance with me. I appreciate all your encouragement and support throughout this journey, to Yu Liu, Yujia Liu, Jinrong Bao, Yiru Ye, Johnathon Cox, you have been a pleasure to research alongside, thank you for the advice and friendship you offered to me.

I would like to express my special thanks to my former lecturer, Professor Carla Molteni, you have provided me with advice and guidance throughout my career, I am very grateful to that.

Finally, I express my eternal gratitude to God, for the guidance and strength I was provided to pursue this research as well as throughout my life and all that is to follow.

# Contents

# List of Figures

# List of Acronyms

1. AQC: Adiabatic Quantum Computing
2. APX: Approximable
3. BBGKY: Bogoliubov-Born-Green-Kirkwood-Yvon
4. BCH: Baker-Campbell-Hausdorff
5. BPP: Bounded-Error Probabilistic Polynomial Time
6. BQP: Bounded-Error Quantum Polynomial Time
7. FPTAS: Fully Polynomial Time Approximation Scheme
8. MA: Merlin-Arthur
9. NP: Nondeterministic Polynomial Time
10. NPC: Nondeterministic Polynomial Time Complete
11. NPO: Nondeterministic Polynomial Time Optimisation
12. NPO APX: Nondeterministic Polynomial Time Optimisation Approximable
13. P: Polynomial Time
14. PBS: Peano-Baker Series
15. PTAS: Polynomial Time Approximation Scheme
16. QCMA: Quantum Classical Merlin-Arthur
17. QMA: Quantum Merlin-Arthur
18. QMAC: Quantum Merlin-Arthur Complete
19. QPT: Quantum Phase Transitions
20. R.E.: Relative Error
21. SDE: Stochastic Differential Equation
22. TDPT: Time Dependent Perturbation Theory
23. TFIH: Transverse Field Ising Hamiltonian

# Chapter 1

# Introduction

The impacts of quantum computing would be far reaching and monumental in modern society with benefits from simulating chemical reactions which contribute to the developments of new drugs, to boosts in machine learning, assisting self driving cars in assessing situations better more efficiently, for improved safety.

Announcements by D-Wave Systems Inc, of the production of working adiabatic quantum computers have led to the ongoing research in the complexity theory it involves. Standard approaches to the success of quantum computing have focused on the quantum gate model. It has been conjectured to achieve a quantum speedup in computation with a tradeoff between time and the probability of the final states [1, 2, 3, 4]. The gate model operates on qubits that encode a solution in an entangled superposition of eigenstates. Experimental achievements in this area include the control and entanglement of approximately 10 qubits to develop a universal computer using the quantum gate model. However, recent experiments have shown that there are cases where classical computers work just as effectively as quantum computers, though for incompressible data, there is no competition that quantum computers have the advantage, still they prove vulnerable to decoherence [1, 2, 3, 4] - the loss of information due to the interactions of the system with the environment.

An alternative more promising approach is adiabatic quantum computing (AQC) [1]. This is more robust against decoherence. The AQC model encodes the solution dictated by the adiabatic theorem, in an easily achievable groundstate of the initial Hamiltonian, $H_I$, evolving the system under an adiabatic parameter such that the system maps the solution to the groundstate in $H_F$. This corresponds to an optimal solution of a given optimisation problem based on quantum annealing algorithms, reducing the vulnerability of the system dephasing [1]. Using the AQC model, D-Wave jointly sponsored by NASA and Google announced the achievement of working quantum chips with 128 and 512 qubits, which is feasible because of the intrinsic features of adiabatic processes rendering the model more

robust against decoherence.

The standard approach to quantum computing uses a heuristic search algorithm, described by quantum annealing. This relies on random walks parameterised Markov chains to solve combinatorial optimisation problems. This gives the prospect of tackling NP-hard problems. The algorithms restrict the final Hamiltonian $H_f$, such that the entire computation need not be confined to the ground state. These algorithms are realised in both classical and AQC computational models, providing a bridge between the two.

For the theoretically ideal AQC, an adiabatically closed system without interference from the environment, the algorithm is probabilistic. The adiabatic theorem is used to bound the tradeoff between computation time and the probability of ending in the groundstate [1]. For a physical quantum platform, based on the superposition of states, the system will inevitably be open such that it is impossible to perfectly isolate the system from the environment, hence noise must be accounted for [5]. In determining the probability of ending in the groundstate, one takes a heuristic search approach. In contrast, the classical platform does not support quantum features of superposition and entanglement, the algorithm is not probabilistic yet much slower by comparison [1].

In development of insights on the measure of quantumness in the AQC model, the Pechukas-Yukawa model has been used to map quantum algorithms to classical models [3]. This allows for classical properties to apply to the highly entangled quantum nature of the system. From this property, we constructed the BBGKY chain of kinetic equations of motion concerning the level dynamics. Sets of approximate kinetic equations for a generalised distribution function of the dynamical variables are obtained by breaking this chain at a particular point. These equations could be factorised, where we found that corrections to the factorized approximation of the distribution function scale as $1/N$, where $N$ is the number of the Pechukas gas particles corresponding to the number of eigenvalues. This is promising in particular for large systems which could reach an efficiency that greatly reduces the speed of numerical simulation.

Under this formalism, decoherences have been modelled such that one could explore their influences. One source of decoherence we considered had been on account of state transitions occuring in the event of level crossings and avoided crossings. We investigated these impacts on an evolving quantum system using the traditional Landau-Zener model. We determined the conditions required for the applicability of the Landau-Zener mode in the Pechukas-Yukawa setting. In extension to this investigation, we determine the influences of noise on the description of avoided crossings. We considered a single source of composite longitudinal Brownian noise. This carries the potential to cause decoherence in a quantum algorithm.

Furthermore, we derived a relationship between the level dynamics and the evolution

of quantum states, allowing for a description of occupation dynamics and the evolution of coherences beyond the Landau-Zener model. Using the relationship between the quantum states and level dynamics, we produced a cumulant expansion with improved efficiency compared to traditional methods to approximate quantum state evolution. Our expansion requires only the initial conditions and the evolution of the perturbation parameter, $\lambda$ to determine its convergence to provide highly accurate approximations. This further enabled us to describe the density matrix, requiring far less information than current approaches. Allowing for investigation of the density matrix dynamics with fewer imposed conditions, one obtains analytical insights on the evolution of quantum states and their populations which can describe better a large quantum coherent system than the currently used approaches which is especially fruitful in the research of sources of decoherence in quantum systems. This expansion carries the potential to investigate adiabatic invariances in a system which could allow for determining the different complexity classes a family of Hamiltonians may fall under. When the distributions for the level dynamics are complemented by the equations for the level occupation numbers and inter-level transition amplitudes, they allow to describe the non-equilibrium evolution of the quantum state of the system. These have potential to improve the designs of quantum algorithms in the development of AQC.

## 1.1 Thesis Overview

The following chapter provides a brief introduction to quantum computing and in particular, the theory of AQC and AQC algorithms. We follow with a background of optimisation problems which is essentially the backbone of quantum computing. In Chapter 3 we detail the Pechukas-Yukawa model, providing a derivation of its mapping of eigenvalue dynamics to a set of coupled ordinary differential equations and its stochastic extension, the stochastic Pechukas-Yukawa model. In Chapter 4 we also offer a brief introduction of the BBGKY hierarchy of kinetic equations of motion. Our work on the statistical treatment of the level dynamics is detailed here, with the derivation for the generalised BBGKY hierarchy in the Pechukas-Yukawa framework, extending the dynamics to account for parametrically evolving quantum systems. We also describe our effecive mean-field approximation. Having determined its accuracy theoretically, we tested numerically our theory using the 2-Qubit Ising model in illustration of the factorisation approximation. In Chapter 5, we establish a connection between the level dynamics and the evolution of the eigenstate expansion coefficients, which allows for characterising the entire system via the level dynamics. We then approximated the evolution of the eigenstate coefficients, exploring different approximations and comparing them numerically. This was extended to describe the evolution of the density ma-

trix such that the entire quantum system could be characterised from eigenvalue dynamics. We identified the strengths and weaknesses of the approximations, identifying the most appropriate description of the occupation dynamics of the exact cover 3-satisfiability problem as a specific example. In Chapter 6, we consider the compatibility of Landau-Zener model in the Pechukas-Yukawa formalism and the conditions governing this marriage. We obtain a description of level crossings, avoided crossings and stochastic avoided crossings satisfied in this setting. Finally, we provide a summary of our works in the conclusions with a brief study of the scope of our work carries for further investigations.

# Chapter 2

# Introduction to Quantum Computing

Manin and Feynman introduced the concept of a quantum computer in 1980 [6] and 1982 [7] respectively. This attracted enormous interest under the promise of a quantum speed-up through exploiting quantum properties such that quantum computations are carried out in asymptotically fewer basic operations than classical computations. However, this leads to a tradeoff in probability of realisation in the final states. The standard approach to quantum computing uses a heuristic search algorithm, yet still due to its susceptibility to decoherence, achieving a practical quantum computer remains a challenging feat.

In this chapter, the properties of a quantum computer are presented, followed by an introduction to adiabatic quantum computing (AQC), one approach to quantum computing, outlining the assumptions required, extending to its applications and vulnerabilities. For details on basic notation on quantum information, refer to Appendix A.

## 2.1 Quantum Computing

Quantum computations operate on qubits which exhibit the quantum properties, superposition and entanglement. Superposition enables storing all $2^n$ states simultaneously. For a single qubit given by $|\phi\rangle = \alpha|0\rangle + \beta|1\rangle$, superposition allows qubits to store information simultaneously in states $|0\rangle$ and $|1\rangle$. Once a qubit is measured, there is probabilistic collapse of $|\phi\rangle$ to one of these states, which can be read off to decode the information it stores. This reasoning can be extended to $n$-qubit systems. Entanglement occurs when qubits interact and are subsequently removed from each other. Despite being physically separated they are no longer independent. For multi-qubit states, after entanglement states cannot be decomposed into products of individual probabilities. The probability of being observed in any given state is correlated, allowing for acting on all $2^n$ states simultaneously. A demonstration of this property is given by the Bell state[8].

In this representation, one can construct quantum logic gates in order to transform qubits by acting on them with a combination of Pauli matrices and the identity matrix. These are used to create all classical logic gates with the crucial difference that quantum gates are reversible; given the output, it is possible to determine the input. From these, quantum circuits can be constructed, capable of computing any classical function $f$ defined on $n$ bits. The general statement here is that for a circuit $C_f$ applied to a register $Q$, the result is a new superposition state $C_f|\phi\rangle = |\phi'\rangle$ where $|\phi'\rangle$ denotes a new superposition. This representation forms the basis of the quantum gate model.

The quantum gate model concerns $n$ qubits in a register $Q$, operated on by quantum circuits $C_i$, where $i \in N$. The circuits operate on $Q$ in parallel and in series such that a computation initialises $Q$ in some known state and after the circuits induce state transformations on $Q$, it is measured resulting in a probabilistic collapse of $Q$ to a classical state, providing the answer which is then returned by the computation. Utilising the quantum properties of superposition and entanglement respectively, $Q$ holds all $2^n$ states simultaneously and the quantum circuits are able to act on all $n$ bits simultaneously in constant time. This quantum parallelism carries the potential to provide significant speedups in computation time compared with classical computers.

Assuming the universal applicability of quantum mechanics, the practical realization of a universal quantum computer remains a rather distant possibility due to the large number of physical qubits necessary for its operation and the extreme fragility of its quantum states with respect to external and internal sources of decoherence [1, 2, 3, 4, 5]. Moreover, as was shown by Feynman, simulation of a large enough quantum coherent system by classical means is impossible due to the dimensionality of the corresponding Hilbert space growing exponentially with the size of the system (e.g. number of qubits) [7, 9]. Unfortunately, the size of a practically useful universal quantum computer greatly exceeds the limits of what is tractable by classical means. This makes the task of determining the degree of quantumness of such a device, its design and optimization exceedingly difficult [1, 2, 3, 4, 10, 11, 12].

An alternative approach to quantum computing is through quantum dynamical systems where the $n$ qubits in a register $Q$ are regarded as dynamical particles evolving over time according to the forces acting on it, characterised by an $N \times N$ time-dependent Hermitian Hamiltonian, where Hermiticity imposes $N$ real eigenvalues, which make up the energy spectrum of the system. When multiple states take the same eigenvalue, they are said to be degenerate states. The groundstate corresponds to the state with the lowest eigenvalue, all other states are then excited states. The Hamiltonian operator changes the state of the system by acting on states just as quantum circuits result in transformations on qubit states, however the Hamiltonian acts continuously on a state in contrast to discrete transformations.

This approach to quantum computers leads on to the foundations of adiabatic quantum computing.

## 2.2 Adiabatic Quantum Computing

Adiabatic Quantum Computing (AQC) offers an alternative approach to the universal quantum gate model [1, 3, 4, 5, 9, 13], based on the continuous adiabatic time evolution of a Hamiltonian, modelling the quantum algorithm. Under this framework, qubits are evolved in accordance with the adiabatic theorem, from an easily achievable groundstate of some initial Hamiltonian such that after time evolution the groundstate is an eigenstate of the final Hamiltonian. This corresponds to an optimal solution. It was shown [1], that the two models are polynomially equivalent.

### 2.2.1 Adiabatic Theorem

The adiabatic theorem, accredited to Born and Fock, states that the instantaneous rate of change of the process is proportional to the energy of the process. For a time-dependent Hamiltonian $H(t)$ system, with wavefunction $|\psi(t)\rangle$ satisfying the Schrodinger equation:

$$i|\dot{\psi}(t)\rangle = H(t)|\psi(t)\rangle, \tag{2.1}$$

where $|E_n(t)\rangle$ denotes the instantaneous eigenstates of $H(t)$ with instantaneous eigenvalues $E_n(t)$. The adiabatic theorem states that, if the system is initialised at $t = 0$, in an eigenstate $|E_n(0)\rangle$ of the Hamiltonian $H(0)$, it will remain in the same instantaneous eigenstate, $|E_n(t)\rangle$, at final time $t = T$ , as long as the evolution of the $H(t)$ is slow enough to satisfy:

$$max_{t\in[0,T]} \left| \frac{\langle E_m(t)|\dot{E}_n(t)\rangle}{E_n(t) - E_m(t)} \right| \ll 1, \tag{2.2}$$

where $m \neq n$ and $\langle E_m(t)|\dot{E}_n(t)\rangle = \langle E_m(t)|\dot{H}(t)|E_n(t)\rangle$. The adiabatic theorem has recently gained renewed attention as the basis of AQC.

However, the adiabatic theorem was subjected to controversy due to the result that if a Hamiltonian, $H(t)$ follows an adiabatic evolution, a related Hamiltonian:

$$\tilde{H}(t) = -U^{\dagger}(t)H(t)U(t), \\ U(t) = Te^{-i\int_0^t H(t)dt}, \tag{2.3}$$

where $T$ represents the time-ordering operator. Then $\tilde{H}(t)$ cannot have an adiabatic evolution even if satisfying Eq. (2.2). It was proven by Amin [14], that there is consistency in the adiabatic theorem, we follow this argument here for a general system with resonant oscillations. Re-writing the wavefunction expanded under the instantaneous eigenstates:

$$|\psi(t)\rangle = \sum_n a_n(t)e^{-i\int_0^t E_n(t')dt'}|E_n(t)\rangle, \tag{2.4}$$

where $a_n(t)$ denotes the instantaneous eigenstate coefficients. For a time-independent Hamiltonian, $a_n(t)$ is a constant whereas for a slowly varying Hamiltonian it is a slow function of time. Substituting Eq. (2.4) and integrating over time, one obtains:

$$a_m(T) - a_m(0) = -\sum_{n\neq m}\int_0^T dt a_n(t)\langle E_m(t)|\dot{E}_n(t)\rangle e^{-i\int_0^t [E_n(t')-E_m(t')]dt'}. \tag{2.5}$$

To assure adiabaticity, the right hand side of this equation should be small. With the initial condition $a_m(0) = \delta_{mn}$. Since the exponential term in the integrand of Eq. (2.5) is a rapidly oscillating function, if the rest of the terms vary very slowly, the integral will be small[14]. Refer to [14] for the more general proof when the system is absent of resonant oscillations, demonstrating the applicability of the adiabatic theorem to construct an AQC.

For a quantum dynamical system modelling an AQC algorithm acting on Q, evolving under $t$ then $\tau(s)$ gives the rate of change of $H(s)$. This gives the equivalent Hamiltonian in timescale $s$ with nondegenerate groundstate. If $\delta_s$ denotes the spectral gap, then $\delta_m = min_s\delta_s$ the minimum spectral gap through $s$.

The adiabatic theorem states: 1) Q is in the groundstate at $s = 0$. 2) $\delta_m > 0$ throughout evolution in $s$. 3) the process is slow enough such that $\tau(s)$ is bounded by the following:

$$\tau(s) \gg \frac{||\frac{d}{ds}H(s)||}{\delta_m^2}. \tag{2.6}$$

The bound on $\tau(s)$ can be bounded from above by a low-degree polynomial in $n$. Given these 3 conditions are satisfied, the process will end in the groundstate of the final Hamilto-

nian with high probability, optimising the problem. A general Hamiltonian can reveal well defined gaps between the eigenvalues in the Hamiltonian spectrum, giving $\delta_m$. The adiabatic theorem does not hold in instances of level crossings given by $\delta_m = 0$ [13]. This is used to govern adiabatic quantum algorithms.

### 2.2.2 Adiabatic Quantum Algorithms

AQC algorithms are designed to minimise an objective function $f$ acting on the register of qubits $Q$, under some constraints. The algorithm is governed by a time-dependent Hamiltonian which can be broken up into three key features: 1) The initial Hamiltonian $H_0$ with an easily achievable ground state. 2) The final Hamiltonian $H_f$, encoding the objective function such that the solution is mapped to the ground state of $H_f$. This yields an optimal solution. 3) An adiabatic evolution path $s(t)$ such that $s : 1 \to 0$ as $t : 0 \to t_f$ for some final time $t_f$, this defines the run-time of the algorithm.

The AQC algorithm describing an adiabatic transition from $H_0$ to $H_f$ can be described by an adiabatic Hamiltonian, a system that remains in its instantaneous eigenstates to optimise the problem, given a perturbation acts slow enough in accordance with the adiabatic theorem.

The adiabatic Hamiltonian for the AQC algorithm is given by the following:

$$H(s(t)) = s(t)H_0 + (1 - s(t))H_f, \tag{2.7}$$

where the solution encoded in the ground state of $H_0$ is mapped to the ground state of $H_f$ given the adiabatic path $\lambda(t)$ is sufficiently slow. Then, if there is a nonzero gap between the ground state and the first excited state of $H(s(t))$ for all $s \in [0, 1]$, the success probability of the algorithm tends to 1 in the infinite run-time limit. This compares with a general Hamiltonian for $\lambda(t)$ taken to be an adiabatic path in the following equation:

$$H(\lambda(t)) = H_0 + \lambda(t)ZH_b, \tag{2.8}$$

where $H_0$ is the unperturbed Hamiltonian, $ZH_b$ is the perturbation in the Hamiltonian and $\lambda$ is a time evolving parameter, especially suited to adiabatic systems. $H_0$ encodes the groundstate solution and $ZH_b$ is a large bias term with $Z \gg 1$. This is especially suited, though not restricted to the description of a large adiabatic Hamiltonian [3, 9]. This formalism is consistent with the notation used in our research groups previous works [3, 4, 5] in this area. It is a reformulation of Eq. (2.7), forming a more natural description of qubits

and the external field. This allows a direct mapping between quantum algorithms and the Pechukas-Yukawa model, describing the evolution of a system via the level dyanmics. This is described in further detail in Sec. III.

To demonstrate this mapping of quantum algorithms, consider the exact cover three-satisfiablity problem. Given a Boolean expression defined on $n$ binary variables $x_1, \dots x_n$. The expression contains $m$ clauses $C_c$ each containing 3 variables $(x_{c1}, x_{c2}, x_{c3})$. Each of these variables are either equal to $x_i$ or $(1 - x_i)$. A clause is satisfied if exactly one of the variables takes the value 1 such that the clause function $f_c(x)$ follows:

$$f_c(x) = (1 - x_{c1} - x_{c2} - x_{c3})^2, \tag{2.9}$$

The objective function $f_{ec}(x)$ is defined as the sum of all the individual clause functions where $f_{ec} \geq 0$, taking the value 0 when all clauses are satisfied. It is defined by the following:

$$f_{ec}(x) = -2m + \sum_{i<j} C_{ij} x_i x_j, \tag{2.10}$$

where $C_{ij}$ counts the number of times $x_i$ and $x_j$ appear together in a clause. To define the final Hamiltonian for this algorithm, $x_i = \frac{1-s_i}{2}$ replacing the binary variables $x_i$, where $s_i$ denote spin variables taking values of $-1$ or 1. The objective function then represents the energy function corresponding to the eigenvalues of a final Hamiltonian, minimised by $H_{ec}$. Under the adiabatic evolution path $s(t) = 1 - \frac{t}{t_f}$, the AQC alorithm for exact cover is given by:

$$\begin{aligned} H(t) &= s(t)H_i + (1 - s(t))Hf \\ &= s(t) \sum_{i=1}^{m} \frac{1 - \sigma_i^x}{2} + (1 - s(t)) \sum_{i<j} C_{ij}(1 - \sigma_i^z)(1 - \sigma_j^z), \end{aligned} \tag{2.11}$$

where $\sigma^z$ is defined by the Pauli matrix as in Appendix A, $H_i = \sum_{i=1}^{m} \frac{1-\sigma_i^x}{2}$ and $H_f = \sum_{i<j} C_{ij}(1 - \sigma_i^z)(1 - \sigma_j^z)$.

## 2.3 Quantum Annealing

A subset of AQC is quantum annealing (QA), describing a heuristic search which minimises a problem defined on $n$ binary variables $x_1 \dots x_n \in [0, 1]^n$, where the objective function $f(x)$

assigns a cost to the solution. The search is applied to combinatorial optimisation problems, restricted on a final Hamiltonian $H_f$, representing a classical objective function.

Initialised in some state $x$, with cost $c$, the system is iterated according to a random walk described by a parameterised Markov chain where each iteration of QA depends on some tunnelling coefficient $\Gamma$ to control the traversibility of the solution landscape. If a search starts at some initial state and moves towards a low-cost state where the algorithm terminates according to some stopping rule. If the landscape moves towards an optimal solution, it takes a greedy-descent approach. However, this encounters problems in the case when there are many local minima, resulting in the greedy-descent approach becoming stuck or moving in circles, never reaching the optimal solution.

$\Gamma$ starts at some high value and is gradually decreased with each iteration against time. When $\Gamma$ decreases slow enough such that $\Gamma(t) \geq \frac{kn}{log(t)}$, where $k$ is a constant, the QA algorithm is guaranteed to provide an optimal solution in the long-time limit. This compares with the adiabatic path $s(t)$. This approach introduces a disordering Hamiltonian, $H_D$ which adds the kinetic energy to the annealing process in the form of quantum fluctuations. $H_D$ does not commute with $H_f$. Then the Hamiltonian is transformed to a new time-dependent Hamiltonian:

$$H(\Gamma(t)) = H_f + \Gamma(t)H_D. \tag{2.12}$$

This is analogous to Eq. (2.8) for an AQC. AQC algorithms determine a bound on the probability to end in the ground state given the problem was encoded in the ground state of some initial Hamiltonian, whereas QA allows the problem being initialised in an arbitrary state and analyses the probability to converge to a solution within a small neighbourhood of the optimal solution.

Analysis of QA depends on the platform it runs on. There are three types of platforms QA algorithms can run from. 1) A theoretically ideal AQC platform: an adiabatically closed system with no interference from the environment. In this case, the algorithm is probabilistic and the adiabatic theorem bounds the tradeoff between the computation time and the probability to end in the ground state. 2) A physical quantum platform: the system will inevitably be open such that it is impossible to perfectly isolate the system from the environment. This results in noise, due to random fluctuations in the environment, reducing the probability of ending in the ground state. 3) A classical platform: a classical computer does not adhere to decoherence due to interactions with the environment, however it does not offer the quantum properties, superposition and entanglement between states that are

available in using a quantum computer.

On a quantum computing platform, quantum properties are utilised such that calculations can occur with increased speeds compared to classical computers. Moreover, quantum computers offer the capability of solving problems that are not tractable on classical computers; the run time for a classical computer algorithm grows polynomially as a function of the input data. In the following section a brief description of the different complexity classes are provided.

## 2.4 Optimisation Problems

Optimisation problems searches for a feasible solution that either maximises or minimises an objective function. It is the crux to AQC, that appears to out-perform the gate model, making it an attractive area of research. These are considered in terms of their approximation complexity; given an instance $I$ in a minimisation problem $P$, with optimal solution $s^*$, to determine the feasibility in returning a solution $s$ with some difference $|f(s)-f(s^*)|$or bound from above $\frac{f(s)}{f(s^*)}$. If an algorithm returns a feasible solution, then the distance is 0 making it an exact algorithm. If it returns a non-trivial bound on the distance or the ratio, it is an approximation algorithm. An **NPO** denotes a class of optimisation problems with a decision counterpart in **NP**, refer to Appendix B for an introduction to the various complexity classes.

All decision problems in **NP** can be solved by an exact algorithm for the analogous problem in **NPO APX** denote the set of problems that can be approximated within the upper bound of the problem in polynomial time. **PTAS** describes a set of problems with a polynomial time approximation scheme. A parameterised algorithm $A_q$ for any $q \in Q$ where $q > 1$, the solution cost is within the upper bound of the problem, returned in polynomial time with respect to the problem size and inversely exponential in $q$. Similarly, **FPTAS** describes a fully-polynomial time approximation scheme. It is a parameterised approximation scheme that returns a solution within the upper bound of the problem, returned in polynomial time in both the size of the problem and $\frac{1}{(1-q)}$.

In the context of AQC, we aim to optimise the solution of a quantum algorithm to speed up calculations beyond that which is achievable in traditional computations.

## 2.5 Summary

In this chapter, we introduced the basic concepts behind a quantum computer, superposition and entanglement. As a result, information can be both stored in $2^N$ simultaneously where $N$ denotes the number of bits, states as well as acted on all states together.

Furthermore, a discussion of the different approaches to quantum computing via the quantum gate model, quantum dynamical systems and AQC, the primary motivation behind our research, developing alternative approaches to investigate nonequilibrium quantum systems. This relies on the adiabatic theorem, where the evolution of the system is sufficiently slow that state transitions do not occur. Formulation of this theorem is given and extended to its applications in the context of AQC algorithms. Following this, quantum annealing is discussed providing the key elements behind initialising and evolving an AQC system.

Finally, a brief discussion of optimisation problems was given. This leads into our work using the Pechukas-Yukawa model as described in the following chapter, carrying the potential to characterise different complexity classes which could prove valuable in designing AQC algorithms.

# Chapter 3

# Pechukas-Yukawa Formalism

The Pechukas-Yukawa model describes a fictitious one-dimensional classical gas with parametric evolution in time[15, 16, 17, 18]. This model provides a homeomorphism between a perturbed quantum system of general Hamiltonian given by $H(\lambda(t)) = H_0 + \lambda(t)ZH_b$, where $H_0$ denotes the free Hamiltonian, $H_b$ a perturbation, $Z$ is some factor and $\lambda(t)$ evolves parametrically in time, to a one-dimensional classical gas, where the level dynamics are described by a set of coupled ordinary differential equations[15, 19], governed by the initial conditions. These equations correspond to the Hamilton's equations for the fictitious classical particles evolving in time. Under this mapping the number of fictitious particles $N$, corresponds to number of eigenvalues. However, in phase space the dimension for the system grows beyond $2N$ in this formalism, as a consequence of particle-particle interactions becoming dynamic variables. This formalism is well suited to highly entangled many level quantum systems with connections to quantum chaos. In [20], it was shown that the system admits a Lax formalism and is completely integrable[20, 21] which has been invaluable in the study of quantum chaos, see Appendix F for details on Lax representation.

This chapter presents a derivation of the Pechukas-Yukawa model, mapping from a general perturbed quantum Hamiltonian to a set of coupled ordinary differential equations of a classical 1D gas. A brief summary of the Pechukas-Yukawa model is provided with an overview of its applications to adiabatically evolving quantum Hamiltonian systems. This is extended to the stochastic Pechukas-Yukawa model, where it was shown that this formalism accommodates for open quantum systems whilst preserving its structure.

## 3.1 Derivation of the Pechukas-Yukawa Gas Equation

Consider a time-dependent Hamiltonian given by, $H(\lambda t) = H_0 + \lambda V \sum_{n=-\infty}^{\infty} \delta(t-n)$ where $H_0$ denoted the free Hamiltonian, $\lambda$ evolving parametrically in time and $V$ some perturbation.

The associated single-period Floquet operators are given as $F = e^{-i\lambda V}e^{-iH_0}$. Assuming the Hilbert space has finite dimension $N$ and that by varying $\lambda$, the eigenvalues and eigenvectors change, then the Floquet operator acting on an eigenstate $|m\rangle$ with $m \in \mathbb{N}$ is governed by,

$$F|m\rangle = e^{-i\phi_m}|m\rangle. \tag{3.1}$$

Taking an approach similar to perturbation theory and expanding Eq. (3.1) in terms of $\lambda$, $F_{mm} = e^{-i\phi_m}$. This can be used to show that $\dot{\phi}_m = V_{mm} + i(\langle \dot{m}|m\rangle + \langle m|\dot{m}\rangle)$. Taking orthonormal eigenstates, $\dot{\phi}_m = V_{mm}$. Then $\dot{V}_{mm} = \sum_n (\langle \dot{m}|n\rangle V_{mm} + V_{mn}\langle n|m\rangle)$.
Differentiating Eq. (3.1) and taking the scalar product with $\langle n|$ where $m \neq n$, we obtain the following:

$$\langle n|\dot{m}\rangle = (\langle \dot{m}|n\rangle)^* = \frac{-iV_{nm}}{1 - e^{-i\phi_{nm}}}, \tag{3.2}$$

the rate of change of $V_{mm}$ is then given as:

$$\dot{V}_{mm} = i\sum_{n\neq m} V_{mn}V_{nm}\left(\frac{1}{1 - e^{-i\phi_{mn}}} - \frac{1}{1 - e^{i\phi_{mn}}}\right), \tag{3.3}$$

where $\phi_{mn} = \phi_m - \phi_n$ describing the difference between 2 quasi-energies. Similarly, the off-diagonal perturbation components (without loss of generality taking gauge factors as zero) are given by:

$$\dot{V}_{mn} = -i\frac{V_{mn}(V_{mm} - V_{nn})}{1 - e^{-i\phi_{mn}}} + i\sum_{k\neq m,n} V_{mk}V_{kn}\left(\frac{1}{1 - e^{-i\phi_{mk}}} - \frac{1}{1 - e^{i\phi_{kn}}}\right). \tag{3.4}$$

The equations for $\dot{\phi}_m, \dot{V}_{mm}$ and $\dot{V}_{mn}$ form a complete set capable of describing the quasi-energies and the perturbation components for any $\lambda$ given the initial conditions are set. Taking a reformulation of these set of equations using the classical Hamiltonian flow, one obtains the following equation:

$$\sum_m \left(\frac{\partial \dot{\phi}_m}{\partial \phi_m} + \frac{\partial \dot{V}_{mm}}{\partial V_{mm}}\right) + \sum_{m\neq n}\frac{\partial \dot{V}_{mn}}{\partial V_{mn}} = -i\sum_{m\neq n}\frac{V_{mm} - V_{nn}}{1 - e^{-i\phi_{mn}}}. \tag{3.5}$$

The flow is non-zero with the only divergence arising from $V_{mn}$, one can replace the off-diagonal terms with $l_{mn} = V_{mn} f_{mn}$, where $f_{mn}$ are factors chosen to cancel the second term in Eq.3.4. This requirement leads to the following:

$$\frac{\dot{f}_{mn}}{f_{mn}} = \frac{i\dot{\phi}_{mn}}{1 - e^{-i\phi_{mn}}} = i\frac{\dot{\phi}_{mn}}{2} + Ln\left(sin\left(\frac{\phi_{mn}}{2}\right)\right). \tag{3.6}$$

This simply integrates to $f_{mn} = Ae^{i\phi_{mn}/2} sin(\phi_{mn}/2)$. Choosing the intgration constant $A$ to be $-2$, $l_{mn} = -2V_{mn}e^{i\phi_{mn}/2} sin(\phi_{mn}/2) = -l^*_{nm}$, where $*$ denotes the complex conjugate. The source free equations can then be written as:

$$\begin{aligned} \dot{\phi}_{mm} &= \rho_m, \\ \dot{\rho}_{mm} &= -\frac{1}{4}\sum_{m\neq n} l_{mn} l_{nm} \frac{cos(\phi_{mn}/2)}{sin^3(\phi_{mn}/2)}, \\ \dot{l}_{mn} &= \frac{1}{4}\sum_{k\neq m,n} l_{mk} l_{kn} \left(\frac{1}{sin^2(\phi_{mk}/2)} - \frac{1}{sin^2(\phi_{kn}/2)}\right), \end{aligned} \tag{3.7}$$

where $\rho_m = V_{mm}$.

The first 2 equations can be interpreted as classical Hamiltonian equations and associated Poisson brackets, $\dot{\phi}_m = \frac{\partial H}{\partial \rho_m} = \{H, \phi_m\}$ and $\dot{\rho}_m = -\frac{\partial H}{\partial \phi_m} = \{H, \rho_m\}$ for an associated Hamiltonian $H = \frac{1}{2}\sum_{m=1}^{N} \rho_m^2 + \sum_{m\neq n} \frac{|l_{mn}|^2}{8sin^2(\phi_{mn}/2)}$. In order to determine the Poisson bracket for $l_{mn}$, we demand its independence of $\phi_m$ and $\rho_m$ such that $\{\rho_m, l_{ij}\} = \{\phi_m, l_{ij}\} = 0$. This follows from the Leibniz product rule and the Jacobi identity. Then, in the unitary class of Floquet operators, $\{l_{mn}, l_{ij}\} = \delta_{in} l_{mj} - \delta_{mj} l_{in}$. One can similarly determine the expressions in the orthogonal and symplectic cases for the Floquet operators. Note that this expression and the Jacobi identity forbids the assumption of identically vanishing diagonal elements $l_{mm}$ but restricts these elements such that $l_{mm} = -l^*_{mm}$ which is unavoidable in the Hamiltonian reformulation. However, one finds that $\{H, l_{mn}\} = 0$ revealing these relative angular momenta terms as constants of motion, then if they vanish at some initial $\lambda$, without loss of generality $l_{mm} = 0$. This leads to the Pechukas-Yukawa gas equations, of the form:

$$\begin{aligned} \dot{x}_m &= \frac{\partial H}{\partial \rho_m}, \\ \dot{\rho}_{mm} &= -\frac{\partial H}{\partial x_m}, \\ \dot{l}_{mn} &= (H, l_{mn}). \end{aligned} \tag{3.8}$$

The following section summarises the model and its applications to AQC systems.

## 3.2 The Pechukas-Yukawa model

The Pechukas-Yukawa model maps from a general Hamiltonin $H(\lambda(t)) = H_0 + \lambda(t)ZH_B$ to a fictitious one-dimensional gas. It is well suited to adiabatic systems with the additional feature that all information of the system is encoded in the initial conditions [15, 16, 17, 18]. The contribution from $H_0$ is fully determined at all times. Information of all initial conditions are obtained through instantaneous matrix elements given by $< m|H_0|n >= E_m(\lambda)\delta_{mn} - \lambda < m|ZH_b|n >$ and $\lambda\,(t)\,Z\mathcal{H}_b$. This relationship maps from a general Hamiltonian to the Pechukas equations [3, 4, 5, 15, 16, 17, 18, 19, 22, 23, 24]. This can be used to model an AQC [3], where the associated Hamiltonian describes the quantum algorithm used to optimise a problem. The Hamiltonian in the Pechukas-Yukawa formalism takes the form:

$$H(\lambda(t)) = \frac{1}{2}\sum_m v_m^2 + \sum_{m\neq n}\frac{|l_{mn}|^2}{(x_m - x_n)^2}, \tag{3.9}$$

where $x_m$ denotes the eigenvalues of the Hamiltonian system, $v_m$ the diagonal entries of the perturbation and $l_{mn}$ the relative angular momenta of the fictitious gas. This governs a complex system that evolves in time parametrically through $\lambda$, described through the instantaneous eigenstates $|m(\lambda)\rangle$ and eigenvalues $E_m(\lambda)$, related by $H(\lambda)|m\rangle = E_m(\lambda)$ where the nature of a system can be determined by its eigenvalues [15, 16, 17, 18]. It has an easily achievable nondegenerate groundstate with the solution found in an eigenstate of the final Hamiltonian, optimising the problem. This describes the quantum annealing procedure.

The level dynamics of this system is governed by the following closed set of ordinary differential equations. These equations enable treating quantum systems in the light of classical dynamics. Under this formalism, one can derive the Pechukas equations, describing the "position" ($x_m$), "velocity" ($v_m$) and "relative angular momentum" ($l_{mn}$), given by the following[15, 16, 17, 18]:

$$\begin{aligned} \dot{x}_m &= v_m \\ \dot{v}_m &= 2\sum_{m\neq n}\frac{|l_{mn}|^2}{(x_m - x_n)^3} \\ \dot{l}_{mn} &= \sum_{k\neq m,n} l_{mk}l_{kn}\left(\frac{1}{(x_m - x_k)^2} - \frac{1}{(x_k - x_n)^2}\right), \end{aligned} \tag{3.10}$$

where $x_m(\lambda) = E_m(\lambda)$, $v_m(\lambda) = \langle m|Z\mathcal{H}_b|m\rangle$ and $l_{mn}(\lambda) = (E_m(\lambda) - E_n(\lambda))\langle m|Z\mathcal{H}_b|n\rangle$ where this is a antisymmetric complex quantity such that $l_{mn} = -l^*_{nm}$. The indices $(m)$ represent the positions, velocities and particle-particle repulsion as determined by the relative angular momenta, for the corresponding $m^{th}$ particle interaction. Here $\lambda$ plays the role of time [3, 4, 15, 16, 17, 18, 19]. This procedure describes the aforementioned mapping of the level dynamics of a system to that of a one-dimensional classical gas, interacting with long range couplings described by the relative angular momenta, valid for an arbitrary choice of $H_0$ and $H_b$ and an arbitrary time dependence of $\lambda$ not necessarily adiabatic. Note that time does not explicitly enter the Pechukas equation, rather concerning the evolution in time parametrically through $\lambda$ which determines the instantaneoues energy levels.

It was shown that the parametric evolution of the system described by Eq. (2.8) can be mapped on the classical Hamiltonian dynamics of a one-dimensional (1D) gas model with long-range repulsion: the Pechukas gas. The level dynamics of a system are given by the evolution of the eigenvalues on a Hamiltonian [15, 16, 17]. Under the Pechukas-Yukawa formalism, there is an exact mapping between adiabatic quantum evolution and the 1D classical Hamiltonian dynamics[3, 4, 5, 9]. Using this approach, described in adiabatic quantum computing, a complex Hamiltonian is considered with a nondegenerate groundstate. This Hamiltonian is mapped to the Pechukas model, a set of ordinary differential equations describing a classical 1D gas with long range repulsion [15, 16, 17]. These govern the effects of adiabatic evolution on the level dynamics. Consider a Hamiltonian of $N$ levels, in phase space there are over $2N$ levels describing the dynamics of the system, as a consequence of the coupling strengths being dynamics variables. The equilibrium statistical mechanics of Pechukas-Yukawa gas turned out a useful tool in justifying the random matrix theory [9]. This approach was successfully used to describe the operation of a small-scale adiabatic quantum computer, but its scaling up was restricted for the same reason as mentioned above, and it was suggested that building the kinetic theory of the Pechukas-Yukawa gas may provide a useful solution. The Pechukas equations had been adapted to a system with noise in order to determine how well this mapping held in the presence of noise [5]. One major challenge to achieving AQC is the decoherence of quantum systems under time evolution is noise, resulting in dissipation in the evolution of states.

## 3.3 Stochastic Pechukas-Yukawa Model

Quantum systems adhere to random fluctuations as a consequence of interactions with the environment and intrinsically due to the Heisenberg uncertainty principle[25]. These result in decoherence in quantum states. Noise inherently enters a system either internally from the

physical system itself or the system may be subject to noise due to external interactions due to the inability to perfectly isolate a system from the environment. As a result, stochastic influences must be accounted for. In our research, we studied the effects of noise on the dynamics of a many-body perturbed quantum system. For simplicity we considered white noise models, however our formalism extends to any general stochastic process. We refer the reader to Appendix C for more background on stochastic dynamics.

An idealised mathematical model of noise is to treat it as white noise $\eta(t)$ [26] having zero expectation, $\langle\eta\rangle = 0$. For $\eta(t)$ and $\eta(t')$ where $t \neq t'$ the noise terms are statistically independent, described as being uncorrelated. This is described by the following:

$$\langle\eta(t)\eta(t')\rangle = \delta(t - t'). \tag{3.11}$$

Formally, white noise is defined as the derivative of a Wiener process $W(t)$, which is a Markovian process on $R^d$, see Appendix D.

These concepts are applied to classical integrable descriptions of quantum systems, such that they carry the added advantage of providing insight on the influences of noise on the nature of eigenstate dynamics via classical elements. This is used to formulate many-body quantum systems analytically using eigenvalue dynamics under the stochastic Pechukas-Yukawa model, which is otherwise intractable. For more background, refer to Appendix E.

The stochastic Pechukas-Yukawa formalism accommodates for noise arising from random fluctuations in the environment, affecting the level dynamics of the system[5]. Using the central limit theorem; noise arises from a number of independent identical sources, therefore it is reasonable to assume the sum of its effect is Gaussian [26, 5]. The noise contribution in the Hamiltonian is denoted as $\delta h(\lambda(t))$ in the Hamiltonian, $H(\lambda(t)) = H_0 + \lambda(t)ZH_b + \delta h(\lambda(t)$. For real eigenvalues, $\delta h$ is Hermitian. We take $\delta h$ to be real, to simplify the system. It is shown that with the added stochastic term, the Pechukas mapping still applies and we can extend Eq. (3.10) to the closed stochastic Pechukas equations. The generalised Pechukas equations are given by the following [5]:

$$
\begin{aligned}
\dot{x}_m &= v_m + \dot{\delta}h_{mm}, \\
\dot{v}_m &= 2\sum_{m\neq n} \frac{|l_{mn}|^2}{(x_m - x_n)^3} + \frac{l_{mn}\dot{\delta}h_{nm} - \dot{\delta}h_{mn}l_{nm}}{(x_m - x_n)^2}, \\
\dot{l}_{mn} &= \sum_{k\neq m,n} l_{mk}l_{kn}\left(\frac{1}{(x_m - x_k)^2} - \frac{1}{(x_k - x_n)^2}\right) + \frac{(x_m - x_n)(l_{mk}\dot{\delta}h_{km} - \dot{\delta}h_{mk}l_{km})}{(x_m - x_k)(x_n - x_k)} \\
&\quad + \dot{\delta}h_{mn}(v_m - v_n) + \frac{l_{mn}(\dot{\delta}h_{mm} - \dot{\delta}h_{nn})}{(x_m - x_n)}.
\end{aligned} \tag{3.12}
$$

The derivative is taken with respect to $\lambda$. The mapping retains its structure; whereby if $\delta h = 0$, Eq. (3.12) reduces to Eq. (3.10). The stochastic Pechukas equations, Eq. (3.12) is independent of any assumptions on the nature of the noise, therefore applicable to a wide range of stochastic systems.

## 3.4 Summary

In this chapter, we presented the Pechukas-Yukawa formalism, describing a fully integrable model for a set of $N$ fictitious particles and their interactions through a coupled set of ordinary differential equations. Under this formalism, one can describe the evolution of highly entangled quantum systems using classical dynamics. Furthermore, the level dynamics are governed by their initial conditions, which is advantageous in regard to adiabatically evolving systems. This carries promise in the theoretical development of adiabatic quantum computing, however we consider this mapping in the general sense with applications to adiabatic quantum algorithms. A derivation of this model has been provided, demonstrating this mapping. Finally, we presented an extended Pechukas-Yukawa model, accounting for general dissipative influences whilst maintaining the properties of integrability, accounting for the dynamics of large entangled out of equilibrium systems governed by initial conditions.

Using this formalism, we construct a statistical mechanical framework to investigate non-equilibrium, nonstationary quantum systems governed by their level dynamics, extending the standard BBGKY hierarchy. Furthermore, we explore the applicability of the Landau-Zener model and the conditions required. We further extend this description to explore the impacts of Brownian noise on these conditions. In extension, we developed the formalism beyond Hamiltonian eigenvalue dynamics to include state dynamics via the density matrix such that the entire quantum system is described through its level dynamics. Whilst these methods provide valuable insights on the solutions and dynamics of a system, an alternative approach to characterise these dynamics is through Lax pairs which enables access to further conser-

vation laws within the system. This description was invaluable to this project as will become more apparent in the following sections. Furthermore, as the Pechukas-Yukawa formalism supports the random matrix theory for equilibrium statistical mechanics, we extended the description to non-equilibrium, nonstationary evolution.

# Chapter 4

# Statistical Treatment of Eigenvalue Dynamics

Extending the standard BBGKY hierarchy of the statistical treatment of particle dynamics, we provide a consistent description of a non-equilibrium, nonstationary evolution of a perturbed quantum system based on the kinetic theory of Pechukas-Yukawa gas. Describing parametrically driven evolution of quantum systems, is especially useful in accommodating for adiabatic systems, however the formalism is applicable to an arbitrary Hamiltonian system with parametric evolution in time given by Eq. (2.8). This formalism explores an important new direction in contemporary physics and open further investigations in order to understand the connection to the physics of the Pechukas gas.

Extending on [5, 24], using probability distributions to investigate eigenvalue dynamics in Landau-Zener transitions, we consider the overall evolution of levels, not restricted to level crossings or anti-crossings, statistically via probability distributions. As in classical kinetic theory, it is expected that the statistical approach to the level dynamics (as functions of the parameter $\lambda$) would allow a reduced description in terms of correlation functions, which can be used as a basis for controlled approximations. This could provide a better insight into what measurable characteristics of a system can be used as criteria of its quantum performance, and make possible an approximate simulation of larger systems than those tractable by other methods.

In this chapter, the standard BBGKY hierarchy is introduced, describing the kinetic equations of motion for an arbitrary Hamiltonian governing $N$ particles via coupled differential equations concerning probability distributions of particle positions and velocities. A derivation of the BBGKY hierarchy in the Pechukas-Yukawa formalism is provided, extending this theory to parametrically driven perturbed quantum systems using the Pechukas-Yukawa model, governing the evolution of the quantum system via the statistical treatment of level

dynamics. A factorisation approximation based on the statistically independent treatment of level dynamics is then investigated, followed by an analytical study of its accuracy. We then test our theory numerically for a small system of two interacting qubits, simulated by a transverse field Ising Hamiltonian (TFIH), summarising our results.

## 4.1 The Standard BBGKY Hierarchy

The standard BBGKY hierarchy arises from the continuity equation in phase space. It is used to describe the evolution of classical reduced distribution functions for a general time-independent Hamiltonian. The chain relates the distribution function for $N$ particles to the distribution function for $N+1$ particles concerning positions and velocities [2, 22, 23, 27, 28, 29].

Consider an arbitrary perturbed Hamiltonian, under the influence of an external field,

$$H = \sum_i \frac{v_i^2}{2m} + \sum_i V(x_i) + \sum_{i<j} V(x_i - x_j), \tag{4.1}$$

where the first term corresponds to a massless free Hamiltonian with positions $x_i$ and velocities $v_i$, $V$ represents the potential such that the second term denotes self-interaction terms as consequence of the potential and the final term being the interaction between other terms associated to the angular momentum. We denote an empirical distribution function, $F_N(x_1 \dots x_N, v_1 \dots v_N)$ averaged over the initial conditions, of the form:

$$F_N(x_1 \dots x_N, v_1 \dots v_N) = \langle \prod_m \delta\left(x_m - \xi_m\right) \delta(v_m - \omega_m) \rangle, \tag{4.2}$$

where $x_n$ denotes the particles in the Hamiltonian systems with respective velocities $v_n$. The averaging procedure is described through:

$$\langle f(x_m, v_n) \rangle := \frac{1}{|I|} \sum_{x^0,\ v^0 \in I} f(x^t, v^t; x^0, v^0), \tag{4.3}$$

where $|I|$ denotes the size of $I$, the set of initial conditions and $f(x^t, v^t; x^0,\ v^0)$ denotes the function evaluated at $(x^t, v^t, t)$, the propagated coordinates up to time $t$, parameterised by $(x^0,\ v^0)$. This is essentially a counting function of where the particles are present.

The BBGKY hierarchy for this arbitrary distribution function $F_N\left(x_1 \dots x_N, v_1 \dots v_N\right)$,

in phase space is defined through the following set of equations:

$$\partial_t F_s = \sum_{j=1}^{s} L_j^0 F_s + \sum_{j=1}^{s} L_j^F F_s + \sum_{j=1}^{s} \sum_{n=1}^{j-1} L_{jn}^I F_s + \sum_{j=1}^{s} \int dx_{s+1} L_{j(s+1)}^I F_{s+1}. \tag{4.4}$$

The reduced distribution function, $F_s := F_s(x_1 \dots x_s, v_1 \dots v_s)$ taken up to the $s$-particle interactions hence it takes into account only the distribution functions of the $s$-particle and the $(s+1)$-particle. The first term, $L^0$ corresponds to the free part of the Hamiltonian, the second term, $L^F$ describes the external field for example, noise. The final two terms associated with $L^I$ correspond to the perturbation contribution of the Hamiltonian as result of interaction [22, 23, 27, 28, 2, 30, 31, 32]. Truncating the system to the first four equations, the equations read:

$$\begin{aligned}
\partial_t F_0 &= 0, \\
(\partial_t - L_1^0 - L_1^F) F_1 &= \int dx_2 dv_2 L_{12}^I F_2, \\
(\partial_t - L_1^0 - L_2^0 - L_1^F - L_2^F) F_2 &= L_{12}^I F_2 + \int dx_3 dv_3 (L_{13}^I + L_{23}^I) F_3, \\
(\partial_t - \sum_1^3 L_j^0 - \sum_1^3 L_j^F) F_3 &= (L_{12}^I + L_{13}^I + L_{23}^I) F_3 + \int dx_4 dv_4 (L_{14}^I + L_{24}^I + L_{34}^I) F_4.
\end{aligned} \tag{4.5}$$

Here we have demonstrated the BBGKY hierarchy up to the $4^{th}$ chain, revealing the relationship between the s-particle distribution functions with the (s+1)-particle distribution functions.

Although this hierarchy produces a scheme which determines the kinetic equations of motion, it does not describe the nature of time dependent non-equilibrium Hamiltonians. In the following section, we derive a generalised BBGKY hierarchy that describes a non-equilibrium parametrically evolving Hamiltonian, using the Pechukas model.

## 4.2 The BBGKY Hierarchy in the Pechukas-Yukawa Model

The BBGKY chain for the Pechukas equations governs the statistical dynamics of the system from the evolution of the probability distribution functions concerning the levels. These levels can be thought of as interacting particles with the respective distribution functions relating that of $N$-particles to $(N+1)$ particles. Consider the distribution with dynamic variables

$x_m, v_n$ and $l_{mn}$: averaging over $\xi,\ \omega,\ \lambda$,

$$F_{N,N(N-1)}(x_1,\ldots,x_n,v_1,\ldots,v_n,l_{12},\ldots,l_{mn}) = \langle \prod_m \delta(x_m-\xi_m)\delta(v_m-\omega_m)\prod_{mn}\delta(l_{mn}-\Lambda_{mn})\rangle, \tag{4.6}$$

following a similar averaging procedure as in Eq. (4.3), where $|S|$ is the size of $S$ being the set of all initial conditions $(x^0,\ v^0, l^0)$ and similar to the classical BBGKY hierarchy of reduced distribution functions, $F_N(x^t, v^t, l^t, t; x^0,\ v^0,\ l^0)$ denotes the function evaluated at $(x^t, v^t, l^t, t)$, the propagated coordinates obtained through the Pechukas equation up to time $t$. We denote the probability distribution function by the following, $F_{N,N(N-1)} := F_{N,N(N-1)}(x_1,\ldots,x_n,v_1,\ldots,v_n,l_{12},\ldots,l_{mn})$ All distribution functions are symmetric with respect to permutations of arguments [15, 16, 19, 23].

Here $x_m, v_n$ and $l_{mn}$ are independent coordinates which describe the centre frame and $\xi,\ \omega$ and $\Lambda$ are shifted coordinates from this centre frame. Taking a total derivative of this distribution with respect to the adiabatic parameter $\lambda$, we obtain the following:

$$\begin{aligned}\frac{d}{d\lambda}F_{N,N(N-1)} = &\sum_{m\neq m'} < \prod_{m'}\frac{\partial}{\partial\xi_m}\delta(x_{m'}-\xi_{m'})\dot{\xi_m}\delta(v_{m'}-\omega_{m'})\prod_{m'n'}\delta(l_{m'n'}-\Lambda_{m'n'}) > \\ &+\sum_{m\neq m'} < \prod_{m}\delta(x_{m'}-\xi_{m'})\frac{\partial}{\partial\omega_m}\delta(v_{m'}-\omega_{m'})\dot{\omega}_m\prod_{m'n'}\delta(l_{m'n'}-\Lambda_{m'n'}) > \\ + < \prod_{m'}\delta(x_{m'}-\xi_{m'})\delta(v_{m'}-\omega_{m'})&\sum_{mn}\prod_{m'n'}\frac{\partial}{\partial\Lambda_{mn}}\delta(l_{m'n'}-\Lambda_{m'n'})\dot{\Lambda}_{mn} > +\frac{\partial}{\partial t}F_{N(N-1)}.\end{aligned} \tag{4.7}$$

Given that $\frac{\partial}{\partial\xi} = -\frac{\partial}{\partial x}$ , $\frac{\partial}{\partial\omega} = -\frac{\partial}{\partial v}$, $\frac{\partial}{\partial\Lambda} = -\frac{\partial}{\partial l}$ where '.' describes differentiation with respect to $\lambda$. Note that time does not explicitly enter these equations but is parameterised by $\lambda$., which plays the same role. We substitute this into the total derivative with the related Pechukas equations. We use the chain rule with respect to time to obtain:

$$\begin{aligned}\frac{d}{d\lambda}F_{N(N-1)} = &-\sum_m v_m\frac{\partial}{\partial\xi_m}F_{N,N(N-1)} - \sum_m\frac{\partial}{\partial v_m}2\sum_{m\neq n}\frac{|l_{mn}|^2}{(x_m-x_n)^3}F_{N,N(N-1)} \\ -\sum_{mn}\frac{\partial}{\partial l_{mn}}\sum_{k\neq m,n}&l_{mk}l_{kn}\left(\frac{1}{(x_m-x_k)^2}-\frac{1}{(x_k-x_n)^2}\right)F_{N,N(N-1)} + \frac{\partial}{\partial t}F_{N,N(N-1)}.\end{aligned} \tag{4.8}$$

Applying Liouville's theorem, which states that the number of particles at the start stays constant in the system as time evolves [15, 16, 19, 23]:

$$\frac{d}{d\lambda}F_{N(N-1)} = 0. \tag{4.9}$$

From this we rearrange the total derivative to express $\frac{\partial}{\partial\lambda}F_{N,N(N-1)}\left(x_m, v_m, l_{mn}\right)$ by the following:

$$\begin{aligned}\frac{\partial}{\partial\lambda}F_{N,N(N-1)} = \sum_m v_m \frac{\partial}{\partial x_m}F_{N,N(N-1)} + \sum_m \frac{\partial}{\partial v_m} 2 \sum_{m\neq n} \frac{|l_{mn}|^2}{(x_m - x_n)^3} F_{N,N(N-1)} \\ + \sum_{mn} \frac{\partial}{\partial l_{mn}} \sum_{k\neq m,n} l_{mk} l_{kn} \left( \frac{1}{(x_m - x_k)^2} - \frac{1}{(x_k - x_n)^2} \right) F_{N,N(N-1)}.\end{aligned} \tag{4.10}$$

In the scheme of BBGKY, we consider $s$ number of particles where $s \leq \{1, \ldots N\}$ in order to build up the chain. For this we consider the way this affects each term of the distribution. The $s$-particle distribution function is thus given by the following:

$$\begin{aligned}F_{s,s(s-1)} := \frac{N!}{(N-s)!} \cdot \frac{(N^2-N)!}{(N^2-N-s(s-1))!} \\ \times \int dx_{s+1} \ldots dx_n dv_{s+1} \ldots dv_n dl_{s+1,s} \ldots dl_{n,n(n-1)} F_{N,N(N-1)}.\end{aligned} \tag{4.11}$$

The normalisation constants in the front of the integral comes from the combinatorics of $x_m$ and $v_m$ for $\frac{N!}{(N-s)!}$ with $N!$ representing the total number of combinations in both $x_m$ and $v_m$ and $(N-s)!$ representing the number of combinations of particles not included in the distribution. Similarly, for $l_{mn}$ we have the total number of possible values in $l_{mn}$ determined by $(N^2-N)!$ where dictated by $s$ there are $s(s-1)$ possible values in the distribution giving rise to the normalisation constant $\frac{(N^2-N)!}{(N^2-N-s(s-1))!}$ included in the definition for $F_{s,s(s-1)}$. These come about from the symmetry in the distribution functions with respect to permutations in their arguments.

Considering the $s$-particle distribution in the above relation for Eq. (4.10) we obtain:

$$\frac{\partial}{\partial\lambda}F_{s,s(s-1)} = \frac{N!}{(N-s)!}.\frac{(N^2-N)!}{(N^2-N-s(s-1))!}\int dx_{s+1}\dots dx_n dv_{s+1}\dots dv_n dl_{s+1,s}\dots dl_{n,n(n-1)}$$
$$\sum_m v_m\frac{\partial}{\partial x_m}F_{N,N(N-1)} + \sum_m \frac{\partial}{\partial v_m}2\sum_{m\neq n}\frac{|l_{mn}|^2}{(x_m-x_n)^3}F_{N,N(N-1)}$$
$$+\sum_{mn}\frac{\partial}{\partial l_{mn}}\sum_{k\neq m,n} l_{mk}l_{kn}\left(\frac{1}{(x_m-x_k)^2}-\frac{1}{(x_k-x_n)^2}\right)F_{N,N(N-1)}. \tag{4.12}$$

Determining the way the first term is affected by the reduced distribution function concerning up to $s$-particle interactions is expressed by the following:

$$\frac{N!}{(N-s)!}.\frac{(N^2-N)!}{(N^2-N-s(s-1))!}\int dx_{s+1}\dots dx_n dv_{s+1}\dots dv_n dl_{s+1,s}\dots dl_{n,n(n-1)}$$
$$\sum_{m=1}^{s} v_m\frac{\partial}{\partial x_m}F_{N,N(N-1)} + \int dx_{s+1}dv_{s+1}\boldsymbol{Dl}_{s+1}\sum_{m=s+1}^{N} v_m\frac{\partial}{\partial x_m}F_{N,N(N-1)}, \tag{4.13}$$

where we denote $\boldsymbol{Dl}_{s+1}$ as the following:

$$\boldsymbol{Dl}_{s+1} = \prod_{i=1}^{s} dl_{s+1,i}dl_{i,s+1}. \tag{4.14}$$

By Green's theorem the last term is equivalent to integrating on the boundary and so vanishes as the system tends to infinity, which reduces the expression as given by the following:

$$\frac{N!}{(N-s)!}.\frac{(N^2-N)!}{(N^2-N-s(s-1))!}$$
$$\times\int dx_{s+1}\dots dx_n dv_{s+1}\dots dv_n dl_{s+1,s}\dots dl_{n,n(n-1)}\sum_{m=1}^{s} v_m\frac{\partial}{\partial x_m}F_{N,N(N-1)}. \tag{4.15}$$

Following this procedure, we determine the way $F_{s,s(s-1)}$ affects the second term in the relation for $\frac{\partial}{\partial\lambda}F_{N,N(N-1)}$ such that it concerns only the $s$-particle distribution and $(s+1)$ particle distribution as determined below:

$$\frac{N!}{(N-s)!}.\frac{(N^2-N)!}{(N^2-N-s(s-1))!}\int dx_{s+1}\dots dx_n dv_{s+1}\dots dv_n dl_{s+1,s}\dots dl_{n,n(n-1)}$$

$$2\sum_{m=1}^{s}\sum_{n=1}^{m-1}\left(\frac{|l_{mn}|^2}{(x_m-x_n)^3}+\frac{|l_{nm}|^2}{(x_n-x_m)^3}\right)\frac{\partial}{\partial v_m}F_{N,N(N-1)}$$
$$+2\int dx_{s+1}dv_{s+1}\boldsymbol{Dl}_{s+1}\sum_{m=1}^{s}\left(\frac{|l_{m(s+1)}|^2}{(x_m-x_{s+1})^3}+\frac{|l_{(s+1)m}|^2}{(x_{s+1}-x_m)^3}\right)\frac{\partial}{\partial v_m}F_{N,N(N-1)}. \quad (4.16)$$

Finally, we determine the way taking $F_{s,s(s-1)}$ affects the last term in the relation for $\frac{\partial}{\partial\lambda}F_{N,N(N-1)}$, where we obtain the following:

$$\frac{N!}{(N-s)!}.\frac{(N^2-N)!}{(N^2-N-s(s-1))!}\int dx_{s+1}\dots dx_n dv_{s+1}\dots dv_n dl_{s+1,s}\dots dl_{n,n(n-1)}$$
$$\sum_{m=1}^{s}\sum_{k=1}^{m-1}\sum_{n=1}^{k-1}l_{mk}l_{kn}\left(\frac{1}{(x_m-x_k)^2}-\frac{1}{(x_k-x_n)^2}\right)\frac{\partial}{\partial l_{mn}}F_{N,N(N-1)}$$
$$+\int dx_{s+1}dv_{s+1}\boldsymbol{Dl}_{s+1}\sum_{k=1}^{s}\sum_{n=1}^{k-1}l_{s+1k}l_{kn}\left(\frac{1}{(x_{s+1}-x_k)^2}-\frac{1}{(x_k-x_n)^2}\right)\frac{\partial}{\partial l_{(s+1)n}}F_{N,N(N-1)}. \quad (4.17)$$

Combining these expressions and simplifying them with the definition for $F_{s,s(s-1)}$ we derive the BBGKY chain for the Pechukas equations as given by the following equations:

$$\frac{\partial}{\partial\lambda}F_{s,s(s-1)}=\sum_{m=1}^{s}v_m\frac{\partial}{\partial x_m}F_{s,s(s-1)}+2\sum_{m=1}^{s}\sum_{n=1}^{m-1}\left(\frac{|l_{mn}|^2}{(x_m-x_n)^3}+\frac{|l_{nm}|^2}{(x_n-x_m)^3}\right)\frac{\partial}{\partial v_m}F_{s,s(s-1)}$$
$$+2\int dx_{s+1}dv_{s+1}\boldsymbol{Dl}_{s+1}\sum_{m=1}^{s}\left(\frac{|l_{m(s+1)}|^2}{(x_m-x_{s+1})^3}+\frac{|l_{(s+1)m}|^2}{(x_{s+1}-x_m)^3}\right)\frac{\partial}{\partial v_m}F_{s+1,s(s+1)}$$
$$+\sum_{m=1}^{s}\sum_{k=1}^{m-1}\sum_{n=1}^{k-1}l_{mk}l_{kn}\left(\frac{1}{(x_m-x_k)^2}-\frac{1}{(x_k-x_n)^2}\right)\frac{\partial}{\partial l_{mn}}F_{s,s(s-1)}$$
$$+\int dx_{s+1}dv_{s+1}\boldsymbol{Dl}_{s+1}\sum_{k=1}^{s}\sum_{n=1}^{k-1}l_{s+1k}l_{kn}\left(\frac{1}{(x_{s+1}-x_k)^2}-\frac{1}{(x_k-x_n)^2}\right)\frac{\partial}{\partial l_{(s+1)n}}F_{s+1,s(s+1)}. \quad (4.18)$$

This gives us the BBGKY hierarchy for the Pechukas model with respect to a full distribution concerning position, velocity and relative angular momentum, where $F_{s,s(s-1)} := F_{s,s(s-1)}(x_1,\dots x_s,v_1,\dots v_s,l_{12},\dots l_{s,s-1})$ describes the reduced distribution function up to $s$-particle interactions and $F_{s+1,s(s+1)} := F_{s+1,s(s+1)}(x_1,\dots x_{s+1},v_1\dots v_{s+1},l_{12},\dots l_{s+1,s})$ being the reduced distribution function concerning the $(s+1)$ particle interactions. This is our main result for this section, providing a coupled set of differential equations concerning the statistical properties of kinetic equations for the level dynamics. These equations extend

the standard BBGKY hierarchy to non-equilibrium, nonstationary parametrically evolving systems.

To illustrate the scheme more explicitly, we write the BBGKY chain up to the $2^{nd}$ equation. We neglect the $s = 0$ level as this merely vanishes on the right hand side of the chain. Starting from $s = 1$ we obtain that $F_{1,0}(x_1,\ v_1)$ the associated chain is:

$$\frac{\partial}{\partial\lambda}F_{1,0} = v_1\frac{\partial}{\partial x_1}F_{1,0} + 2\int dx_2dv_2dl_{12}dl_{21}\left(\frac{|l_{12}|^2}{(x_1-x_2)^3} + \frac{|l_{21}|^2}{(x_2-x_1)^3}\right)\frac{\partial}{\partial v_1}F_{2,2}. \quad (4.19)$$

In the same manner, the chain has been explicitly built up for $s = 2$ with $F_{2,2}\,(x_1, x_2, v_1,\ v_2, l_{12,}\ \ l_{21})$. For $s = 2$, we obtain:

$$\begin{aligned}\frac{\partial}{\partial\lambda}F_{2,2} &= v_1\frac{\partial}{\partial x_1}F_{2,2} + v_2\frac{\partial}{\partial x_2}F_{2,2} + 2\left(\frac{|l_{12}|^2}{(x_1-x_2)^3} + \frac{|l_{21}|^2}{(x_2-x_1)^3}\right)\frac{\partial}{\partial v_2}F_{2,2}\\ &+2\int dx_3dv_3dl_{13}dl_{31}dl_{23}dl_{32}\left(\frac{|l_{13}|^2}{(x_1-x_3)^3} + \frac{|l_{31}|^2}{(x_3-x_1)^3}\right)\frac{\partial}{\partial v_1}F_{3,6} \quad (4.20)\\ &+2\int dx_3dv_3dl_{13}dl_{31}dl_{23}dl_{32}\left(\frac{|l_{23}|^2}{(x_2-x_3)^3} + \frac{|l_{32}|^2}{(x_3-x_2)^3}\right)\frac{\partial}{\partial v_2}F_{3,6}.\end{aligned}$$

These provide insights on the evolution of the statistical dynamics of the levels. However, the BBGKY heirarchy cannot be solved without truncation. We have considered the factorisation approximation in order to truncate this hierarchy.

## 4.3 Factorisation Approximation of the BBGKY Heirarchy in the Pechukas-Yukawa Formalism

Eq. (4.18) extends the BBGKY hierarchy to non-equilibrium parametrically evolving systems, using the Pechukas model. The coupled differential equations determine the kinetics of the distribution functions associated to the level dynamics of the Pechukas-Yukawa gas. The hierarchy clearly demonstrates the relationship between the associated distribution functions of the $s$-particles to $(s + 1)$ interacting particles. We make the approximation that the distribution functions of the system can be expressed as a product of $F_{1,0}\,(x_1, v_1)$ distributions.

Taking into account the chain for $s = 1$, we introduce a factorisation approximation based on the independence of the the set of coordinates $x_m, v_m$ and the set of relative angular momenta terms $l_{mn}$ such that we can construct probability distribution functions of $x_m$ and

$v_m$ that are independent of the probability distribution functions of $l_{mn}$. As a consequence, the distribution $F_{N,N(N-1)}$ can be factorised in terms of the one-particle distribution and the distribution of $l_{mn}$ separately. Under the approximation, $F_{2,2}\left(x_1, x_2, v_1,\ v_2, l_{12}, l_{21}\right)$ can be factorised in terms of the distribution functions of $F_{1,0}\left(x_1, v_1\right)$, $F_{1,0}\left(x_2, v_2\right)$ and $h(l_{12,}\ \ l_{21})$ with negligible contributions from the mixed terms. This is expressed below:

$$F_{2,2}(x_1, x_2, v_1, v_2, l_{12}, l_{21}) \approx F_{1,0}(x_1, v_1) F_{1,0}(x_2, v_2) h(l_{12}, l_{21}). \tag{4.21}$$

Considering the approximation, Eq. (4.19) can be transformed in a way that precisely reflects an effective mean field theory, where the definitions of $F_{1,0}\left(x_1, v_1\right)$, $F_{1,0}\left(x_2, v_2\right)$ and $h(l_{12,}\ \ l_{21})$ are expressed in the same way as the generalised $F_{s,s(s-1)}$.

Substituting Eq. (4.21) into Eq. (4.19) and using the product rule under the integral, (including the arguments for clarity), we obtain the following:

$$\begin{aligned}
\frac{\partial}{\partial\lambda} F_{1,0}(x_1, v_1) &= v_1 \frac{\partial}{\partial x_1} F_{1,0}(x_1, v_1) \\
+2 \int dx_2 dv_2 dl_{12} dl_{21} &\left( \frac{|l_{12}|^2}{(x_1 - x_2)^3} + \frac{|l_{21}|^2}{(x_2 - x_1)^3} \right) \left( \frac{\partial}{\partial v_1} F_{1,0}(x_1, v_1) \right) F_{1,0}(x_2, v_2) h(l_{12}, l_{21}) \\
&+ F_{1,0}(x_1, v_1) \left( \frac{\partial}{\partial v_1} F_{1,0}(x_2, v_2) \right) h(l_{12}, l_{21}) + F_{1,0}(x_1, v_1) F_{1,0}(x_2, v_2) \left( \frac{\partial}{\partial v_1} h(l_{12}, l_{21}) \right).
\end{aligned} \tag{4.22}$$

It is clear to see that the last two terms vanish and $\left(\frac{\partial}{\partial v_1} F_{1,0}\left(x_1,\ v_1\right)\right)$ can be taken out from under the integral obtaining:

$$\begin{aligned}
\frac{\partial}{\partial\lambda} F_{1,0}(x_1, v_1) &= v_1 \frac{\partial}{\partial x_1} F_{1,0}(x_1, v_1) \\
+2 \frac{\partial}{\partial v_1} F_{1,0}(x_1, v_1) &\int dx_2 dv_2 dl_{12} dl_{21} \left( \frac{|l_{12}|^2}{(x_1 - x_2)^3} + \frac{|l_{21}|^2}{(x_2 - x_1)^3} \right) F_{1,0}(x_2, v_2) h(l_{12}, l_{21}).
\end{aligned} \tag{4.23}$$

Using this approximation, we reduce the chain after breaking it at the first link such that it only concerns the $F_{1,0}\left(x_1, v_1\right)$, $F_{1,0}\left(x_2, v_2\right)$ and $h(l_{12,}\ \ l_{21})$ distributions hence reducing to a one-body problem. This approximation extends to an $N$-body system, rendering the heirarchy solvable.

### 4.3.1 Accuracy of the Factorisation Approximation

In this section, we estimate the accuracy of the factorisation approximation as this is important to know the validity of the effective mean field approximation. Taking the definition for $F_{N,N(N-1)}\left(x_m, v_n, l_{mn}\right)$ and evaluating the integral in Eq. (4.12) we obtain the distribution for $F_{2,2}\left(x_1, x_2, v_1,\ v_2, l_{12}, l_{21}\right)$ expressed as the product of $\delta$ functions:

$$\begin{aligned} &F_{2,2}(x_1, x_2, v_1, v_2, l_{12}, l_{21}) = \\ &< \delta(x_1 - \xi_1)\delta(x_2 - \xi_2)\delta(v_1 - \omega_1)\delta(v_2 - \omega_2)\delta(l_{12} - \lambda_{12})\delta(l_{21} - \lambda_{21}) > . \end{aligned} \tag{4.24}$$

Similarly the product of the distributions $F_{1,0}\left(x_1,\ v_1\right),\ F_{1,0}(x_2,\ v_2)$ and $h(l_{12,}\ l_{21})$ obtained from evaluating Eq. (4.23) specifically with these distribution functions takes the same form with the only difference being the normalisation constants,

$$\begin{aligned} &F_{1,0}(x_1, v_1)F_{1,0}(x_2, v_2)h(l_{12}, l_{21}) = \\ &< \delta(x_1 - \xi_1)\delta(v_1 - \omega_1) >< \delta(x_2 - \xi_2)\delta(v_2 - \omega_2) >< \delta(l_{12} - \lambda_{12})\delta(l_{21} - \lambda_{21}) > . \end{aligned} \tag{4.25}$$

In order to verify the factorisation approximation holds, depends solely on the normalisation constants used in the averaging procedure as defined in Eq. (4.12) such that Eq. (4.21) holds. The normalisation constant for Eq. (4.24) can be expressed by the following:

$$\frac{N!}{(N-2)!}.\frac{(N^2-N)!}{((N^2-N)-2)!} = N(N-1)(N^2-N)(N^2-N-1). \tag{4.26}$$

On the other hand, for Eq. (4.25), the normalisation constant is similarly determined from the following:

$$\left(\frac{N!}{(N-1)!}\right)^2.\frac{(N^2-N)!}{((N^2-N)-2)!} = N^2(N^2-N)(N^2-N-1). \tag{4.27}$$

The normalisation constant relating to $l_{mn}$ is the same in both equations. This is a consequence of the fact that the $l_{mn}$ term from $h(l_{12}, l_{21})$ comes from a system associated to the $F_{2,2}\left(x_1, x_2, v_1,\ v_2, l_{12}, l_{21}\right)$ distribution function. We determine the relative error, $\mathcal{E}_r$ from the difference of these normalisations given by the following expression:

$$\mathcal{E}_r := \frac{F_{1,0}(x_1, v_1)F_{1,0}(x_2, v_2)h_{1,0}(l_{12}, l_{21}) - F_{2,2}(x_1, x_2, v_1, v_2, l_{12}, l_{21})}{F_{2,2}(x_1, x_2, v_1, v_2, l_{12}, l_{21})}. \tag{4.28}$$

Using this expression, we obtain the following:

$$\mathcal{E}_r = \frac{N-(N-1)}{(N-1)} = O(\frac{1}{N}). \tag{4.29}$$

Taking a large limit of the number $N$ of particles, it is possible to determine exactly the ground state and to encode solutions into through brute force. For the limit that $N \to \infty$ we find that $\mathcal{E}_r$ decays asymptotically. This comes as a consequence of pairwise interactions between particles having less significance in a large system such that it can be essentially decoupled, validating the factorisation approximation.

We extend this further to consider the factorisation approximation for a general $s$-particle distribution function $F_{s,s(s-1)}$ such that it can be factorised as $s$ one particle distributions and $\frac{s(s-1)}{2}$ number of $h$ distributions. Using the same idea as the case for $F_{2,2}(x_1, x_2, v_1, v_2, l_{12}, l_{21})$ we consider the way the normalisations constants will differ and the $\mathcal{E}_r$ between them. Taking the same approach, for the generalised factorisation for an $N$-particle distribution function composed as the product of $N$ one-particle distributions functions.

The normalisation constant for $F_{s,s(s-1)}$ is expressed as the following:

$$\begin{gathered}\frac{N!}{(N-s)!}.\frac{(N^2-N)!}{(N^2-N-s(s-1))!} = \\ N(N-1)\dots(N-s-1).(N^2-N)(N^2-N-1)\dots(N^2-N-s(s-1)-1).\end{gathered} \tag{4.30}$$

In contrast to this, the factorisation has normalisation constants expressed by the following:

$$(\frac{N!}{(N-1)!})^s.(\frac{(N^2-N)!}{(N^2-N-2)!})^{\frac{s(s-1)}{2}} = N^s.((N^2-N)(N^2-N-1))^{\frac{s(s-1)}{2}}. \tag{4.31}$$

Then $\mathcal{E}_r$ reads:

$$\begin{aligned}\mathcal{E}_r = \frac{N^s}{N(N-1)\dots(N-s-1)}.\frac{((N^2-N)(N^2-N-1))^{\frac{s(s-1)}{2}}}{(N^2-N)(N^2-N-1)\dots(N^2-N-s(s-1)-1)} - 1 \\ = O(\frac{1}{N}).\end{aligned} \tag{4.32}$$

From these results, it can be inferred that to solve the BBGKY chain for the Pechukas equations at the first link, only distributions functions for $F_{1,0}\,(x_1,\ v_1)$ and $h(l_{12,}\ l_{21})$ are required. The same rationale can be extended for higher order interactions in writing these distribution functions as products of one-particle distribution functions. We further illustrate this model on a two-qubit system.

### 4.3.2 Accuracy of the Factorisation Approximation in the Two Qubit Ising Model

We consider a two qubit system described by the Ising model in order to test the BBGKY hierarchy for the Pechukas equations. We take the TFIH as the Hamiltonian that governs the two qubit system:

$$\mathcal{H}(\lambda(t)) = J\sigma_1^z\sigma_2^z + \lambda Z h_1\sigma_1^x + \lambda Z h_2\sigma_2^x, \tag{4.33}$$

where $\sigma_j^z$ and $\sigma_j^x$ represent the corresponding Pauli matrices for the $j$-th qubit.

For the case that $J > 0$ the interaction favours antiferromagnetism whereas for $J < 0$, it favors ferromagnetism. We take random values for $J$, Gaussian distributed with mean 0 and standard deviation 1, reflecting the different initial conditions. When $J \gg \lambda Z h_1, \lambda Z h_2$ the system is in the ground state. We obtain the values for $x_n$ from the eigenvalues of the system given by $x_n(\lambda) = E_n(\lambda) =< n\,|\mathcal{H}_0|\,n >$. The perturbation matrix defined by $ZH_b(\lambda) = \lambda Z h_1\sigma_1^x + \lambda Z h_2\sigma_2^x$ determines the variables for velocity as $v_n(\lambda) =< n\,|Z\mathcal{H}_b|\,n >$ and relative angular momentum, $l_{mn}$ using its definition that $l_{mn}(\lambda) = (E_m(\lambda) - E_n(\lambda)) < m\,|Z\mathcal{H}_b|\,n >$.

The Hamiltonian reads:

$$\mathcal{H}(\lambda(t)) = J\begin{pmatrix} 1 & 0 & 0 & 0 \\ 0 & -1 & 0 & 0 \\ 0 & 0 & -1 & 0 \\ 0 & 0 & 0 & 1 \end{pmatrix} + \lambda Z h_1 \begin{pmatrix} 0 & 0 & 1 & 0 \\ 0 & 0 & 0 & 1 \\ 1 & 0 & 0 & 0 \\ 0 & 1 & 0 & 0 \end{pmatrix} + \lambda Z h_2 \begin{pmatrix} 0 & 1 & 0 & 0 \\ 1 & 0 & 0 & 0 \\ 0 & 0 & 0 & 1 \\ 0 & 0 & 1 & 0 \end{pmatrix}. \tag{4.34}$$

Diagonalising the Hamiltonian and using their respective definitions, we determine the values for $x_n,\ v_n,\ l_{mn}$ in order to construct the distribution functions for $f_1(\xi,\omega)$, $f_1(\xi',\omega')$, $f_2(\xi,\xi',\omega,\omega',l,l')$ and $h(l,\ l')$ as in Eq. (4.11), where $\xi,\xi',\omega,\omega',l,l'$ are the running variables of the probability distribution functions parameterising the coordinates $x_n,\ v_n,\ l_{mn}$ respectively.

The coordinates for $x_n$ are of the form $J+\lambda H_n$. Given that the values for $J$ are Gaussian distributed, $J \sim \mathcal{N}(\mu,\sigma)$ the values for each $x_n$ are Gaussian distributed varying only by a translation by $H_n$, randomising the initial conditions hence, $x_n \sim \mathcal{N}(\mu+\lambda H_n,\sigma) = \mathcal{N}(\lambda H_n, 1) := \tilde{\mathcal{N}}_n$, with the same mean and standard deviation where $H_n = \{-h_1-h_2,\ -h_1+h_2, h_1-h_2, h_1+h_2\}$. The values for $v_n$ are deterministic, we define them as $v_n \sim \delta_{H_n}$. We

observe that the terms describing $l_{mn}$ determined from its definiton are translated Gaussian distributions, which we denote by $L_{i,j}$. Using these definitions we build the distributions for $f_1(\xi,\omega)$, $f_1(\xi',\omega')$, $f_2(\xi,\xi',\omega,\omega',l,l')$ and $h(l,\ l')$ as given below:

$$f_1(\xi,\omega) = \frac{1}{4}\sum_{n=1}^{4}\tilde{\mathcal{N}}_n(\xi)\delta_{H_n}(\omega),$$

$$h(l,l') = \frac{10!}{12!}\sum_{i\neq j}L_{ij}(l)\sum_{i'\neq i,j'}L'_{i',j'}(l'),$$

$$f_2(\xi,\xi',\omega,\omega',l,l') = \frac{10!}{4!12!}\sum_{i\neq j}L_{ij}(l)\sum_{i'\neq i,j'}L'_{i',j'}(l')\sum_{n\neq n',n,n'=1}^{4}\tilde{\mathcal{N}}_n(\xi)\delta_{H_n}(\omega)\tilde{\mathcal{N}}_{n'}(\xi')\delta_{H_{n'}}(\omega'). \tag{4.35}$$

Substituting the definitions in Eq. (4.28), we analytically determine $\mathcal{E}_r$ for this system. We reduce the $\mathcal{E}_r$ as given in the expression below. Keeping concise, we omit the arguments of the distributions:

$$\mathcal{E}_r = \frac{3}{2}\left(\frac{\tilde{\mathcal{N}}_1\delta_{H_1}\tilde{\mathcal{N}}_{1'}\delta_{H_{1'}} + \tilde{\mathcal{N}}_2\delta_{H_2}\tilde{\mathcal{N}}_{2'}\delta_{H_{2'}} + \tilde{\mathcal{N}}_3\delta_{H_3}\tilde{\mathcal{N}}_{3'}\delta_{H_{3'}} + \tilde{\mathcal{N}}_4\delta_{H_4}\tilde{\mathcal{N}}_{4'}\delta_{H_{4'}}}{\sum_{n\neq n',n,n'=1}^{4}\tilde{\mathcal{N}}_n\delta_{H_n}\tilde{\mathcal{N}}_{n'}\delta_{H_{n'}}}\right) + \frac{1}{2}. \tag{4.36}$$

Bounding the error from above by maximising the numerator with $4(\tilde{\mathcal{N}}_4(\xi)\delta_{H_4}(\omega)\tilde{\mathcal{N}}_{4'}(\xi')\delta_{H_{4'}}(\omega'))$ where $(\tilde{\mathcal{N}}_4(\xi)\delta_{H_4}(\omega)\tilde{\mathcal{N}}_{4'}(\xi')\delta_{H_{4'}}(\omega'))$ takes the largest value, and minimising the denominator with $12(\tilde{\mathcal{N}}_4(\xi)\delta_{H_4}(\omega)N_{1'}(\xi')\delta_{H_{1'}}(\omega'))$ as this divides by the smallest of these terms in $f_2(\xi,\xi',\omega,\omega',l,l')$. Using the normal distribution density, we expand these terms to obtain the following, again omitting the arguments in the distributions:

$$\mathcal{E}_r \leq \frac{1}{2} + \frac{3}{2}.\frac{4}{12}\left(\frac{\tilde{\mathcal{N}}_4\delta_{H_4}\tilde{\mathcal{N}}_{4'}\delta_{H_{4'}}}{\tilde{\mathcal{N}}_4\delta_{H_4}\tilde{\mathcal{N}}_{1'}\delta_{H_{1'}}}\right) \leq \frac{1}{2} + \frac{1}{2}\frac{\left(\frac{e^{\lambda(h_1+h_2)(\xi+\xi')}}{e^{\frac{\xi^2+\xi'^2}{2}}e^{\lambda^2(h_1+h_2)^2}}\right)\delta_{H_{4'}}}{\left(\frac{e^{\lambda(h_1+h_2)\xi}e^{\lambda(-h_1-h_2)\xi'}}{e^{\frac{\xi^2+\xi'^2}{2}}e^{\frac{\lambda^2(h_1+h_2)^2}{2}}e^{\frac{\lambda^2(-h_1-h_2)^2}{2}}}\right)\delta_{H_{1'}}}.$$

Cancelling common terms, this bound reduces to the following:

$$\mathcal{E}_r \leq \frac{1}{2} + \frac{1}{2}e^{2\lambda\xi'(h_1+h_2)}. \tag{4.37}$$

Similarly, bounding from below by minimising the numerator using $\tilde{\mathcal{N}}_3(\xi)\delta_{H_3}(\omega)\tilde{\mathcal{N}}_{3'}(\xi')\delta_{H_{3'}}(\omega')$ and maximising the denominator with $12(\tilde{\mathcal{N}}_3(\xi)\delta_{H_3}(\omega)\tilde{\mathcal{N}}_{2'}(\xi')\delta_{H_{2'}}(\omega'))$ where we find the following, omitting the arguments in the distributions:

$$\mathcal{E}_r \geq \frac{3}{2}.\frac{1}{12}\left(\frac{N_3\delta_{H_3}N_{3'}\delta_{H_{3'}}}{N_3\delta_{H_3}N_{2'}\delta_{H_{2'}}}\right) \geq \frac{1}{8}\frac{\left(\frac{e^{\lambda(h_1-h_2)(\xi+\xi')}}{e^{\frac{\xi^2+\xi'^2}{2}}e^{\lambda^2(h_1-h_2)^2}}\right)\delta_{H_{3'}}}{\left(\frac{e^{\lambda(h_1-h_2)\xi}e^{\lambda(-h_1+h_2)\xi'}}{e^{\frac{\xi^2+\xi'^2}{2}}e^{\frac{\lambda^2(h_1-h_2)^2}{2}}e^{\frac{\lambda^2(-h_1+h_2)^2}{2}}}\right)\delta_{H_{2'}}}.$$

We bound $\mathcal{E}_r$ from above and below to examine the applicability of the factorisation approximation. This reduces to the following:

$$\frac{1}{8}e^{2\lambda\xi'(h_1-h_2)} \leq \mathcal{E}_r \leq \frac{1}{2}+\frac{1}{2}e^{2\lambda\xi'(h_1+h_2)}. \tag{4.38}$$

Using these bounds, we find that the factorisation approximation does not hold. This is expected because to approximate well a probability distribution function as a product of one-particle distribution functions, the system must be essentially uncorrelated. In the specific case of the two qubit system the qubits are not statistically independent because the eigenvalues of the system are related as there is only one $J$. In order to explore this error further we test the system numerically using cloud dynamics and determine the distribution functions associated to the interactions. We draw 100 trials of $J \sim \mathcal{N}(0,1)$ terms, diagonalising the system to determine its eigenvalues, as demonstrated in Fig. 1. Choosing a large bias such that $Z = 10$, we take $h_1 = 0.01$ and $h_2 = 0.02$, keeping these values small so as to reduce their impact on $\mathcal{E}_r$. However, to explore the dynamics of these values we observe the system when $h_1$ as 0.1 and $h_2$ as 0.2 such that the perturbation is of the same order of the values of $J$ associated to the unperturbed Hamiltonian as in Eq. (4.33) as demonstrated in Fig. 4.1.

Further to this, we construct the normalised distribution functions for $f_2(\xi,\xi',\omega,\omega',l,l')$ and that of $f_1(\xi,\omega)$, $f_1(\xi',\omega')$ and $h(l,\ l')$ in order to test the factorisation approximation for the first link of the BBGKY hierarchy using the Pechukas model. To build these distribution functions, we split the time interval in 0.1 from initial time at 0 and final time at 1, each of these distributions had been normalised. We determine the values of $v_n$ through taking $x_{n+1} - x_n$ and dividing it through by the time step of 0.1. We obtain values for $l_{mn}$ using its definition described above. From this we produce the distribution for $f_1(\xi,\omega)$ shown in Fig. 4.2.

In Fig. 4.2 we observe how the probability distributions of the level dynamics in Fig. 4.1, demonstrating the statistical consistence between the evolution of the eigenvalues and their respective evolution of probability distribution functions.

From the distribution functions, it is evident that the factorisation approximation does not hold for a two qubit system as discussed above. We use Eq. (4.28) to determine $\mathcal{E}_r$ and

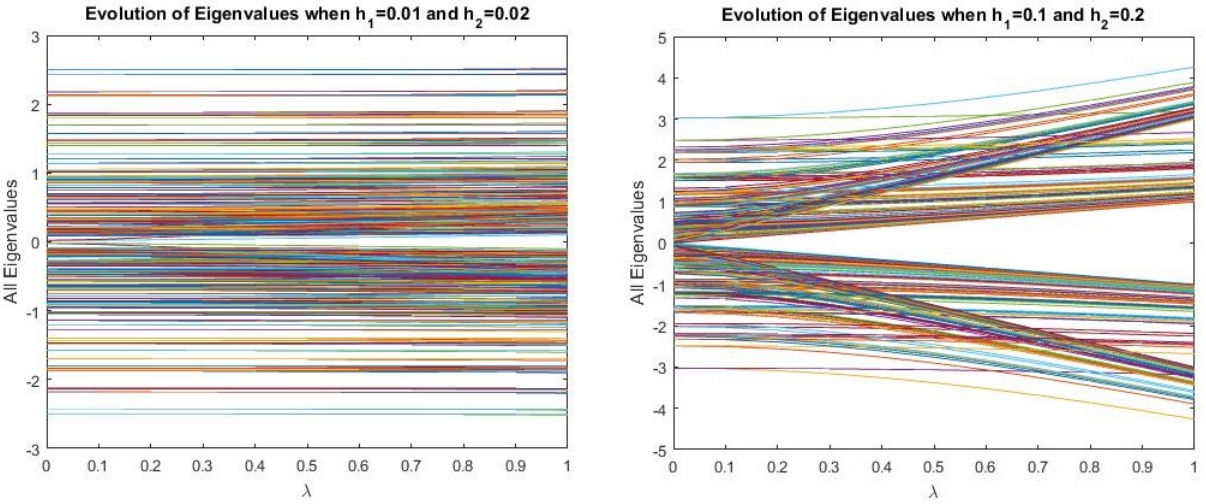


Figure 4.1: Evolution of eigenvalues: all the eigenvalues of Hamiltonian Eq. (4.33) for 100 simulations with random initial conditions obtained from the different values of $J$. These eigenvalues are of the form $J + \lambda H_n$, they are Gaussian distributed as $J$ is Gaussian distributed with mean 0 and standard deviation 1, through their evolution in $\lambda$ from 0 to 1 in steps of 0.1. When the perturbation is much weaker than the interaction $J$, the system stays close to its ground state see left panel. When the perturbation is of the same order as $J$, the eigenvalues deviate from an initially Gaussian distribution, evolving into four distinct peaks, see right panel.

how it varies through the evolution of the adiabatic parameter, considering nonzero points between the factorised distributions and that of $f_2(\xi, \xi', \omega, \omega', l, l')$. The results are presented in the Table 1 below:

| $\lambda$ | 0.1 | 0.2 | 0.3 | 0.4 | 0.5 | 0.6 | 0.7 | 0.8 | 0.9 |
|---|---|---|---|---|---|---|---|---|---|
| $\langle \mathcal{E}_r \rangle$ | 0.668 | 3.203 | 0.578 | 1.18 | 0.335 | 1.54 | 0.4803 | 0.0659 | 0.366 |
| SD of $\mathcal{E}_r$ | 0.00127 | 0.00393 | 0.00119 | 0.00216 | 0.00120 | 0.00312 | 0.00142 | 0.00109 | 0.00153 |

Table 1: the average $\mathcal{E}_r$ and its standard deviation (SD) are described through time up to 3 significant figures, to determine the accuracy of the factorisation approximation, using the Pechukas model for a two qubit system.

The verdict is that the factorisation approximation does not hold for a two qubit system due to the interaction term. We note that $\mathcal{E}_r$'s standard deviation remains below 0.005 throughout the evolution of the adiabatic parameter. We observe, anomalous averaged relative errors as in the cases for $\lambda$ being 0.2 ,0.4 and 0.6 that which do not fall in the range of the analytic bounds determined from Eq. (4.38). This is a result of the sample being taken from 100 trials. However $\mathcal{E}_r$ follows the prediction of Eq. (4.29) with $\mathcal{E}_r$ expected to be 1 for a two qubit system whereas Eq. (4.38) suggests an exponential growth in the upper

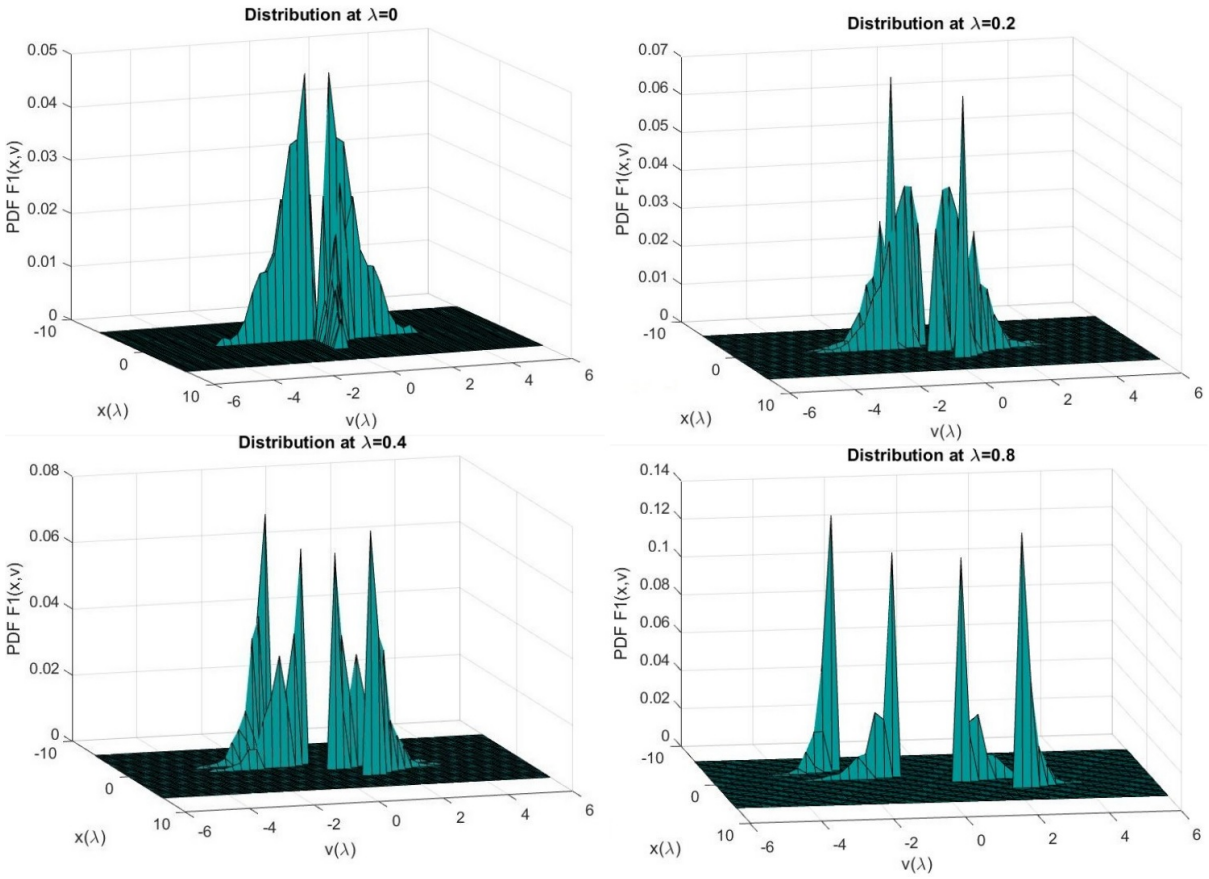


Figure 4.2: One-particle distributions: this gives the evolution of $F_{1,0}(x_1,\ v_1)$ as the time parameter increases, clearly it is seen that it is initially Gaussian distributed about a single peak however as time increases, it settles into 4 equally distributed peaks due to the large perturbation as expected. The velocities here are deterministic, as such the distribution is centred around the four velocity points.

bound for a two qubit system with a minimum of $\frac{1}{2}$. This is a consequence of the system having its eigenvalues determining $x_n$ and, in turn, both $v_n$ and $l_{mn}$ being related through the coupling constant $J$. The influence of $J$ reduces significantly as $N$ grows. Though the factorisation approximation has not been numerically tested for large $N$, we have shown that $\mathcal{E}_r$ scales as $1/N$, suggesting that it is possible to reduce the BBGKY chain to a factorisation of $F_{1,0}\left(x_1,\ v_1\right)$ distributions. We leave the numerical demonstration of this for future work as it is beyond the scope of the present analytical study. We note that in the $z$ basis, for large $\lambda$ the $J$ terms are negligible where the two qubit Ising model could be completely decoupled as such we would expect the factorisation approximation to hold, however in the basis used in this investigation, we do not make such observations.

Using this approach, we have determined the statistical level dynamics of a general nonequillibrum system through the Pechukas equations. In the realms of AQC, level crossings of the system result in state transfer, resulting in decoherence in the system. We explore these further in the following section.

## 4.4 Summary

Using the BBGKY hierarchy in the Pechukas formalism to develop a set of coupled kinetic equations of motion, one can investigate the level dynamics of a quantum perturbed system, statistically. This extends the kinetic equations concerning the level dynamics to parametrically driven evolution of a quantum system which is especially convenient for the investigation of adiabatically evolving systems however the formalism is not strictly adiabatic and is applicable to a general system of parametric time evolution with arbitrary time dependence in $\lambda$.

In extension, a factorisation approximation is constructed such that the $s$-particle reduced probability distribution functions can be constructed from a product of $s$ one-particle distributions. This approximation is motivated by the fact that the coordinates in the Pechukas equations are independent and so may lead to effectively independent probability distribution functions, reducing the many body systems to that of a one-body system. This is a great simplification as it amounts to solving the BBGKY hierarchy by solving just the one-body system. All the information of the level dynamics can be determined from the one-particle distribution functions. To test the factorisation approximation, we analytically considered the way the factorisations vary from the many particle probability distribution functions giving an effective mean field theory approximation. We find that the relative error $\epsilon_r$ decays asymptotically as $\mathcal{O}(1/N)$ as the number of the interacting particles tend to infinity. This gives confidence that for systems with large number of particle interactions,

the approximation holds.

To illustrate the theory, we consider the simplest possible system of two qubits, and compared it with the exact solution of the Hamiltonian. Breaking the BBGKY hierarchy at its first chain, we built the related $s$-particle distributions, where we found that the factorisation approximation is not accurate due to coupling between the eigenvalues where the energy levels are not mutually independent for any given $\lambda$.

This research has significance to the study occupation dynamics at eigenvalue crossings and avoided crossings with current relevance to a range of applications, two directly related realms would be AQC and photonic systems, both of which carry great prospect.

# Chapter 5

# Evolution of Quantum States

In this chapter, we study how the evolution of the eigenvalues provides useful information on the evolution of the energy gap and the distribution of avoided crossings. Using the Pechukas-Yukawa model, we connect the level dynamics of a system to the quantum states through the evolution of eigenstate coefficients,$C(t)$ for a wavefunction expanded in the instantaneous eigenstates. The advantage under this description for a quantum coherent system is that the instantaneous eigenstates include all higher level entanglements.

One can extend this description from eigenvalue dynamics to determine the form of the density matrices. This provides insight in the dynamics of occupation numbers and the coherences in the system which will prove useful in determining the probability for the system to remain in its initial state. Using this description, one can, for example, determine the effects of avoided level crossings on the systems evolution and the extent to which the noise affects the population of states. Our work here extends the standard Pechukas-Yukawa model from the statistical mechanics of energy levels to the description of quantum states themselves. It is worth stressing that these works build a general scheme applicable to the investigation of AQC, however, they are not restricted to AQC.

To proceed we use a Magnus series expansion to approximate $C(t)$, a convenient way to obtain an asymptotic expansion. This approach is contrasted against both the adiabatic approximation and the time dependent perturbation theory (TDPT). We determine the coefficients of the eigenstates to compare how well these approximations accommodate adiabatic parameters [33, 34]. Using the Magnus series, $C(t)$ can be approximated by a cumulant expansion to re-sum the TDPT, in powers of $\dot{\lambda} = d\lambda/dt$, with respect to the adiabaticity. Each term of the expansion corresponds to a sum of an infinite number of terms in a direct expansion of the density matrix. Given the Magnus series converges, the cumulant expansion provides a source of improved efficiency in the result. This is important to study the adiabatic invariants of the system. Knowledge of this could yield important features of the

behaviour of an AQC. This description may provide useful analytics to study sources of decoherence in highly entangled systems using the eigenvalue expansion coefficients. Moreover this can be used to investigate dissipative influences on occupation numbers and coherences which can be extended to study the effects of multi-level Landau-Zener transitions. Furthermore, our analysis shows that the convergence of the Magnus series approximating the evolution of $C(t)$ is governed by the initial conditions. This could provide better insight into what measurable characteristics of a system can be used as a criterion for its quantum performance. Additionally, this carries the potential to specify Hamiltonians of different complexity classes, governed by the initial conditions in the PechukasYukawa formalism. It may be possible to extend the argument to stoquastic (stochastic quantum) systems where noise is added; this may prove crucial experimentally.

This chapter is as follows: we provide a derivation of the evolution of the occupation eigenstate coefficients under the Pechukas-Yukawa formalism which forms the main results of this chapter. This is followed with approximations to solve for the eigenstate coefficients both analytically and numerically. Analytically, we consider the Magnus series approximation that we develop to study the evolution of the perturbed quantum system. The Magnus series is compared numerically against two other approximations; the adiabatic approximation and the time dependent perturbation theory (TDPT), investigating its limitations. These results are numerically tested by use of an example, determining the occupation dynamics numerically for the exact cover 3 NP-complete problem.

## 5.1 Derivation of the Evolution of Occupation Eigenstate Coefficients

In this section, we establish the relationship between the occupation numbers and the level dynamics through the Pechukas model. Recall that a wave function on a Hilbert space can be expressed as the sum of linear combination of eigenstates that is:

$$|\psi(t)\rangle = \sum_n C_n(t)|n(t)\rangle. \tag{5.1}$$

For eigenstate coefficients for each fixed instant in time $C_n(t) \in \mathbb{C}$ , related to the occupation numbers (the number of states at energy level $n$) $N_n$ by the following:

$$|C_n(t)|^2 = N_n. \tag{5.2}$$

The evolution of $C_n$ associated to the eigenvalues of the state is obtained by:

$$\mathcal{H}(t)|\psi(t)\rangle = i\frac{\partial}{\partial t}|\psi\rangle = i\frac{\partial}{\partial t}\sum_n C_n(t)|n(t)\rangle = \sum_n E_n(t)|\psi(t)\rangle. \tag{5.3}$$

Here $E_m(t)$ denotes the eigenvalues of the system for state $|m(t)\rangle$. Taking time derivative: $\dot{.} = \frac{\partial}{\partial t}$ using Leibniz rule, we obtain:

$$i\frac{\partial|\psi\rangle}{\partial t} = i\sum_n \dot{C}_n(t)|n(t)\rangle + C_n(t)|\dot{n}(t)\rangle = \sum_n C_n(t)E_n(t)|n(t)\rangle. \tag{5.4}$$

Applying $\langle m(t)|$ on both sides and through linearity we obtain the dynamics of these coefficients through time with regards to the eigenvalues of the state,

$$i\sum_n \dot{C}_n(t)\delta_{mn} + \langle m(t)|C_n(t)|\dot{n}(t)\rangle = \sum_n C_n(t)E_n(t)\delta_{mn}. \tag{5.5}$$

Hence by evaluating the $\delta$-distributions and rearranging the expression we have the following:

$$i\dot{C_m}(t) - C_m(t)E_m = -i\sum_{n\neq m} C_n(t)\langle m(t)|\frac{\partial}{\partial\lambda}|n(t)\rangle\dot{\lambda}, \tag{5.6}$$

where $E_m(t)$ are the eigenvalues of the system and $\langle m(t)|$ and $|n(t)\rangle$ denote the eigenstates. In order to evaluate the dynamics with respect to the level dynamics, it is necessary to determine $\sum_n iC_n(t)\langle m(t)|\frac{\partial}{\partial\lambda}|n\,(t)\rangle\dot{\lambda}$ where the term vanishes for $m(t) = n(t)$. We adopt the Pechukas-Yukawa model in order to express the evolution of $C_n(t)$ in terms of variables describing level dynamics. The evolution of $\langle m(t)\,\big|\frac{\partial}{\partial\lambda}\big|\,n(t)\rangle$ is determined from the following argument:

$$\frac{\partial}{\partial\lambda}E_n(t)|n(t)\rangle \;=\; \frac{\partial}{\partial\lambda}\mathcal{H}(t)|n(t)\rangle. \tag{5.7}$$

Applying Leibniz rule on both sides we obtain the following:

$$E_n(t)(\frac{\partial}{\partial\lambda}|n(t)\rangle) + |n(t)\rangle(\frac{\partial}{\partial\lambda}E_n(t)) = V(t)|n(t)\rangle + H(t)\frac{\partial}{\partial\lambda}|n(t)\rangle,$$

where $V(t)$ represents the potential. We act on both sides with $\langle m(t)|$ and through linearity such that $m \neq n$, we find that the dynamics reads:

$$E_n(t)\langle m(t)|\frac{\partial}{\partial\lambda}|n(t)\rangle = \langle m(t)|V(t)|n(t)\rangle + E_m(t)\langle m(t)|\frac{\partial}{\partial\lambda}|n(t)\rangle. \tag{5.8}$$

Hence,

$$(E_n(t) - E_m(t))\langle m(t)|\frac{\partial}{\partial\lambda}|n(t)\rangle = \langle m(t)|V(t)|n(t)\rangle. \tag{5.9}$$

By applying the Pechukas equations, for determining $l_{mn}$ described in Eq. (3.10), giving $\langle m(t)|V(T)|n(t)\rangle = \frac{l_{mn}}{E_m - E_n}$, we are able to determine the evolution of $\langle m(t)\left|\frac{\partial}{\partial\lambda}\right|n(t)\rangle$ entirely using level dynamics:

$$(x_n - x_m)\langle m(t)|\frac{\partial}{\partial\lambda}|n(t)\rangle \ = \frac{l_{mn}}{x_m - x_n}. \tag{5.10}$$

Thus,

$$\langle m(t)|\frac{\partial}{\partial\lambda}|n(t)\rangle = \frac{-l_{mn}}{(x_m - x_n)^2}. \tag{5.11}$$

Substituting Eq. (5.11) into Eq. (5.6) the dynamics of the occupation numbers are given through the following relation, which provides us with the main result of this chapter:

$$i\dot{C_m}(t) - C_m x_m = i\dot{\lambda}\sum_{n\neq m} C_n \frac{l_{mn}}{(x_m - x_n)^2}. \tag{5.12}$$

This describes the wavefunction in its entirety at any given time. We established the relationship between the occupation numbers and the level dynamics through the Pechukas-Yukawa model, given by Eq. (5.12). For the simplified case that $\dot{\lambda} = 0$, we solve this ordinary differential equation to find that $C_m(t) = C_m(0)e^{-i\int_0^t x_m(s)ds}$, describing an adiabatically evolving system. We consider the case that Eq. (5.12) is inhomogeneous.
We denote:

$$X = \mathrm{diag}\,(x_1 \dots x_n)\,,$$

$P = p_{mn}$, where $p_{mn} = \frac{l_{mn}}{(x_m - x_n)^2}$ and $p_{mm} = 0$,

$C(t) = (C_1(t) \dots C_n(t))^T$.

Here $X$ is diagonal and $P$ is skew-Hermitian as $l_{mn} = -l^*_{nm}$, thus diagonalisable. Then Eq (5.12) can be written as the following:

$$i\frac{\partial}{\partial t}C(t) = A(t)C(t). \tag{5.13}$$

where $A = (iX + \dot{\lambda}(t)P)$ does not commute with itself at different time instances.

## 5.2 Approximating the Evolution of the Eigenstate Coefficients

In the present work, we investigate approximate methods to solve for $C(t)$, from which the occupation numbers are obtained. Using the Peano-Baker series[35] (PBS) we find that the solution comes in the form:

$$\mathrm{C(t;t_0)}=\mathbf{1}+\sum_{n=1}^{\infty}\mathcal{I}_n(t), \tag{5.14}$$

where $t_0$ is the initial time and $\mathcal{I}_n$ is expressed as the following:

$$\mathcal{I}_\mathrm{n}(\mathrm{t}) := \int_{t_0}^{t} A(\tau_1) \int_{t_0}^{\tau_1} A(\tau_2) \cdots \int_{t_0}^{\tau_{n-1}} A(\tau_n) d\tau_n \dots d\tau_1. \tag{5.15}$$

We are interested in a nonzero constant $\dot{\lambda}$ such that the adiabatic parameter evolves slow enough that the system is not excited from its eigenstate. In the case $A(t)$ commutes with itself at each instant in time, we may use classic linear algebra to determine $C_n(t)$ at each instance through the following relation:

$$C(t) = e^{-i\int_0^t A(s)ds} C_0. \tag{5.16}$$

This expression holds only for the case that $A\,(t)$ can be approximated as constant. Using PBS, we demonstrate that a solution exists for a general $\dot{\lambda}(t)$, however obtaining an explicit

form to determine $C_n(t)$ at each instant is much more complicated. Instead, it is useful to consider an alternative approximation.

## 5.3 Discretising the Evolution of Eigenstate Coefficients

Treating Eq. (5.13) as constant at each instant in time, we model the system through step functions such that $X, P$ and $\dot{\lambda}$ are constant at each instant time. This discretises the system, essentially building a piecewise constant approximation such that the solution is of the following form, where $0 < t_0 < t_1 < \cdots < t_I$:

$$C(t) = e^{(t-t_I)(-iX_I - \dot{\lambda}(t_I)P_I)} \ldots e^{(t_2-t_1)(-iX_1-\dot{\lambda}(t_1)P_1} e^{t_1(-iX_0-\dot{\lambda}(t_0)P_0)} C_0, \tag{5.17}$$

where $X_i$ and $P_i$ represent matrices $X(\lambda(t))$ and $P(\lambda(t))$ at time step $i$. Note, these matrices do not depend explicitly on time but rather implicitly through $\lambda(t)$. $C_0$ denotes the initial condition of the eigenstate coefficient.

Numerically choosing $\delta t = \frac{T}{N}$, small such that the approximation is close, we model the eigenstate expansion coefficients. This is used as our true value of the solution such that further approximations are compared against this model to determine their accuracy.

This method is tractable numerically, providing a close characterisation of the eigenstate coefficients for small $\delta t$, however it does not provide information related to the influence of $\dot{\lambda}(t)$ on the evolution of $C(t)$. Using the discretised solution of Eq. (5.13), we contrast against the time dependent perturbation theory, the adiabatic approximation and the Magnus series truncated at different orders of $\lambda(t)$ to calculate the relative error. This allows us to evaluate the accuracy of the adiabatic theorem against the other approximations to verify whether the non-adiabatic contributions are negligible.

## 5.4 Standard Eigenstate Coefficient Approximations

The adiabatic approximation assumes the rate of evolution in the perturbation of a system is sufficiently slow such that $\dot{\lambda} \to 0$ in Eq. (3.9), having negligible influence on the evolution of eigenstate coefficients. Then the solution to Eq. (5.13) is simply given as:

$$C(t) = e^{-i\int_0^t X(s)ds} C_0. \tag{5.18}$$

This corresponds to a first order correction to the standard TDPT expansion. In our

research, we determined higher order contributions in $C_n(t)$ to contrast accuracies against the adiabatic theorem.

TDPT uses an iterative procedure to construct an expansion of the eigenstate coefficients. Approximated up to the $n^{th}$ excited eigenstate state, the solution to Eq. (5.13) is given as the following infinite sum truncated to $n$:

$$C_n(t) = \sum_{i=0}^{n} C_n^i, \tag{5.19}$$

where $C_n^i$ represent orders in corrections of the eigenstate coefficients $C_n(t)$, of general form as below,

$$C_n^i(t) = \int_0^t (-iX(\lambda(s)) - \dot{\lambda}(s)P(\lambda(s)))C_n^{i-1}(s)ds. \tag{5.20}$$

This offers higher corrections to the eigenstate coefficients than given by the adiabatic approximation. We take up to 10 iterations, compared against the piecewise constant approach to determine its relative error. This allows us to evaluate the the different accuracies between the different approximations, accommodating for non-adiabatic parameters. We further compare against the Magnus series approximation.

## 5.5 Magnus Series Expansion

Like the TDPT, the Magnus series approximation offers a solution for the eigenstate coefficients whilst accounting for non-adiabatic parameters. It is given as a cumulant expansion, in powers of $\dot{\lambda} = d\lambda/dt$, where each term of the expansion corresponds to a sum of an infinite number of terms in a direct expansion of the density matrix.

The Magnus series provides a solution to Eq. (5.13), taking into account the non-commutativity of $A(t)$[36, 37, 38, 39]. We begin by writing $C(t)$ in the form:

$$\begin{aligned} C(t) &= e^{\Omega(t)}C_0, \\ \Omega(t) &= \sum_{k=1}^{\infty} \Omega_k(t), \end{aligned} \tag{5.21}$$

where $C_0 = C(0)$ is the initial conditions for $C(t)$. Here $\Omega_k$ corresponds to the $k^{th}$ order term of the Baker-Campbell-Hausdorff (BCH) formula [36, 39] and is given as integrals of

successive commutators. This can be used to construct an infinite hierarchy of $\dot{\lambda}$ terms from a cumulant expansion, which both improves the efficiency of the series and allows for the study of the adiabatic properties of the system related to $C(t)$. The first two terms of the series for $\Omega_k(t)$ read:

$$\begin{aligned} \Omega_1(t) &= \int_0^t A(s)ds, \\ \Omega_2(t) &= \frac{1}{2}\int_0^t \int_0^s [A(s), A(s')]ds'ds. \end{aligned} \tag{5.22}$$

Since the full Magnus series is not tractable, one resorts to a truncation, approximating the solution. Investigating the asymptotic convergence of this series would be of interest in future research. In our subsequent analysis, we truncate the Magnus series to the $2^{nd}$ order and test it numerically. If the Magnus series converges, the cumulant expansion provides a source of improved efficiency in the result, relevant to studying the adiabatic invariants of the system. Knowledge of this could yield important features of the behaviour of an AQC, improving our understanding of the relationship between control parameters which may significantly affect adiabatic algorithm designs.

### 5.5.1 Convergence of the Magnus series

In the Pechukas model, all information for the Hamiltonian dynamics is encoded in its initial conditions; we translate the conditions for convergence of the full Magnus series in terms of initial conditions. The Magnus series converges if[36, 37, 38, 39]:

$$\int_0^t ||A(s)||ds < \pi. \tag{5.23}$$

Using the triangle inequality and the expression for $A(t)$, it suffices to show that:

$$\int_0^t ||X||ds + \int_0^t \dot{\lambda}(s)||P||ds < \pi. \tag{5.24}$$

Rewriting the $||X||$ integral in Eq. (5.24) in terms of initial conditions $x_n(0), v_n(0), l_{mn}(0)$, we consider the Lax formalism in order to express the Pechukas equations Eq. (3.10) in Lax formalism[20, 40, 41]:

$$\begin{aligned} \dot{X} &= W + [P, X], \\ \dot{W} &= [P, W], \\ \dot{L} &= [P, L], \end{aligned} \tag{5.25}$$

where $P$ is as expressed in Eq. (5.13) and matrices $W$ and $L$ are skew-Hermitian, given by:

$$W = w_{mn} \text{ where } w_{mn} = \frac{l_{mn}}{(x_m - x_n)} \text{ and } w_{mm} = 0,$$

$$L = l_{mn} \text{ and } l_{mm} = 0.$$

As before, $X = \text{diag}\,(x_1 \dots x_n)$ denotes the diagonal matrix of the eigenvalues of the system. $X$ can be transformed, through a unitary transformation to a nondiagonal matrix $Y$ (the reason will become apparent in later in this section), $X = UYU^{-1}$, where $U$ is a matrix of eigenvectors. The matrix $Q$ is defined by:

$$Q = W + \text{diag}\,(v_1 \dots v_n)\,.$$

In Lax formalism, $Y$ is then expressed in terms of the initial conditions[41]:

$$Y(t) = \lambda(t)Q(0) + X(0). \tag{5.26}$$

Time dependence exists solely through the evolution of $\lambda$. Using the unitary transformation of $X$ and Eq. (5.26),

$$||X(t)|| = ||Y(t)|| = \sqrt{Tr(Y^*(t)Y(t))} = \sqrt{||X(0)||^2 + \lambda(t)Tr(X(0)Q(0)) + \lambda^2(t)||Q(0)||^2}. \tag{5.27}$$

Substituting this for the $||X||$ integral in Eq. (5.24). From this we describe the $||X||$ integral by the following:

$$\begin{aligned}&\int_0^t \sqrt{||X(0)||^2 + \lambda(s)Tr(X(0)Q(0)) + \lambda^2(s)||Q(0)||^2}ds \\ &\leq t||X(0)|| + \sqrt{Tr(X(0)Q(0))}\int_0^t \sqrt{\lambda(s)}ds + ||Q(0)||\int_0^t |\lambda(s)|ds.\end{aligned} \tag{5.28}$$

Thereby the convergence of the first integral is reduced solely to the dependence of initial conditions and the time evolution of $\lambda$. This method however, is restricted to finite times such that initial conditions can be set to satisfy Eq. (5.24). As $t \to \infty$, it is not possible to meet this convergence criteria regardless of the restrictions on the initial conditions.

Similarly, for $||P||$, using that the square root of a sum is less than the sum of the square roots and interchanging the sum and integral using Tonelli's theorem, we can rewrite the second integral in Eq. (5.24):

$$\int_0^t \dot{\lambda}(s)||P||ds \leq \sum_{m\neq n}\int_0^t \dot{\lambda}(s)p_{mn}ds. \tag{5.29}$$

Taylor expanding around the initial time for short time intervals, $p_{mn}$ is expressed in terms of initial conditions, $p_{mn} = p_{mn}(0) + \delta\lambda(s)\dot{p}_{mn}(0)$ (using our definition of $p_{mn}$ from before) where $\delta\lambda(s) = (\lambda(s) - \lambda(0))$. Then Eq. (5.29) becomes:

$$\int_0^t \dot{\lambda}(s)(p_{mn}(0) + \delta\lambda\dot{p}_{mn}(0))ds = \frac{\dot{p}_{mn}(0)}{2}(\lambda^2(t) - \lambda^2(0)) + \delta\lambda(t)(p_{mn}(0) - \lambda(0)\dot{p}_{mn}(0)), \tag{5.30}$$

where $\dot{p}_{mn}$ can be computed entirely from $x_m(0), v_m(0)$ and $l_{mn}(0)$. We conclude that using Eq. (5.24), Eq. (5.28) and Eq. (5.30), the convergence of Magnus series is guaranteed and is expressed entirely through its parametric evolution, $\lambda$ and initial conditions.

A potential source of divergence of the Magnus series involves level crossings; in the case of Landau-Zener transitions, the system is simplified to 2 levels with linear evolution in $\lambda$ hence $\dot{\lambda}$ is constant. We show that level crossings can be disregarded as they have zero measure.

### 5.5.2 Convergence of the Magnus Series: Level Crossings

Level crossings may result in Landau-Zener transitions of the population of states. These occur at a $\lambda^*$, potentially involving multiple levels which is considered separately. Note that

in the $N = 2$ case described by the Landau-Zener model, the system collapses to the Calegro-Sutherland model with constant $l_{mn}$ terms. We show in this section that level crossings due to the symmetries of the Hamiltonian, have zero measure.

For a level crossing $x_m = x_n$ at $\lambda^*$ , then Eq. (3.10) implies $l_{mn} = 0$ and $\dot{l}_{mn} = 0$. The converse is not necessarily true, that is if $l_{mn} = 0$ does not imply $x_m = x_n$. Expanding both numerator and denominator of $||P||$ about this point with $\delta\lambda^* = (\lambda - \lambda^*)$, we obtain the following expression for the upper bound on Eq. (5.29):

$$\sum_{m\neq n}^{N} \frac{|l_{mn}(\lambda^*) + \delta\lambda \dot{l}_{mn}(\lambda^*) + \frac{1}{2}\delta\lambda^2 \ddot{l}_{mn}|}{(x_m(\lambda^*) - x_n(\lambda^*))^2 + 2\delta\lambda(x_m(\lambda^*) - x_n(\lambda^*))(v_m(\lambda^*) - v_n(\lambda^*)) + \delta\lambda^2(v_m(\lambda^*) - v_n(\lambda^*))^2} + \mathcal{O}(\lambda^3), \tag{5.31}$$

where $\ddot{l}_{mn}$ is given by $\sum_{k\neq m,n}^{N} \frac{-2l_{mk}l_{kn}(v_m - v_n)}{(x_m - x_k)^3}$. Cancelling zero valued terms and substituting $\ddot{l}_{mn}$ into Eq. (5.31),

$$\frac{|l_{mn}|}{(x_m - x_n)^2} = \sum_{k\neq m,n}^{N} \frac{|l_{mk}l_{kn} + \mathcal{O}(\lambda^3)|}{(x_m - x_k)^3(v_m - v_n) + \mathcal{O}(\lambda^3)}\bigg|_{\lambda^*}. \tag{5.32}$$

This series diverges in two scenarios, case 1: degenerate level crossings: $x_k = x_m = x_n$ for some $k$, which again by Eq. (3.10) gives $l_{mn}, l_{mk}, l_{nk}$ vanishes and case 2: that $v_m = v_n$ describing a system where levels coalesce. For case 1, as both numerator and denominator are zero, warrants the application of l'Hopital's rule on Eq. (5.32). At its third iteration, we obtain:

$$\frac{|l_{mn}|}{(x_m - x_n)^2} = \sum_{k\neq m,n} \frac{0 + \mathcal{O}(\lambda^3)}{6(v_m - v_n)(v_m - v_k)^3 + \mathcal{O}(\lambda^3)}. \tag{5.33}$$

The expression converges to zero at the critical point $\lambda^*$, implying that degenerate level crossing do not cause Eq. (5.32) to diverge.

Exploring case 2, we use the interpretation of the Pechukas equations as describing a 1D gas. As $\lambda$ approaches $\lambda^*$; $\lambda^- = \lambda^* - \epsilon$ and without loss of generality $x_m^- > x_n^-$, it is clear that $v_m = \lim_{\epsilon\to 0} \frac{x_m - x_m^-}{\epsilon}$ hence $(v_m - v_n) \approx \frac{(x_m^- - x_n^-)}{\epsilon}$ greater than 0 by assumption. By symmetry, this argument holds for $x_n^- > x_m^-$. In the case $v_m = v_n$, at $\lambda^*$ we consider the difference between acceleration terms given by the following:

$$\frac{(\dot{v}_m - \dot{v}_n)}{2} = \sum_{k \neq m,n}^{N} \left( \frac{|l_{mk}|^2}{(x_m - x_k)^3} - \frac{|l_{nk}|^2}{(x_n - x_k)^3} \right) + \frac{|l_{mn}|^2 + |l_{nm}|^2}{(x_m - x_n)^3}. \tag{5.34}$$

The latter term corresponding to the level crossing, tends to 0 as $\lambda \to \lambda^*$ as determined by the application of l'Hopital's rule three times, however the terms in the sum are non-zero, describing acceleration between the levels at $\lambda^*$, modelling repulsion such that levels do not coalesce. This shows that level crossings occur only for an instant $\lambda^*$ rather than an interval, as such they do not contribute to Eq. (5.29) as they have zero measure.

From these expressions, one can determine (from the initial conditions encoding the evolution of the system) when the convergence criterion outlined in Eq. (5.24) are met.

## 5.6 Numerically Comparing the Magnus Series Against the Adiabatic Approximation and TDPT

We compare numerically the Magnus series (up to its second order) against the adiabatic approximation, treating $\dot{\lambda}$ as negligible. Under the adiabatic approximation, $C(t) = e^{-i\int_0^t X(s)ds} C_0$. Both these approximations are contrasted against the TDPT expanding $C(t)$ in powers of the interaction. The TDPT is useful for exactly solvable systems with an interaction to its environment described by a small perturbation[42]. Under this description, $C(t) \approx \sum_{i=0}^{\infty} C^i(t)$, where $C^i(t) = \int_0^t A(s)C^{i-1}(s)ds$, represent higher order corrections. These are obtained iteratively for 10 iterations. This solution breaks down for the TDPT when perturbations are large. To avoid this, initial levels are chosen with a minimum spacing of 0.01 and 0.05. This ensures that initial $||P||$ is not large as a consequence of level (avoided) crossings. Levels tend to diverge away from each other as the system evolves, hence $||P||$ decreases with time. However, it is unavoidable that for large $N$ level (avoided) crossings would not occur. This approach is sensitive to the time steps of evolution, requiring that they be small. The TDPT depends on the quantum states $C(t)$; unlike both the Magnus series and the adiabatic approximation, where comparisons are made between matrix propagators in determining relative error.

To compare these methods numerically, we take a piecewise constant approximation. Treating $A$ as constant over sufficiently small time steps, such that the TDPT is applicable, we break the interval of evolution in steps of 0.01. This approximation numerically converges to the true solution. This explicit solution is given by:

$$C(t) = \prod_{i=0} e^{(t_i - t_{i-1})A_i} C_0, \tag{5.35}$$

where $0 \leq t_0 < t_1 < \cdots \leq t$ and $A_i$ is constant on interval $[t_{i-1}, t_i]$.

We investigate different classes of Hamiltonians, each parameterised by their initial conditions $H(\lambda(t); x^0, v^0, l^0)$ with $x^0, v^0$ and $l^0$ describing the initial time level dynamics, governed by functions of $\lambda$(t): 1) linear $\lambda(t) = 10^{-3}t$, 2) cubic $\lambda(t) = 10^{-3}(t^3 + t^2 + t)$ and 3) exponential decay; $\lambda(t) = 10^{-3}e^{-t}$. In accordance to Eq. (5.28) and Eq. (5.30), the upper bound on the convergence criterion of the Magnus series grows as $\mathcal{O}(t^2)$ for linear functions of $\lambda$, $\mathcal{O}(t^6)$ for the cubic function and $\mathcal{O}(t)$ for the exponential decay. This suggests the convergences are expected to hold longest for an exponential decay. Under the same initial conditions, these different $\lambda$ yield the same level dynamics. Fig. 5.1 depicts the level dynamics for a linear function of $\lambda$.

We use the Euler method with random initial conditions uniformly distributed over a ball of radius $\frac{\pi}{6}$ to evolve the general Pechukas-Yukawa equations Eq. (3.10), such that the conditions outlined in Eq. (5.24) are met for 0-1 in steps of 0.01 for 1000 simulations to average over the random initial conditions for $x, v, l$. We evolve the dynamics up to $t = 100$, without amending initial conditions in order to observe the limitations of the Magnus series. We compare the logarithm of the relative errors between the piecewise constant approach given by Eq. (5.35). The average relative error (R.E.), at each time step per simulation is given by:

$$R.E. = \frac{1}{1000} \sum_{i=1}^{1000} \frac{||\tilde{C}[i] - C_{PC}[i]||}{||C_{PC}[i]||}, \tag{5.36}$$

where $\tilde{C}[i]$ describes the approximation of $C(t)$ and $C_{PC}[i]$ the piecewise constant solution at time step $i$. Taking the norm provides a real valued relative error to plot against time. We take $N = 2, 4, 8$ excited states for an initial minimum level spacing of 0.01 and $N = 2, 4, 5$ excited states for 0.05 to check the effectiveness of the methods as the dimensionality increases. Note that for a radius of $\frac{\pi}{6}$ for the distribution of initial conditions, it is not possible for a minimum level spacing of 0.05 beyond $N = 5$. Comparative results are given in Figs. 5.2, 5.3 and 5.4 for minimum initial level spacing 0.01 and 0.05. These detail the growth of the logarithmic relative errors with time between the approximations, for each function of $\lambda$.

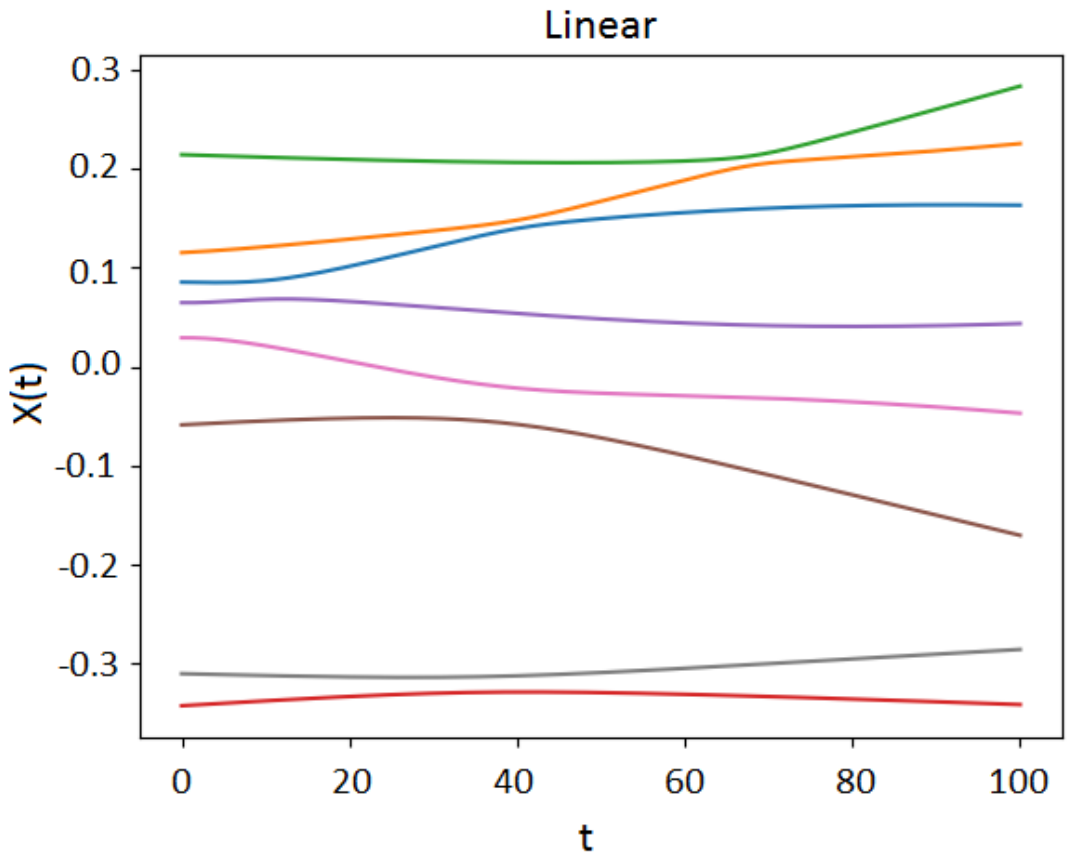


Figure 5.1: The time evolution of an 8 level system under the Pechukas-Yukawa model, for $t \in [0, 100]$. Levels are initially Gaussian distributed with al minimum spacing of 0.05. The dynamics is encoded in the initial conditions, governed by $\lambda$ being the linear function of time. Different $\lambda$ correspond to different nonlinear stretchings in the dynamics against time. Given the inital conditions are the same, the dynamics are the same. We observe multiple avoided crossings between the different levels during their dynamics. We note that the levels are seen to be moving away from each other as time evolves.

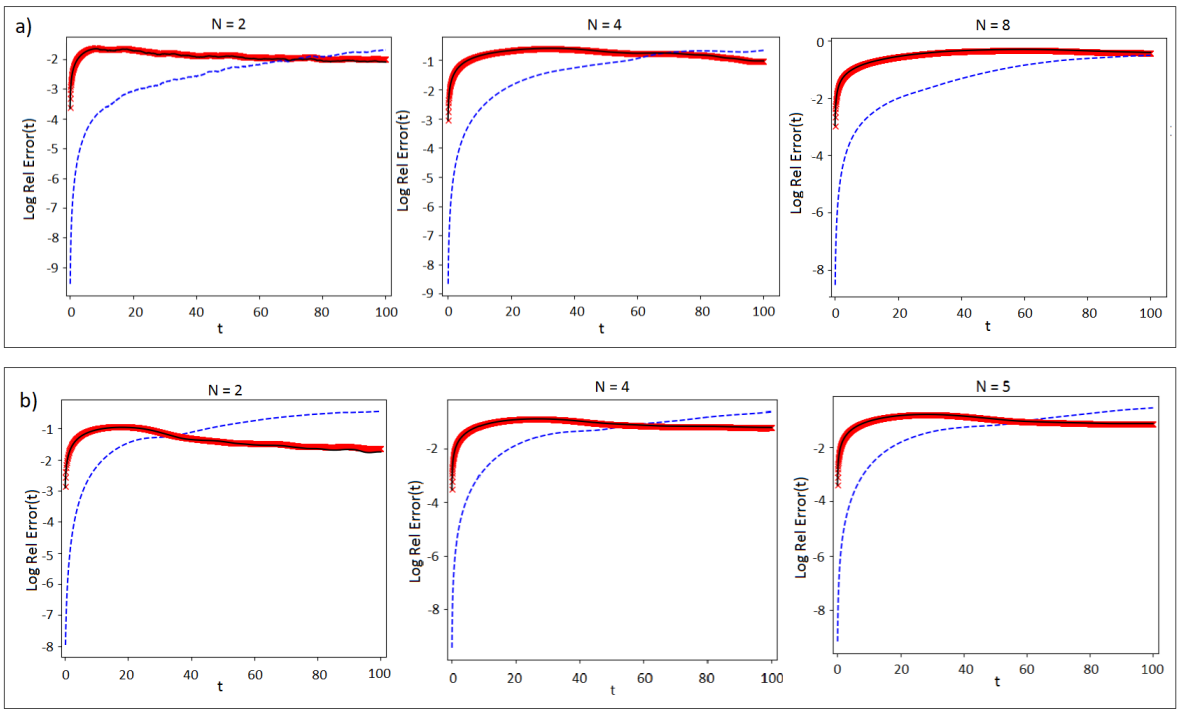


Figure 5.2: **(a)** The logarithmic relative error (R.E.) between the piecewise constant approach and the Magnus series (dashed blue line), the adiabatic approximation (solid black line) and the TDPT approximation (red crosses) against time for the linear case: $\lambda(t) = 10^{-3}t$. These errors have been investigated for different dimensions; $N = 2, 4$ and 8, with a minimum level spacing of 0.01. The Magnus series best approximates $C(t)$, when $t \leq 60$. The accuracy improves with dimension, a consequence of the increased number of level crossings and anti-crossings which are handled better using the Magnus series. For $N = 8$, the Magnus series best approximates $C(t)$ for $t \leq 100$. This demonstrates that the point of intersection between these R.E.s shift to the right as dimension grows. During the evolution, the R.E.s are bounded by $10^0$ for all approximations through time. The R.E. for the Magnus series increases with time as the system approaches a limit such that the convergence criterion in Eq. (5.23) does not hold. The errors for the adiabatic approximation overlaps with the TDPT. **(b)** Similar to (a) with an initial minimum level spacing of 0.05. These errors have been investigated for dimensions; $N = 2, 4$ and 5. One observes at $N = 2$, the Magnus series best approximates $C(t)$ for $t \leq 40$, again this period increases with dimension, at $N = 5$, reaching $t \leq 50$. This demonstrates that the point of intersection between these R.E.s shift to the right as dimension grows. During the evolution, the R.E.s are bounded by $10^0$ for all approximations. Only for $N = 2$ does the Magnus series approach $10^0$. There is a growth in R.E with time as the system approaches a limit such that the convergence criterion in Eq. (5.23) does not hold. The errors for the adiabatic approximation overlaps with the TDPT, both appear to decrease as time grows large as levels spread further apart, so level crossings and avoided crossings are less frequent. Compared against (a), the periods before the intersection between the Magnus series and the TDPT and adiabatic approximations are shorter as having a larger minimum separation between levels improves the accuracy in both the latter approximations.

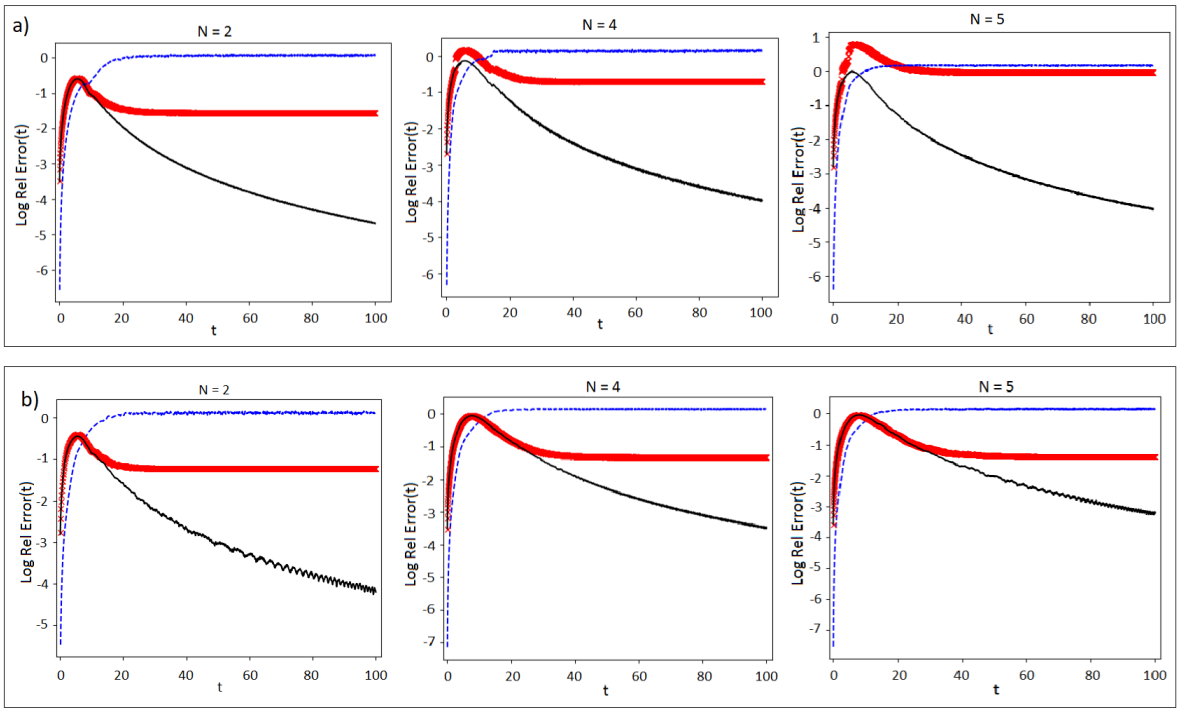


Figure 5.3: **(a)** Same as in Fig. 5.2 (a), averaged over the same initial conditions, for cubic $\lambda(t) = 10^{-3}(t^3+t^2+t)$. The errors have been obtained for $N = 2, 4$ and 5, it was not possible to obtain results for larger $N$ as the approximations broke down. The Magnus series best approximates $C(t)$ when $t \leq 10$, and plateaus at $10^0$, demonstrating a break down in meeting Eq. (5.23) for the Magnus series. This is expected as the cubic function grows faster than all other classes of $\lambda$ considered in this paper. The relative error for TDPT peaks initially and also plateaus at $10^0$, whereas the R.E. for the adiabatic approximation decreases with time as the levels spread further apart in this system, resulting in fewer level crossings and avoided crossings. **(b)** Same as in 5.2 (b), averaged over the same initial conditions, with cubic $\lambda(t) = 10^{-3}(t^3 + t^2 + t)$. The Magnus series best approximates $C(t)$ for $t \leq 10$. This interval is shorter than for all other classes of $\lambda$, as the cubic function grows faster than all other classes of $\lambda$ considered in this paper. The R.E. for the Magnus series plateaus at $10^0$ for all dimensions, demonstrating a break down in meeting Eq. (5.23). One observes the errors for the adiabatic approximation overlaps with the TDPT. One observes the duration in the overlap increases with dimension however, as time increases the adiabatic approximation is most accurate, decreasing with time, whereas the TDPT plateaus at $10^{-1}$. Again, compared against (a), the periods before the intersection between the Magnus series and the TDPT and adiabatic approximations are shorter as having a larger minimum separation between levels improves the accuracy in both the latter approximations.

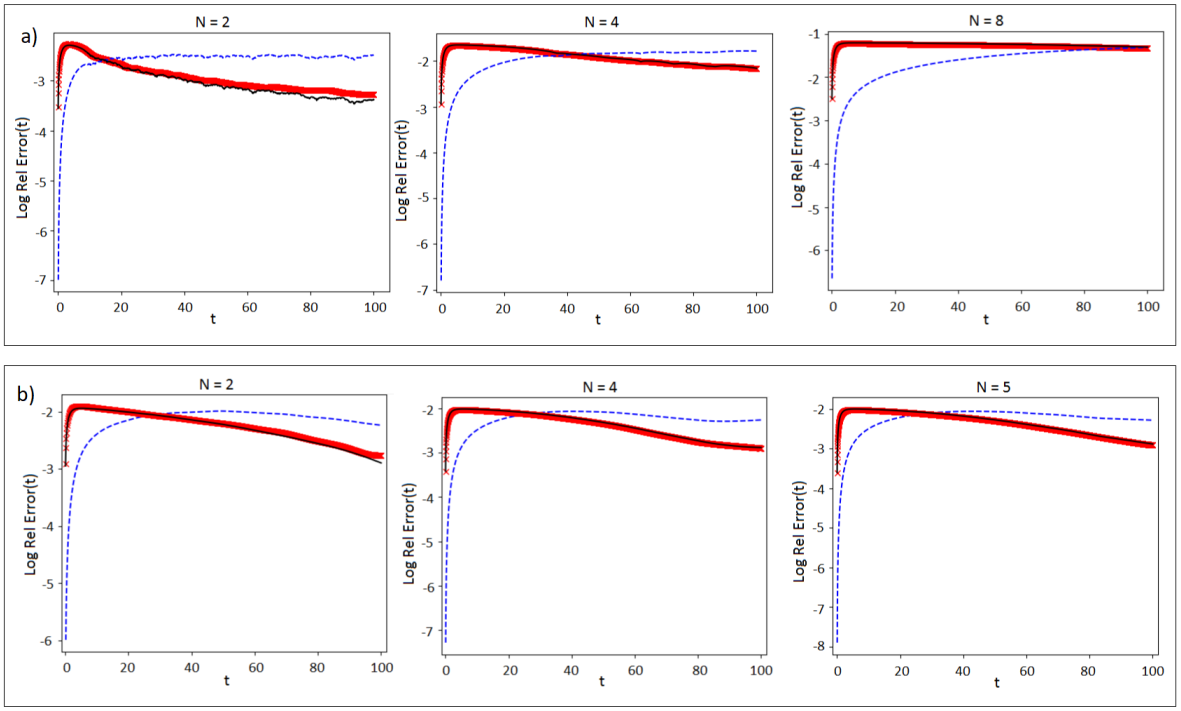


Figure 5.4: Same as in Fig. 5.2 (a), again averaged over the same initial conditions, for exponential decay $\lambda(t) = 10^{-3}e^{-t}$. For $t \leq 10$ and $N = 2$, the Magnus series best approximates $C(t)$. This period increases with dimension, going beyond $t = 100$ for $N = 8$, where the point of intersection between the R.E.s shift to the right as dimension grows. For the exponential decay, the R.E.s for all approximations remain bounded below $10^{-1}$, as time grows large the Magnus series plateaus yet provides accurate results throughout the evolution, demonstrating thus far the Magnus series convergence criterion is met. Again, the errors for the adiabatic approximation overlaps with the TDPT, where their errors plateau below $10^{-1}$. **(b)** Same as in Fig. 5.2 (b), again averaged the same initial conditions, for exponential decay $\lambda(t) = 10^{-3}e^{-t}$. For $t \leq 20$, the Magnus series best approximates $C(t)$. This period increases with dimension, reaching $t \leq 30$ at $N = 5$, where, again the point of intersection between the R.E.s shift to the right as dimension grows. For the exponential decay, the R.E.s for all approximations remains below $10^{-2}$, as time grows large the Magnus series plateaus yet provides accurate results throughout the evolution, demonstrating thus far the Magnus series convergence criterion is met. Again, the errors for the adiabatic approximation overlaps with the TDPT, both seen to decrease as time grows large at the same rate such that beyond $t = 30$, these provide better approximations for $C(t)$ a consequence of the levels moving further apart hence level crossings and avoided crossings are less frequent. Compared against (a), again one observes the periods before the intersection between the Magnus series and the TDPT and adiabatic approximations are shorter as having a larger minimum separation between levels improves the accuracy in both the latter approximations.

We observe for short time intervals, the best approximation for $C(t)$ is the Magnus series. However, as time grows large there is a break down in meeting the convergence criteria Eq. (5.23) for the set initial conditions. Exponential decay is an exception case; the growth of the system is slow enough that the R.E saturates before reaching errors of $10^{-2}$. This provides accurate solutions throughout the evolution. The R.E.s from the adiabatic approximation and the TDPT decrease below the Magnus series R.E. as time grows large, a consequence of the levels becoming further apart resulting in $||P||$ becoming less significant. We note that this weakens the approach. The Magnus series in contrast is well suited to the 'spaghetti regime' where levels are close, a result of the Magnus series being less vulnerable to the effects of level crossings (as shown in Appendix B). This is observed in the general trend, that for larger N where level interactions are more frequent, the Magnus series relative errors overtake the errors for both the adiabatic and TDPT approximations at later times.

## 5.7 Density Matrix Evolution

Using the Pechukas-Yukawa formalism, we obtain an explicit description of both the occupation numbers and coherences of a quantum system continuous through time from the level dynamics. This has great potential for the development of AQC, providing insight on the decoherences of a system, a major challenge faced by AQC. We later extend our investigation to the study of Landau-Zener transitions occurring at level crossings and avoided crossings leading to decoherences. Decoherences arise from a number of various elements intrinsically and from the environment ranging from level crossings and avoided crossings to random dissipative influences from the environment, however the investigation of these various sources are beyond the scope of this paper.

The density matrix is determined from the eigenstate coefficients, $C(t)$:

$$\rho(t) = C(t) \bigotimes C^{*T}(t). \tag{5.37}$$

This provides insight on both the dynamics of occupation numbers (the probability of remaining in a state after level "collisions") and the coherences (interlevel correlations). One gains crucial insights on the decoherence of the system in relation to its initial conditions.

Taking the Magnus series expansion to approximate $C(t)$, one obtains a convenient asymptotic cumulant expansion in powers of $\dot{\lambda}$, improving the efficiency of the result given that the series converges. Each term of the expansion corresponds to a sum of an infinite number of terms in a direct expansion of the density matrix. The convergence of this approx-

imation is governed by the initial conditions and the evolution of $\lambda$ such that these solely characterise the entire system dynamics.

This description is well suited to nonequilibrium systems where levels are close together, described by the "spaghetti" regime. Using this description, one can investigate the effects of level crossings and avoided crossings on the system's evolution and the extent to which these affects the population of states[43].
Under the Magnus series approximation, the occupation numbers are given by,

$$\rho_{mm}(t) = \sum_{n=1}^{N} \left( e^{\int_0^t A(s)ds + \frac{1}{2}\int_0^t \int_0^s [A(s),A(s')]ds'ds} \right)_{mn} \times C_{1n}(0) C_{n1}^{*} \left( e^{\int_0^t A(s)ds + \frac{1}{2}\int_0^t \int_0^s [A(s),A(s')]ds'ds} \right)_{nm}. \tag{5.38}$$

This describes continuously through time, the probability of remaining in the same quantum states as the system evolves. The diagonal elements of the density matrix describe the probability of states remaining in the same state, accounting for the influences of interference on the system. We apply these properties of the Magnus series, comparing against the different approximations for a concrete example.

## 5.8 Occupation Dynamics for the Exact Cover Algorithm: A Variation on 3-Satisfiability

Applying our approach to a concrete example, the exact cover 3-satisfiability problem, we compare the applicability of the different approximations to this problem. We determine the eigenstate coefficients from which one obtains the occupation dynamics crucial to the understanding of sources of decoherences in a quantum system.

The exact cover algorithm, belongs to the class of NP-complete problems[44, 45], first proposed by Knuth[44]. It has since been extended to the AQC setting[1], cast as a variation on 3-satisfiability[1, 10, 45]. The problem is described by a Boolean expression, the intersection of all clauses for a string of $N$ binary variables in a set $S$, constrained by $M$ clauses, each acting on three variables; $y_\alpha, y_\beta$ and $y_\gamma$ with $\alpha, \beta, \gamma \in \mathbb{N}$. The clause is satisfied if and only if one of the three variables takes the value 1 whilst the other two take 0; $y_\alpha + y_\beta + y_\gamma = 1$, described by the clause function such that each violated clause is associated with a fixed energy penalty[45]: $\sum_{Clauses}(y_\alpha + y_\beta + y_\gamma - 1)^2$ used to obtain a solution to the problem. The Hamiltonian describing this problem can be translated to an $M$-qubit problem, given by the following:

$$H = \lambda \sum_{i=1}^{M} \frac{1-\sigma_i^x}{2} + (1-\lambda) \sum_{i<j}^{M} C_{ij}(1-\sigma_i^z)(1-\sigma_j^z), \tag{5.39}$$

where $C_{ij} \in \mathbb{N}$ counts the pairwise occurrence of any two distinct variables in the clauses and $\sigma^x$ and $\sigma^z$ are given by the Pauli spin matrices, translating the description through qubits.

We consider three distinct clauses with $C_{12} = C_{23} = 2$ and $C_{13} = 1$ with an exponential decay function for $\lambda = 10^{-3}e^{-t}$. The energy spectrum is determined by diagonalising Eq. (5.39), giving the eigenvalues. Combined with Eq. (3.10) we determine the evolution of the level dynamics. We note here that the initial conditions do not meet Eq. (5.23). However, as one observes in Figs. 5.2 and 5.4, the Magnus series is robust in that despite the initial conditions having not satisfied the criterion outlined in Eq. (5.23) for in the interval [0, 1], the approximation had accurately provided solutions far beyond this duration. Using this flexibility, we compare the different approximations explored in Sec. 5.6 to obtain the evolution of the eigenstate coefficients, up to $t = 100$ in steps of 0.01 with Gaussian distributed initial conditions, normalised for $C(0)$. We determine the logarithm of the relative errors compared against the piecewise constant approach for each approximation through time in Fig. 5.5.

We observe the Magnus series best approximates the evolution of the eigenstate coefficients throughout the duration, with the error bounded below $10^{-2}$ up to $t \leq 35$. Using the relation $\rho = C(t) \otimes C^{*T}(t)$, where $C^{*T}(t)$ denotes the complex conjugate transpose of $C(t)$, we determine the evolution of the density matrix for this system hence we obtain the dynamics of the occupation numbers, given in Fig. 5.5 (b).

One obtains the evolution of the occupation numbers from diagonalising the density matrices, these describe the probability of remaining in the initial states where the off-diagonal terms describe the dynamics of the coherences, giving the probability of state transitions. Using this description, one can explore various sources of decoherence from stochastic processes as well as Landau-Zener transitions from interactions between the levels and their impact on the population of states.

These investigations on the evolution of eigenstate coefficients could be realised experimentally. For example, consider the experiments by D-Wave One concerning 108 qubits[46]. One could translate their quantum annealed Hamiltonian based on the Ising model to the Pechukas-Yukawa setting using Eq. (3.10); choosing some function of $\lambda(t)$ to satisfy the start and end points of an interval such that it simulates time over $t \in [0, t_f]$[46]. Under this description, one could then approximate the eigenstate coefficients which can then be used to determine the occupation numbers and coherences as the system evolves in time.

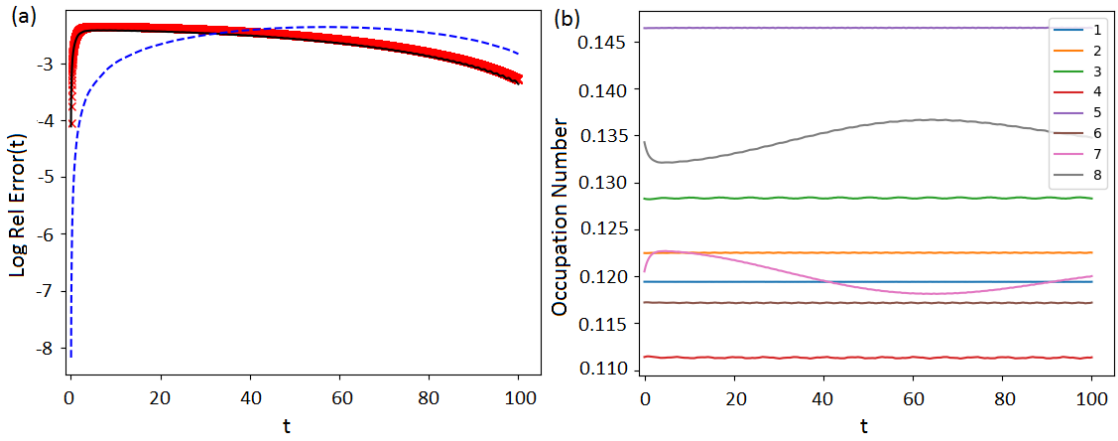


Figure 5.5: **(a)** The logarithm of the relative error against time for the adiabatic approximation (thick crosses), the TDPT (solid line) and the Magnus series approximation (dashed line). One observes the errors throughout the evolution, in all cases are bounded by $10^{-2}$. The adiabatic approximation overlaps with the TDPT, however up to $t \leq 35$, the Magnus series best approximates $C(t)$ providing accurately the dynamics of the eigenstate coefficients. **(b)** The evolution of the occupation numbers of the 3-Satisfiablity qubit system to study the exact cover 3 problem of 8 bits. We observe the presence of an avoided crossing between states 7 and 8, resulting in a reflection in their occupation dynamics, suggesting a transfer in the population of states. In contrast, all other states have remained essentially constant despite a level crossing between states 7, 1 and 2. It would be of interest to determine the dynamics under the influence of noise modelling interactions with the environment.

## 5.9 Summary

In this chapter, we derived the relationship between the evolution of quantum states and level dynamics under the Pechukas-Yukawa formalism. This allows for describing a non-equilibrium, nonstationary quantum system in its entirety via level dynamics and their initial conditions. Solving for the eigenstate coefficients under three different approximation schemes, the adiabatic approximation, TDPT and Magnus series expansion, we compared the suitability of each regime. Determining the convergence criterion for the Magnus series, we determine the theoretical bounds on the approximation. We found the Magnus series held better in a "spaghetti" regime where level crossings and avoided crossings are frequent. Furthermore, the Magnus series admits a cumulant exapansion which could prove insightful in the investigation of adiabatic invariants, which could yield promising in the design of AQC features.

Comparing numerically the different schemes, we show the Magnus series had up to 4 orders of log errors below the adiabatic and TDPT approximation. Moreover, we found the Magnus series accuracy against both the adiabatic and TDPT approximations improved with larger systems. This can be attributed to the fact that Magnus series is well suited to level crossings and avoided crossings which become more frequent for larger systems whereas the TDPT is prone to divergences as a result. We also found that the TDPT adds no improved accuracy than the adiabatic approximation.

Finally, we discuss the evolution of the density matrix in the Pechukas-Yukawa formalism, describing the entirety of the quantum system via level dynamics. Using this description, one can study sources of decoherence on quantum systems via occupation numbers and coherences. Under this formalism, we determine the evolution of the occupation numbers for the 3-Satisfiability exact cover algorithm using these three approximations. Despite the initial conditions not meeting the convergence criterion for the Magnus series, it was shown that the logarithm of the relative error for Magnus series was 4 orders less than the adiabatic approximation and TDPT expansion, demonstrating the robustness of the Magnus series.

This description of occupation numbers through level dynamics, related directly with Landau-Zener transitions. In extension to our description of occupation numbers, we verify the description of Landau-Zener transitions in the Pechukas-Yukawa formalism for level dynamics.

# Chapter 6

# Investigating the Landau-Zener Tunnelling Model via Eigenvalue Dynamics

Quantum systems experience decoherence from both intrinsic interactions as well as random fluctuations from the environment. We investigate the influence of noise on the dynamics of an adiabatic quantum computer using the Pechukas-Yukawa formalism. Under this description, the level dynamics of a parametrically perturbed quantum Hamiltonian are mapped to the dynamics of 1D classical gas.

We develop the Landau-Zener model in the Pechukas-Yukawa formalism to gain insight on the effects of random fluctuations on the evolution of quantum states. It is well equipped for the description of a non-equilibrium interacting system of highly entangled states and especially for the understanding of the dynamics of a system and its vulnerability to decoherence. Under the this formalism, we investigate the compatibility of the Landau-Zener model through determining the requirements in the Pechukas-Yukawa formalism for the conditions necessary for the Landau-Zener model to be applicable. We further explore the impact of Brownian noise on these requirements. Under these conditions, we explore the behaviour of levels approaching the point of minimum distance under the influence of noise. We aim at developing basic elements of such an approach, which would seem especially useful for, but not necessarily restricted to, modelling adiabatic quantum computers.

As discussed earlier, decoherence is one of the key challenges in AQC. This could be investigated using the Landau-Zener transition model, detailing changes in the occupation umbers of quantum states as a consequence the non-adiabatic population transfer at level crossings and avoided crossings in perturbed Hamiltonian systems or quantum phase transitions. These describe fundamental results of nonstationary quantum mechanics. The

Landau-Zener model has been extended to stoquastic systems. This details the probabilities of state transitions under random environmental influences, which may additionally lead to decoherence in the system.

### 6.0.1 Landau-Zener Transitions

Landau-Zener transitions occur at level crossings or avoided crossings, where they reach minimum separation at a $\lambda^*$ and repel. They can occur degenerately and these cases are considered separately. The Pechukas equations, Eq. (3.10) are well equipped to describe level crossings and avoided crossings in a system. In the deterministic case, level crossings occur when $x_m(\lambda^*) = x_n(\lambda^*)$ describing degeneracies[47, 48, 49], as a result $l_{mn}(\lambda^*) = 0$ at some level crossing at $\lambda^*$ (converse is not necessarily true[3, 4, 9]). Avoided crossings arise when levels approach a minimum non-zero distance before repelling.

The conditions to apply the Landau-Zener transition model to a time-dependent Hamiltonian are based on meeting the following simplifications. 1) The energy separation is a linear function of time: $x_m - x_n = \alpha t$ where $\alpha$ is a constant. 2) The perturbation parameter, $\lambda$ is a linear function of time. 3) The perturbation takes a $\frac{1}{r}$ potential with radius $r$. The standard approach to model the interactions assumes all other level interactions are negligible. This comes from the assumption that level crossings are locally more dominant than all other interactions during this period, reducing the system to 2 interacting levels at any time. Multi-level crossings are rare occurrences, their statistical significance is negligible.

Avoided crossings are parameterised by the size of the gap at closest approach and the asymptotic slope of the curves[49, 50, 51]. For an isolated avoided crossing, the energy levels take hyperbolic form: $x^{\pm}(\lambda) = x(\lambda^*) + B(\lambda - \lambda^*) \pm \frac{1}{2}(\Delta_{min}^2 + A^2(\lambda - \lambda^*))^{\frac{1}{2}}$ with $\Delta_{min}$ denoting the minimum gap size, $B(\lambda - \lambda^*)$ and $A(\lambda - \lambda^*)$ respectively describing the mean and the difference in the asymptotic slopes[49, 50].

The Landau-Zener model is used to describe these interactions through a statistical distribution of gap sizes, governing the rate of excitation due to non-adiabatic population transfers. This gives the probability to remain in its initial state after a level crossing or avoided crossing. The non-adiabatic transition probability is given by the following probability distribution, $P_{LZ}$[3, 52]:

$$P_{LZ} = e^{-\frac{\Delta_{min}^2}{4\pi|\langle m|ZH_b|n\rangle|\dot{\lambda}}}. \tag{6.1}$$

This provides a useful description for avoided crossings in a system independent of external noise. Given the outlined Landau-Zener conditions are satisfied, the transition time is $\tau_{LZ} =$

$\frac{\Delta_{min}}{\dot{\lambda}}$, defined by the interval in time the levels interact in a small neighbourhood of each other which we denote by $\gamma$, (for a level crossing this interaction is instantaneous)[47, 49, 53, 54, 55]. Under the Pechukas-Yukawa formalism, one can determine from the initial conditions whether a system will exhibit quantum phase transitions. This allows for the investigation of "quantum phase transition friendly" initial conditions. Additionally, this could be used to provide insight on the effects of quantum phase transitions. It was suggested[56] that one can expect quantum phase transitions to occur if there is a fast initial compression of the whole spectrum, leading to sharp scatterings, however this investigation is beyond the scope of our current work. In the setting of bosonic systems, this compares with the works by Gangardt in [57] where it was shown for coupling strengths in the interval (1, 2) the system can be described as a quasi-super-solid where the potential energies are of the same order as the kinetic energies. The coupling constant in our system is given by the golden ratio.

## 6.1 The Landau-Zener Model in the Pechukas-Yukawa Formalism

To ensure compatibility between the Landau-Zener model and the Pechukas-Yukawa formalism, it is necessary that Landau-Zener conditions are satisfied. In the neighbourhood of a level crossing or avoided crossing, both $\lambda$ and the level separation must be a linear function of time. Expanding about $\lambda^*$, we linearise the system in regards to level crossings, avoided crossings with and without the influences of noise to verify the Landau-Zener model conditions are met. Given these conditions are satisfied, one can extend the traditional description of state dynamics through the lens of level dynamics which could yield fruitful in the development of quantum computing system, however this carries potentials beyond AQC for general state transitioning systems.

## 6.2 Level Crossings

Recall our earlier investigation on level crossings in Sec. 5.5.2, we determine how these results compare when considering the applicability of the Landau-Zener model in the Pechukas-Yukawa formalism. We use the underlying assumption that levels outside the $\gamma$ neighbourhood of the level crossings or avoided crossings are far away such that their coupling interactions are by comparison negligible. Under these assumptions, we investigated the impacts on the Pechukas equations, Eqs.(3.10) to show that in the Pechukas-Yukawa formalism, the $N$ level system can be reduced to solely the interacting levels. Furthermore, we find that the

Pechukas-Yukawa formalism can indeed be simplified to linear level separations. We examine the behaviour of the level separations about $\lambda^*$ using a Taylor expansion. For a level crossing, we have shown the relative angular momenta terms are constantly 0 and the acceleration terms independently tend to 0. This demonstrates linear evolution in level separations. We show that when there is a level crossing, all non-interacting levels are considered far apart. Then, the Pechukas-Yukawa equations can be reduced to only the interacting levels.

Suppose $x_m = x_n$ are the interacting levels and all other levels are far apart, i.e. $x_m - x_k$ and $x_n - x_k$ large for $k \neq n, m$ and angular moment $l_{mk}l_{kn}$ are small, the quotient is small and so one takes the following approximation:

$$\dot{l}_{mn} = \sum_{k \neq m,n} l_{mk}l_{kn} \left( \frac{1}{(x_m - x_k)^2} - \frac{1}{(x_k - x_n)^2} \right) \approx 0. \tag{6.2}$$

It is known that when $x_m = x_n$ that $l_{mn} = 0$ hence stays constantly zero throughout the transition time. Similarly, the other non-interacting angular momentum can be paired into the following coupled differential equations. All other terms are negligible. These are approximated as follows: for $i \neq m, n$

$$\begin{aligned} \dot{l}_{mi} &\approx l_{mn}l_{ni} \left( \frac{1}{(x_m - x_n)^2} \right), \\ \dot{l}_{ni} &\approx l_{nm}l_{mi} \left( \frac{1}{(x_n - x_m)^2} \right). \end{aligned} \tag{6.3}$$

Applying l'Hopital on this term twice, we have shown this term tends to 0 as $\lambda \to \lambda^*$ demonstrating the relative angular momenta terms can be reduced to only the interacting levels. Under this approximation, it follows that the acceleration terms are also independent of all other level interactions, determined by the following:

$$\begin{aligned} \dot{v}_m &= 2 \sum_{i \neq n} \frac{|l_{mi}|^2}{(x_m - x_i)^3} + \frac{|l_{mn}|^2}{(x_m - x_n)^3}, \\ \dot{v}_i &= 2 \sum_{i,j \neq m,n} \frac{|l_{ij}|^2}{(x_i - x_j)^3} + \frac{|l_{mj}|^2}{(x_m - x_j)^3} + \frac{|l_{nj}|^2}{(x_n - x_j)^3}. \end{aligned} \tag{6.4}$$

For the $\dot{v}_i$ expression, all terms are negligible. Again the same argument holds for $\dot{v}_n$ as does $\dot{v}_m$. Using the expressions in Eq. (6.2), $l_{mi}$ is constant hence the terms under the sum in $\dot{v}_m$ are negligible. After performing l'Hopital 3 times, the expression $\frac{|l_{mn}|^2}{(x_m - x_n)^3}$ was found to tend

to 0 as $\lambda \to \lambda^*$. Expanding about $\lambda^*$, level separation is described by $x_m - x_n = \delta\lambda(v_m - v_n) + \delta\lambda^2(\dot{v}_m - \dot{v}_n) + \mathcal{O}(\delta\lambda^3)$, where acceleration terms independently tend to 0 at a level crossing. This linearises level separations in this region during the Landau-Zener transition. For $v_m = v_n$, the numerator and denominator in the acceleration terms, identically go to 0, thus one can treat $\dot{v}_m$ as constant, such that for small $\delta\lambda$ level separation can be taken as linear. These compare against Eq. (5.34), where outside the Landau-Zener framework, level accelerations are non-zero in the event of a level crossing.

This demonstrates the applicability of the Pechukas-Yukawa formalism to the Landau-Zener model as one can indeed reduce and $N$ level system down to 2, neglecting all other interactions. Additionally, for a level crossing $\tau_{LZ} \to 0$ which reflects a strong repulsion between the levels such that the transition time is instantaneous. Given that multi-level crossings are statistically negligible and that no more than 2 levels in a close vicinity cross at a single point hence the level crossings are independent of each other and the Landau-Zener model in the Pechukas-Yukawa formalism applies.

## 6.3 Avoided Crossings

Avoided crossings occur when levels approaching each other, reach a local minimum before deflecting away. To verify the compatibility of the Landau-Zener model in the Pechukas-Yukawa formalism, it is required that the Landau-Zener conditions are satisfied for the avoided crossing. In such cases, $x_m - x_n = \Delta_{min}$ and $l_{mn}$ is not necessarily 0. In the same way, Eq. (6.2) and Eq. (6.4) apply. Under the same approximation that all other levels are far away, again $\dot{l}_{mn} = 0$ thus $l_{mn} = \beta$ where $\beta$ is a constant. Considering the equations for $l_{mi}$ and $l_{ni}$, the terms under the sum are negligible as is the final term, leaving the only surviving term:

$$\begin{aligned} \dot{l}_{mi} &= l_{mn} l_{ni} \left( \frac{1}{(x_m - x_n)^2} \right) = l_{ni}\beta \left( \frac{1}{{\Delta_{min}}^2} \right), \\ \dot{l}_{ni} &= l_{mn} l_{mi} \left( \frac{1}{(x_n - x_m)^2} \right) = -l_{mi}\beta^* \left( \frac{1}{{\Delta_{min}}^2} \right). \end{aligned} \tag{6.5}$$

We obtain coupled differential equations. Rewritten as $\begin{pmatrix} \dot{l}_{mi} \\ \dot{l}_{ni} \end{pmatrix} = \frac{1}{\Delta_{min}^2} \begin{pmatrix} 0 & \beta \\ -\beta^* & 0 \end{pmatrix} \begin{pmatrix} l_{mi} \\ l_{ni} \end{pmatrix}$. The system is readily solved as:

$$
\begin{aligned}
l_{mi} &= \frac{i\beta}{|\beta|}\frac{1}{2}\left(e^{\frac{i|\beta|}{\Delta^2_{min}}} + e^{\frac{-i|\beta|}{\Delta^2_{min}}}\right) = \frac{i\beta}{|\beta|}\cos\left(\frac{|\beta|}{\Delta^2_{min}}\right), \\
l_{ni} &= \frac{-1}{2}(e^{\frac{i|\beta|}{\Delta^2_{min}}} - e^{-\frac{i|\beta|}{\Delta^2_{min}}}) = -i\sin\left(\frac{|\beta|}{\Delta^2_{min}}\right)
\end{aligned}
\tag{6.6}
$$

Then about $\lambda^*$, the relative angular momenta $l_{mn}$ are constants independent of all other levels. We further showed, $l_{mi}$ and $l_{ni}$ are constants with $Re(l_{mi}) = 0$ and $Re(l_{ni}) = 0$ with $Im(l_{mi})$ and $Im(l_{ni})$, bounded between [-1, 1]. This demonstrates the couplings are weak between the levels involved in an avoided crossing and those that are not. This allows for treating the avoided crossing, independent of all other levels. Substituting these results into Eq. (6.4), $\dot{v}_i = 0$, the only surviving terms in $\dot{v}_m$ and $\dot{v}_n$ evaluated at $\lambda^*$ are constants; $(\dot{v}_m - \dot{v}_n) = \frac{4|\beta|^2}{{\Delta_{min}}^3}$. For small enough $\delta\lambda$, one can linearise the level separations such that level evolutions are reduced to only the interacting levels, then it is justifiable in applying the Pechukas-Yukawa formalism to the Landau-Zener model for avoided crossings. Under these approximations, the Pechukas-Yukawa formalism is reduced to the Calogero-Sutherland model.

To ensure that non-interacting levels are negligible in a Landau-Zener transition, we must ensure that level crossings are isolated from each other. We compare the differences in the transition times between level crossings or avoided crossings in a close vicinity of each other. Given that the transition times do not overlap, these level crossings and avoided crossings can be regarded as independent of each other. Considering 2 level avoided crossings occurring in a close vicinity with minimum level separations at $\lambda^*$ and $\lambda^{**} = \lambda^* + \delta$ and transition times $\tau_{LZ}$ and $\tau'_{LZ}$ respectively. We take symmetric avoided crossings such that $\tau_{LZ} = 2\xi$. Recall that in the adiabatic regime, $\tau_{LZ} = \frac{\Delta_{min}}{\lambda}$. These avoided crossings are considered isolated given that their respective transition times do not overlap such that $(\lambda^{**} - \xi') - (\lambda^* + \xi) > 0$. Then, the Landau-Zener transition model is applicable to describe the probabilities of population transitions.

We denote level separations as $d(\lambda) = x_1 - x_2$, where $d(\lambda^*) = \Delta_{min}$. Let $\delta\lambda = \lambda - \lambda^*$, then expanding about $\lambda^*$, $d(\lambda) = \Delta_{min} + \delta\lambda(v_1 - v_2 + \dot{\delta}h_{11} - \dot{\delta}h_{22}) + \delta\lambda^2(\frac{4\beta^2}{\Delta^3_{min}} + \ddot{\delta}h_{11} - \ddot{\delta}h_{22}) + \mathcal{O}(\delta\lambda^3)$. Given that $d(\lambda)$ reaches a local minimum at $\lambda^*$, then $v_1 - v_2 + \dot{\delta}h_{11} - \dot{\delta}h_{22} = 0$, we have the following:

$$
d(\lambda) = \Delta_{min} + \delta\lambda^2\frac{4\beta^2}{\Delta^3_{min}}. \tag{6.7}
$$

Take $d(\lambda^* + \xi) = \gamma$, such that one could rearrange the equation to obtain:

$$\Delta_{min} = \gamma - \xi^2 \frac{4\beta^2}{\Delta_{min}^3}. \tag{6.8}$$

In order to ensure that avoided crossings can be treated independently, $(\lambda^{**} - \xi^{'}) - (\lambda^{*} + \xi) > 0$ where $\lambda^{**} = \lambda^{*} + \delta$. Recall $\tau_{LZ} = \frac{\Delta_{min}}{\dot{\lambda}} = 2\xi$ for a symmetric avoided crossing. Then it is essentially $\tau_{LZ} < 2(\delta - \xi^{'})$. One could rearrange this bound for $\Delta_{min}$,

$$\gamma - \xi^2 \frac{4\beta^2}{\Delta_{min}^3} < 2\dot{\lambda}(\delta - \xi^{'}). \tag{6.9}$$

Given that $\delta > \frac{1}{2\dot{\lambda}}(\gamma - \frac{4\beta^2}{\Delta_{min}^3}\xi^2) + \xi'$, the conditions for level crossings to be treated independently are satisfied.

In contrast to the level crossing case, avoided crossings have constant relative angular momenta,

between levels at the level crossing or avoided crossing. In this case all other relative angular momenta $l_{mi}$ and $l_{ni}$, are constants where $Re(l_{mi}), Re(l_{ni}) = 0$ and $Im(l_{mi}), Im(l_{ni})$ are bounded in the interval $[-1, 1]$. The difference between the acceleration terms of the interacting levels is constant, $\frac{4|\beta|^2}{\Delta_{min}^3}$ at $\lambda^{*}$. Choosing a sufficiently small $\delta\lambda$, these terms are negligible therefore linearising the level separations. We extend this investigation to account for the impacts of noise on these conditions. This enables further understanding of dissipative influences on the properties of level interactions.

## 6.4 Stochastic Avoided Crossings

In a stochastically perturbed Hamiltonian, Landau-Zener transitions manifest as avoided level crossings (under the effects of noise, levels do not cross). We explore the influences of noise on a quantum system. Depending on the nature of the noise, whether the source is longitudinal (with only diagonal elements) or transverse (with only off-diagonal elements), the system behaves differently. Longitudinal contributions result in decoherence in the system whereas transverse noise results in couplings to the environment. Our analysis could be extended to various types of noise, here we consider intrinsic longitudinal noise modelled as a single composite source of Brownian noise $\delta h$ such that $\dot{\delta} h = \epsilon \eta M$. Here $\eta$ is white noise, a random normal distributed stochastic process[53, 54], $M$ represents a general diagonal matrix and $\epsilon$ denotes the noise amplitude. As explained earlier, for white noise the expectation is zero and the autocorrelation function is given by $\langle \eta_{mn}(\lambda), \eta_{mn}(\lambda^{'}) \rangle = \delta(\lambda - \lambda^{'})$

and $\langle \epsilon\eta_{mn}(\lambda), \epsilon\eta_{mn}(\lambda')\rangle = \epsilon^2\delta(\lambda-\lambda')$. The correlation time $\tau_c = 0$. White noise is the formal derivative of a Wiener process, $W(t)$.

To ensure the applicability of the Landau-Zener model, we reduce the system from $N$ levels to 2. Again, under the assumption that levels outside the avoided crossings are far away with weaker coupling interactions we show that the avoided crossing is independent of all non-interacting level contributions. The Pechukas-Yukawa model is highly entangled, hence it is important to verify that the conditions required for the Landau-Zener description are met. The model described in Eq. (3.12), must be regarded as independent of all non-interacting levels about an avoided crossing.

To determine the applicability of the Pechukas-Yukawa formalism under dissiptive influences, it is neccessary to ensure that level interactions in an avoided crossing are independent of all other interactions. Again, $x_m - x_n = \Delta_{min}$ at some $\lambda^*$ (denoting the point of minimum separation) and $l_{mn}$ is not neccessarily 0. Similarly to Eq. (6.17), we have the following for the coupling between levels at an avoided crossing,

$$\dot{l}_{mn} = \sum_{k\neq m,n} l_{mk}l_{kn}\left(\frac{1}{(x_m-x_k)^2} - \frac{1}{(x_k-x_n)^2}\right) + \frac{(x_m-x_n)(l_{mk}\dot{\delta}h_{km} - \dot{\delta}h_{mk}l_{kn})}{(x_m-x_k)(x_n-x_k)} + \dot{\delta}h_{mn}(v_m-v_n) + \frac{l_{mn}(\dot{\delta}h_{mm}-\dot{\delta}h_{nn})}{(x_m-x_n)}. \tag{6.10}$$

We consider a single source of composite longitudinal Brownian noise. Again, assuming all non-interacting couplings are negligible and the levels are far away from the level crossing. This simplifies the relative angular moment dynamics to the following:

$$\dot{l}_{mn} \approx \frac{l_{mn}(\dot{\delta}h_{mm}-\dot{\delta}h_{nn})}{(x_m-x_n)} \approx \frac{l_{mn}}{\Delta_{min}}\epsilon\mu\eta, \tag{6.11}$$

where $\epsilon$ denotes the noise amplitude, $\mu$ is a constant giving the difference between the noise components and $\eta$ represents a stochastic white noise term. Let $\sigma = \frac{\epsilon\mu}{\Delta_{min}}$. We consider separately real and imaginary components. In each component, we observe a driftless geometric Brownian motion:

$$\begin{aligned} \dot{R}e(l_{mn}) &= \sigma Re(l_{mn})\eta, \\ \dot{I}m(l_{mn}) &= \sigma Im(l_{mn})\eta. \end{aligned} \tag{6.12}$$

Using the Euler-Maruyama method to solve these stochastic differential equations, we

rewrite the expression for $Re(l_{mn})$ as $dRe(l_{mn}) = \sigma Re(l_{mn})dW$. Integrating these terms, where we zero out noise at $\lambda^* - \xi$, we obtain the following:

$$\int_{\lambda^*-\xi}^{\lambda} \frac{dRe(l_{mn})}{l_{mn}} = \sigma dW. \tag{6.13}$$

We apply Ito's formula such that $d(Ln(Re(l_{mn}))) = \frac{dRe(l_{mn})}{l_{mn}} - \frac{1}{2}\frac{1}{Re(l_{mn})^2}dRe(l_{mn})dRe(l_{mn})$ where $dRe(l_{mn})dRe(l_{mn})$ is the quadratic variation of the stochastic differential equation such that $dRe(l_{mn})dRe(l_{mn}) = \sigma^2 Re(l_{mn})^2 d\lambda$. Substituting this into the integral, we have:

$$\int_{\lambda^*-\xi}^{\lambda} d(Ln(Re(l_{mn}))) + \frac{\sigma^2}{2} = \sigma dW. \tag{6.14}$$

Then,

$$Ln\left(\frac{Re(l_{mn}(\lambda))}{Re(l_{mn}(\lambda^* - \xi))}\right) = -\frac{1}{2}\sigma^2(\lambda - (\lambda^* - \xi)) + \sigma W(\lambda). \tag{6.15}$$

The start time of the levels approaching a minimum separation in a $\gamma$ neighbourhood of each other is taken as $(\lambda^* - \xi)$, and $\mu$ denotes the difference in the noise components. Exponentiating the result, we find that $Re(l_{mn}(\lambda)) = Re(l_{mn}(\lambda^* - \xi))e^{-\frac{\sigma^2}{2}(\lambda-(\lambda^*-\xi))+\sigma W(\lambda)}$. Using the same method to solve for the imaginary components, we have $Im(l_{mn}(\lambda)) = Im(l_{mn}(\lambda^* - \xi))e^{-\frac{\sigma^2}{2}(\lambda-(\lambda^*-\xi))+\sigma W(\lambda)}$. Combining these terms, $l_{mn}(\lambda) = l_{mn}(\lambda^* - \xi)e^{-\frac{\sigma^2}{2}(\lambda-(\lambda^*-\xi))+\sigma\eta(\lambda)}$ in the region of the transition time. This term has expectation, $E(l_{mn}) = l_{mn}(\lambda^* - \xi)$ and variance $Var(l_{mn}) = |l_{mn}(\lambda^* - \xi)|^2(e^{\frac{\sigma^2}{2}(\lambda-(\lambda^*-\xi))} - 1)$. Here, $(\lambda^* - \xi)$ represents the start time of levels approaching a minimum separation in a $\gamma$ neighbourhood of each other. This describes $l_{mn}$ as a martingale (the conditional probability of the next step is dependent only on the current step) where for $\lambda \to \infty, l_{mn} \to 0$ with probability 1, which follows from the law of iterative logarithm.

The equations for $l_{mi}$ are given by the following:

$$\dot{l}_{mi} = \sum_{k\neq m,i;i\neq n} l_{mk}l_{ki}\left(\frac{1}{(x_m-x_k)^2}-\frac{1}{(x_k-x_i)^2}\right)+\frac{(x_m-x_i)(l_{mk}\dot{\delta}h_{km}-\dot{\delta}h_{mk}l_{ki})}{(x_m-x_k)(x_i-x_k)}+$$
$$\dot{\delta}h_{mn}(v_m-v_i)+\frac{l_{mi}(\delta h_{mm}-\delta h_{ii})}{(x_m-x_i)}+l_{mk}l_{kn}\left(\frac{1}{(x_m-x_k)^2}-\frac{1}{(x_k-x_n)^2}\right) \tag{6.16}$$
$$+\frac{(x_m-x_n)(l_{mk}\dot{\delta}h_{km}-\dot{\delta}h_{mk}l_{kn})}{(x_m-x_k)(x_n-x_k)}+\dot{\delta}h_{mn}(v_m-v_n)+\frac{l_{mn}(\delta h_{mm}-\delta h_{nn})}{(x_m-x_n)}.$$

We consider a single source of longitudinal noise such that off-diagonal components are 0. Under the Landau-Zener assumption that all other levels have weaker couplings and large level separations, we obtain pairs of coupled differential equations:

$$\begin{aligned}\dot{l}_{mi} &\approx l_{mn}l_{ni}\left(\frac{1}{(x_m-x_n)^2}\right)=l_{mn}l_{ni}\left(\frac{1}{{\Delta_{min}}^2}\right),\\ \dot{l}_{ni} &\approx l_{nm}l_{mi}\left(\frac{1}{(x_n-x_m)^2}\right)=-l^*_{mn}l_{mi}\left(\frac{1}{{\Delta_{min}}^2}\right).\end{aligned} \tag{6.17}$$

Taking a matrix of ordinary differential equations,

$$\begin{pmatrix}\dot{l}_{mi}\\ \dot{l}_{ni}\end{pmatrix}=\frac{f(\lambda)}{\Delta^2_{min}}\begin{pmatrix}0 & l_{mn}(\lambda^*-\xi)\\ -l^*_{mn}(\lambda^*-\xi) & 0\end{pmatrix}\begin{pmatrix}l_{mi}\\ l_{ni}\end{pmatrix}, \tag{6.18}$$

where $f(\lambda)=e^{\frac{\sigma^2}{2}(\lambda-(\lambda^*-\xi))+\sigma\eta(\lambda)}$, capturing the stochastic element. Diagonalising the matrix and changing bases to the eigenvectors, we can simply integrate the decoupled set of equations. We obtain the following:

$$\begin{aligned}l_{mi} &= \frac{il_{mn}}{2|l_{mn}|}\left(e^{i\frac{f(\lambda)}{\Delta^2_{min}}|l_{mn}|}+e^{-i\frac{f(\lambda)}{\Delta^2_{min}}|l_{mn}|}\right)=\frac{il_{mn}}{|l_{mn}|}cos\left(\frac{f(\lambda)}{\Delta^2_{min}}|l_{mn}|\right),\\ l_{ni} &= -\frac{1}{2}\left(e^{i\frac{f(\lambda)}{\Delta^2_{min}}|l_{mn}|}-e^{-i\frac{f(\lambda)}{\Delta^2_{min}}|l_{mn}|}\right)=-isin\left(\frac{f(\lambda)}{\Delta^2_{min}}|l_{mn}|\right).\end{aligned} \tag{6.19}$$

Then, $l_{mi}$ and $l_{ni}$ are stochastic terms, where $Re(l_{mi})=0$ and $Re(l_{ni})=0$ with $Im(l_{mi}), Im(l_{ni})$ bounded in the interval $[-1,1]$. Taking $\delta\lambda$ sufficiently small, these terms are negligible in the avoided crossing. Applying these relative angular momenta formulae to the acceleration terms (again taking account that the noise source comes from a single longitudinal Brownian source) we have the following:

$$\begin{aligned}
\dot{v}_m &= 2\sum_{i\neq n}\frac{|l_{mi}|^2}{(x_m-x_i)^3}+\frac{2\dot{\delta}h_{mi}Re(l_{mi})}{(x_m-x_i)^2}+\frac{|l_{mn}|^2}{(x_m-x_n)^3}+\frac{2\dot{\delta}h_{mn}Re(l_{mn})}{(x_m-x_n)^2},\\
\dot{v}_i &= 2\sum_{i,j\neq m,n}\frac{|l_{ij}|^2}{(x_i-x_j)^3}+\frac{2\dot{\delta}h_{ij}Re(l_{ij})}{(x_i-x_j)^2}+\frac{|l_{im}|^2}{(x_i-x_m)^3}+\frac{2\dot{\delta}h_{im}Re(l_{im})}{(x_i-x_m)^2}\\
&\quad+\frac{|l_{in}|^2}{(x_i-x_n)^3}+\frac{2\dot{\delta}h_{in}Re(l_{in})}{(x_i-x_n)^2}.
\end{aligned}\tag{6.20}$$

All terms are negligible for $v_i$ under the approximation on the level separation in this region is negligible.

For the difference between $\dot{v}_m$ and $\dot{v}_n$, all terms under the sum are negligible except for $l_{mn}\not\approx 0$ is given by $\frac{4|l_{mn}|^2}{{\Delta_{min}}^3}$, independent of all other levels. Here, $l_{mn}$ is a martingale with constant expectation. To determine the effects of the stochastic terms on the difference between accelerations, we consider the expectation during $\tau_{LZ}$. The expectation of $|l_{mn}|^2$ is given by,

$$\begin{aligned}
|l_{mn}|^2 &= Re(l_{mn})^2+Im(l_{mn})^2,\\
E|l_{mn}|^2 &= E(Re(l_{mn})^2)+E(Im(l_{mn})^2)\\
&= Var(Re(l_{mn}))+Var(Im(l_{mn}))+E^2(Re(l_{mn}))+E^2(Im(l_{mn}))\\
&= |l_{mn}(\lambda^*+\xi)|^2 e^{\frac{\sigma^2}{2}(\lambda-(\lambda^*-\xi))}.
\end{aligned}\tag{6.21}$$

Then the expectation of the difference between the acceleration terms are given by $\frac{4|l_{mn}(\lambda^*+\xi)|^2}{\Delta^3_{min}}e^{\frac{\sigma^2}{2}(\lambda-(\lambda^*-\xi))}$. These dynamics are bounded between $[\frac{4|l_{mn}(\lambda^*+\xi)|^2}{\Delta^3_{min}}, \frac{4|l_{mn}(\lambda^*+\xi)|^2}{\Delta^3_{min}}e^{\xi\sigma^2}]$ where $\lambda\in[\lambda^*-\xi,\lambda^*+\xi]$. For $\tau_{LZ}$ being short time durations, this motion is under stricter bounds, near-constant. Choosing $\delta\lambda$ small enough, the difference in acceleration terms are negligible, linearising the level separations. Then it is observed that indeed the Pechukas-Yukawa formalism under the influence of noise is applicable to the Landau-Zener model, reducing the system from N levels to 2. This analysis can be extended to various types of noise.

In order for the Landau-Zener model to hold in the stochastic sense, it is necessary to consider avoided crossings in a close vicinity of each other, such that they can be regarded as isolated crossings. The transition time of an avoided crossing is changed under the influence of noise. Of particular interest are the influences of noise on the minimum separation. These in turn have an impact on both the probability of transitions and the transition times. By the central limit theorem, white noise is a reasonable model for noise from many stochastic

influences however, an attractive extension of these works involve the consideration of avoided crossings under more realistic models of noise such as coloured noise.

## 6.5 Summary

In this chapter, we outline the conditions required for the applicability of the Landau-Zener model. Considering each case separately for level crossings, avoided crossings and stochastic avoided crossings, we show the Landau-Zener conditions are met in the Pechukas-Yukawa formalism. Utilising the close relation between level dynamics and the evolution of quantum states, we demonstrate that state transitions can be investigated through level dynamics.

Having shown that the Landau-Zener model is compatible with the Pechukas-Yukawa formalism, we provided the justification of the investigations by Zagoskin[3] and Wilson[5] where it was observed that there is a significant difference between the scaling exponents of the escape probability for the edge states and intermediate states. We provide analytical expressions which can be used to investigate the reasons for their differences.

Moreover, the marriage of the Landau-Zener model and the Pechukas-Yukawa formalism provides one example of the relationship between level dynamics and state dynamics. A generalisation of this scheme would be to include state dynamic outside of Landau-Zener transitions via level dynamics, independent of the imposed conditions, allowing for the description of state dynamics for nonstationary, dissipative systems. This may be achieved using a quantum master equation in the Pechukas-Yukawa formalism, reducing the description of the density matrix through eigenvalue dynamics however, goes beyond the extent of our current investigation.

# Chapter 7

# Conclusions

In this project, we developed a novel approach to the theoretical description of large quantum coherent systems out of equilibrium, based on the Pechukas-Yukawa formalism. Under this description, the dynamics of energy levels are mapped to a fictitious one-dimensional classical gas with long-range repulsion.

We developed a consistent description of non-equilibrium, nonstationary evolution of a perturbed quantum system based on the kinetic theory of the Pechukas-Yukawa model. Under this formalism, we obtained non-equilibrium statistical kinetic equations of motion for the level dynamics of the system, from the application of the BBGKY hierarchy to the Pechukas-Yukawa model, which extends the kinetic equations concerning level dynamics to parametrically driven evolution of a quantum system. This procedure provides a fundamental extension of previous study which establish the use of the Pechukas-Yukawa model and the random matrix theory in equilibrium statistical mechanics of level dynamics. The application of the BBGKY hierarchy to the Pechukas-Yukawa model describing a parametrically driven evolution of a quantum system, especially convenient in accomodating adiabatic systems. However, the formalism is applicable to a general system with parametric evolution in time, exploring an important new direction in contemporary physics which opens further investigations to understand the connection to the physics of the Pechukas gas.

Statistical approach to level dynamics would allow a reduced description of correlation functions. Given that coordinates in the Pechukas-Yukawa framework are independent, we investigate the factorisation approximation where sets of approximations are obtained from breaking the chain at a particular point such that higher-order reduced distribution functions can be constructed from a product of lower-order ones under this factorisation approximation. This describes an $s$-particle reduced probability distribution function from a product of $s$ one-particle distribution functions. Moreover this results in independent probability distribution functions, reducing the many-body system to a single-body system,

where the number of particles correspond to the number of energy levels in the system. This is a great simplification that enables solving the BBGKY hierarchy from solving just the one-body system. Under this approximation one can infer the statistical properties of the level dynamics using only one-particle distribution functions.

Analytically considering the accuracy of the factorisation approximation, providing an effective mean field theory approximation, we find that corrections to the factorised approximation of the distribution function scale as $1/N$, where $N$ is the number of energy levels in the system. This is shown from the asymptotic decay in the relative error of order $O\left(\frac{1}{N}\right)$ as $N$ tends to infinity. This provides confidence that for large systems, this approximation holds.

To illustrate this theory, we considered a simple system of two-qubits compared against the exact solution of the Hamiltonian. Using the eigenvalues in accordance with the Pechukas equations, the velocities and relative angular momenta were determined. Then the distribution functions involved in the first chain of the BBGKY hierarchy were constructed to test the factorisation approximation for higher order chains. In the case of two-qubits, this approximation was not accurate as the energy levels were not mutually independent at any given $\lambda$, however a comprehensive numerical comparison for larger systems is impractical as it proves more challenging to diagonalise the corresponding Hamiltonian. This description is advantageous as it is expected to have significant developments in non-equilibrium processes such as decoherence, with fruitful extensions into the description of AQC.

Furthermore, we obtain equations for the for level occupations and inter-level transition amplitudes, which allow for the description of the evolution of quantum states in non-equilibrium systems. This description of a quantum coherent system is advantageous as it includes all higher level entanglements. Having established the relationship between the level dynamics and the occupation numbers as a function of time using the PechukasYukawa model, we provide a description of the full wavefunction under the Pechukas-Yukawa formalism, detailing the system in its entirety. Then, it is possible to determine the groundstate of large systems efficiently and hence demonstrate that AQC is a viable alternative to quantum computing. Moreover, this provides scope to better describe a large quantum coherent system than approaches currently in practice.

Through the evolution of the eigenstate coefficients, we considered the dynamics of quantum states using the Magnus series. This approach was contrasted against the TDPT and the adiabatic approximation compared with a direct numeric simulation. The Magnus series provides an infinite hierarchy in powers of $\dot{\lambda}$ parameters. The structure is that of a cumulant expansion and it would be of interest to consider asymptotic convergences in the series which would improve the efficiency of the result. Considering the eigenstate coefficents

in the adiabatic limit, one can explore the significance of these terms with respect to the development of adiabatic invariants which has the potential to significantly impact features of the adiabatic algorithm design. We also showed the convergence of the Magnus series is governed by the initial conditions in the Pechukas-Yukawa formalism which could gain better insight into what measurable characteristics of a system could be used as a criterion for its quantum performance. This carries the potential to specify Hamiltonians of different complexity classes, governed by the initial conditions of the system.

We investigated the limits of the Magnus series, reducing the convergence criterion such that the entire evolution of the system is governed by the initial conditions and the choice in $\lambda$. Numerically, it was found that for short intervals, where the convergence criterion is satisfied, the Magnus series was most accurate with its relative errors lower than the relative errors for both the TDPT and the adiabatic approximation by multiple orders. We found that the Magnus series is robust, as time evolves, the error increases yet the Magnus series remains the better approximation far beyond the interval where he convergence criterion is met. It was also shown that for larger systems with a greater number of interacting levels, the relative error for the Magnus series overtook the relative errors for the TDPT and adiabatic approximations at later times, demonstrating that the Magnus series is better suited to the "spaghetti" regime. The Magnus series is less prone to divergences in the error due to level crossings and avoided crossings, which become more prevalent in higher dimensions of excited states.

Finding that the Magnus series offers an especially convenient description of non-adiabatic evolution, we explored the relationship between the level dynamics and that of the evolution of the quantum states described by the density matrix. We obtained the occupation dynamics for the 3-Sat problem, providing insight on the population of states which offers analytical insights on the sources of decoherence on the evolution of a quantum system. This approach is general and has applications beyond quantum algorithms.

Separately, we developed the Landau-Zener model in the Pechukas-Yukawa formalism, showing that our framework coincides with the results of the classical Landau-Zener transitions upon linearisation. As a starting point, we take all assumptions that form the basis of the Landau-Zener model and explore the conditions they impose on the Pechukas-Yukawa formalism to be applicable. This led to the developments in the understanding of level crossings and avoided crossings in this setting, identifying various properties of the level interaction. Particularly, we provide a detailed insight on the level repulsions extended to the influence of external noise and its impacts on the minimum separations characterising avoided crossings. The investigation of level repulsions at an avoided crossing under the influence of longitudinal noise was not possible without a thorough description of the level

dynamics given by the Pechukas-Yukawa formalism. From this, we built on earlier works by Zagoskin[3] and Wilson[5], to gain insight on level interactions beyond the Landau-Zener probability. Under this description, one could investigate the differences in the scaling properties observed in these earlier works.

An attractive development to this investigation would be to apply the Landau-Zener probability to the Pechukas-Yukawa description of quantum states which could lead to the exploration of quantum phase transitions through the initial condition of the eigenvalues of a quantum Hamiltonian system. The eigenstate coefficients have been expressed using the Pechukas equations such that one could extend this description to obtain both the occupation dynamics and the coherences of the system, crucial to the development of AQC. An interesting extension of these works would be to consider the effects of different types of noise such as coloured noise and the impacts of transverse components.

In continuation of our investigation, using the Magnus series, we obtain an explicit analytical description of both the occupation numbers and coherences of a general quantum system, continuously through time. Discretising the occupation numbers and averaging over the levels, we gain statistical insight in the changes of the occupation dynamics as a consequence of Landau-Zener transitions. Under this description, we contrasted between edge and intermediate states in exploration of the differences in the Landau-Zener transitions and their impacts on the transition probabilities. This allows us to investigate the scaling relations found by Zagoskin[3] and Wilson[5], so we can identify the reasons for their apparent differences. Statistically, the primary contributions for the differences between the transitions can be attributed to the differences in the frequency of occurrences which enables one to consider these impacts on decoherences.

Additionally, these results would serve as a starting point to gain insight on multi-state Landau-Zener transitions. The standard Landau-Zener model only deals with 2 interacting levels. Extending to multi-state problems could yield more interesting physics. The Pechukas-Yukawa model concerns an interacting system of $N$ entangled levels hence it is highly equipped to consider interacting systems with entangled states. A further extension it would be useful to consider detailed analytics of multiple level interactions and their influence on each other's dynamics. This approach can be used to describe a non-equilibrium interacting system of highly entangled states, especially the dynamics of a system and its vulnerability to decoherence. Future scope in this realm would be to investigate the analytical expressions under the influences of external noise. Furthermore, it would be interesting to develop on the evolution of quantum states, independent of the Landau-Zener transition model and the assumptions it demands.

## 7.1 Further Investigations

Theoretical description of quantum many-body systems is a critical area of research with strong connections to modern nuclear physics of nuclei far from equilibrium, optical systems and quantum technologies. It has led to significant developments in the theory of quantum computing, with one of the most viable competing theories being adiabatic quantum computing (AQC). However, due to the persisting obstacle of decoherence, the realisation of quantum computers remains a challenging task. The similarities between the theory of AQC and quantum phase transitions (QPT) have instigated research on decoherence through QPT. Most of these works consider only equilibrium systems, however for a physical quantum platform, based on the superposition of states, the system will inevitably be open due to the impossibility of perfectly isolating the system from its environment[5], hence noise must be accounted for. One can develop on the theory of AQC from out of equilibrium QTP, building a formalism capable of describing highly entangled many-body interactions, under stochastic influences using Hamiltonian dynamics which is a novel concept. Under this description, one can provide an improved understanding of the relationship between nonequilibrium QPTs and decoherence which has significant impacts to a wide range of applications from the development of AQC, the understanding of strongly interacting many-body optical systems to describing shape-phase transitions in the nucleus.

The scope of the impacts of a quantum computer would be far reaching and monumental in modern society with benefits from simulating chemical reactions, enabling insights on the developments of new drugs and how they react to boosts in machine learning, assisting self-driving cars in assessing situations more efficiently, for improved safety. Optical systems are both economically advantageous and highly beneficial to optical computing systems allowing for high speed data transmission where data growth has become large, a prominent limitation to electronic systems. Another advantage photonic systems offer is their robustness against synchronisation problems, unavoidable in electronic systems. Optical correlation systems also have the advantage of accessing individual lattices experimentally offering the ability to design quantum-mechanical devices for quantum information processes. These compare with quantum signal transmission, understood through simple qubit systems with extensions to complex artificial structures enabling the utilisation of quantum properties in data transmission, improving efficiencies.

A major challenge to the realisation of a practical quantum computer is the fragility of quantum states and their susceptibility to decoherence (the loss of information due to the interactions with the environment). A promising alternative approach is AQC, encoding the system in an easily achievable groundstate of the initial Hamiltonian and evolving the system

under an adiabatic parameter such that the system maps the system to the groundstate of the final Hamiltonian. This corresponds to an optimal solution. The groundstate is more robust against decoherence however it is not immune to it.

There is a remarkable similarity between AQC algorithms and QPT in their Hamiltonians governing their dynamics; $H(\lambda(t)) = H_0 + \lambda(t)H_1$. There have been studies of algorithms bringing a quantum system near critical points, similar to that observed in QPT, which are relevant to the study of evolving quantum systems and the development in the study of sources of decoherence, prevalent for many-body systems. There exist various models that seek to describe the relations between quantum phase transitions, decoherence and entanglement, however these models are often reliant on mean field approximations to simplify the system due to the large amounts of information required; this research offers a seamless description for all these properties from the eigenvalue dynamics of a quantum system out of equilibrium. The Pechukas-Yukawa model is also expressible in Lax formalism enabling the study of symmetries and conserved quantities in QPT, however this area of research on out of equilibrium steady states is still a very young field with much to consider.

QPT under dissipative influences result in the manifestation of critical behaviour in steady states rather than groundstates. Adiabatic systems initialised in some steady state, remain in the steady state throughout the duration of the system exhibiting criticalities. For a single steady state, this has the advantage that when the system deviates from the steady state because of stochastic influences, it returns to the steady state. In the realms of AQC, decoherence could be monitored such that the system approaches a desired steady state manifold under controlled dissipative systems. Our understanding of non-equilibrium QPT is limited in contrast to equilibrium QPT, despite its relevance in the studies of quantum computing, atomic molecular and optical systems. One reason for this is that simulating the evolution of a master equation proves more difficult than Hamiltonian dynamics due to the sheer amount of information required for the density matrix in contrast to wavefunctions.

The Pechukas-Yukawa model has the capability of studying the evolution of the density matrix without restriction on the type of noise, understood through eigenvalue dynamics. This provides great insights to and beyond AQC, to the development of non-equilibrium QPT analytically and within grasp of experimental testing which plays a crucial role to the understanding of dynamical phase transitions. Through this understanding of eigenvalue dynamics, the Pechukas-Yukawa formalism could be used to develop on this alternate theory of AQC, under a new framework using Hamiltonian dynamics to understand stochastic QPT to investigate steady states and how their properties could be harnessed for the development of AQC, which has never been considered. This allows for an immersive detail into this relatively new field of study.

# Chapter 8

# Appendix

## 8.1 Appendix A: Quantum Information

Classical computations rely on a register of bits, taking values either 1 or 0. For quantum computations, a register of qubits are used to exploit quantum properties which offer significantly improved speeds in execution of computer algorithms. They store information in a register of $2^n$ quantum states for $n$ qubits rather than the classical analogue of a register of bits.

**Qubit:** A two-level quantum system that lives in the Hilbert space, used to carry quantum information also referred to as a quantum bit.
The basis vectors are given by the following:

$$|0\rangle = \begin{pmatrix} 1 \\ 0 \end{pmatrix}, |1\rangle = \begin{pmatrix} 0 \\ 1 \end{pmatrix}.$$

A qubit can be represented as a linear combination of these basis eigenvectors, given as $|\phi\rangle = \alpha|0\rangle + \beta|1\rangle$, with $\alpha, \beta \in \mathbb{C}$. Then, the probability of observing the qubit in state $|0\rangle$ is given by $|\alpha|^2$ and $|\beta|^2$ for the probability of observing the qubit in state $|1\rangle$. The combined probability, $|\alpha|^2 + |\beta|^2 = 1$. This state vector can be mapped directly to the Bloch sphere, where the poles are given by the eigenvectors $|0\rangle$ and $|1\rangle$. One can represent a collection of qubits through taking a tensor product of their state vectors.

Quantum information is carried in a set of $n$ qubits, the Hilbert space is given the $n$-tupe tensor product, a $2^n$ complex space with a general basis of $|N\rangle$ where $N$ is a binary string of length $n$ given by $N = (N_1 \dots N_n) \in 0, 1^n$. In tensor notation, $|N\rangle = |N_1\rangle \otimes \cdots \otimes |N_n\rangle = |N_1 \dots N_n\rangle$. Then, any vector denoting the information stored in the quantum register of qubits is given as a linear combination of basis states given by $|\phi\rangle = \sum_{N \in 1,0^n} \alpha_N |N\rangle$, where $\alpha_N \in \mathbb{C}$. These qubits are manipulated via quantum operators also referred to as quantum

logic gates.

Quantum operators in the two-dimensional Hilbert space are made up of the three fundamental rotation operators given by the Pauli matrices which are both unitary and Hermitian, and the identity transformation 1. The Pauli matrices each have two eigenvalues $+1$ and $-1$ from acting on the two basis vectors. These are used to construct quantum gates used in quantum computing, discussed in the following section.

## 8.2 Appedix B: Complexity Classes

Complexity classes can be categorised into three different types of computable problems; decision problems, optimisation problems and counting problems.

### 8.2.1 Decision Problems

Decision problems contains the most diversity in the different problem classes, with at least ten other subclasses. The defining feature of this class of problems are that their outcome is binary, yes or no instances. **P**, **: PSPACE**, **EXPTIME**, **NP** and **NPC** make up the majority of classes in this set. These are familiar between both deterministic and non-deterministic computations. **P** problems have runtimes that grow polynomially with the size of the problem whereas **NP** problems take polynomial time to verify a problem. **NPC** problems, also referred to as **NP**-Complete form a subset of **NP** problems with the property that any **NP** problem can be translated as an **NPC** in polynomial time.

An open challenge in relating these problems remain; given a polynomial time algorithm for an **NPC**, the algorithm could be used as a subroutine to solve all other **NPC** problems in polynomial time.

Another class of decision problems is bounded-error probabilistic polynomial time (**BPP**). A probabilistic problem that returns an answer, correct to some fixed probability $p$. It is solved in polynomial time, using a probabilistic algorithm with an error of $1 - p$. Another probabilistic algorithm is the Merlin-Arthur computation class (**MA**), defined as the probabilistic analog of **NP**. In this class of problems, Merlin is computationally unbounded, providing a certificate that Arthur can verfiy using a **BPP** computer.

In contrast, we have the quantum analogs of these classes of problems. The bounded-error quantum polynomial time (**BQP**) describes the quantum analog of the **BPP**, where a quantum model of computation based on the arrangements of quantum circuits operating on qubits. Quantum Merlin-Arthur(**QMA**), represents the set of problems where the binary output is verified polynomially in time with an error $1 - p$. This type of problem defines the quantum analog to both **MA** and **NP**. Similarly, **QMAC** defines the quantum analog

of **NPC** problems, defined in the same way however operating on a circuit of qubits to take advantage of quantum properties. A related class of problems is Quantum-Classical Merlin-Arthur (**QCMA**), similar to **QMA**, however the binary value for a 'yes'-instance is required to take the form of a classical string.

### 8.2.2 Counting Problems

Counting problems are defined by those that count the number of optimal solutions. One example of this group is the sharp-**P** set of problems which carry decision analogues in **NP** and optimisation analogues in **NPO**, returning the number of optimum solutions.

### 8.2.3 NP-Hard Problems

A problem is **NP**-hard if there is a polynomial time reduction from an **NPC** to the problem. This reduction implies that an algorithm to solve the problem in polynomial time could be used as a subroutine to solve the **NPC** problem, hence all **NPC** problems. The set of problems, **NPC**, **QMAC**, **QCMA**, **NPO**, **APX** and **PTAS** fall into the group of **NP**-hard problems.

## 8.3 Appendix C: Density Matrix Formalism

The density matrix is a statistical operator which takes the role of state vectors, encoding all information of the quantum system including incoherent mixtures of the system, indescribable through pure states $|\psi\rangle$. Consider an ensemble of objects in the set states $|\psi_i\rangle$. If all objects are in the same state, the ensemble is represented by a pure state. Take the state $|\psi\rangle$ expanded in the eigenstates of an operator $D$; $|\psi\rangle = \sum_n C_n|n\rangle$ where $C_n$ denote the eigenstate coefficients, then the expectation value of $D$ is given by,

$$\langle D\rangle = \sum_n |C_n|^2 d_n = \sum_n \frac{N_n}{N} d_n, \tag{8.1}$$

where $d_n$ denotes the eigenvalues of $D$, $|C_n|^2$ gives the probability of obtaining the eigenvalue $d_n$, corresponding to the fraction $\frac{N_n}{N}$, where $N_n$ gives the number of times eigenvalue $d_n$ is measured out of an ensemble of $N$ objects. This can be described in the form of a density matrix, characterised by pure states:

$$\rho := |\psi\rangle\langle\psi|. \tag{8.2}$$

This matrix has the following four properties respectively, 1. being a projector: $\rho^2 = \rho$, 2. hermiticity: $\rho^\dagger = \rho$, 3. normalisation: $Tr(\rho) = 1$ and 4. positivity: $\rho \geq 0$. The first two properties can be shown directly from the definition Eq. (8.2), 3. follows from the definition of the trace of an operator. Consider an operator $D$, then the trace of $D$ is given by $TrD := \sum_n \langle n|D|n\rangle$, where $|n\rangle$ is an orthonormal eigenbasis. In the case that $D = \rho$, $Tr\rho = \sum_n \langle n|\rho|n\rangle = \sum_n \langle n|\psi\rangle\langle\psi|n\rangle$, then by unitary projection, property 3. is satisfied. Property 4. implies that the eigenvalues of $\rho$ are greater or equal to 0. This is important as the eigenvalues of $\rho$ correspond to probabilities, hence they must always be greater or equal to 0.

Under this density matrix formalism, one can determine the expectation of an observable $O$ by the following:

$$\langle O\rangle = Tr(\rho O). \tag{8.3}$$

This can be shown from the definition of the trace operation. In the pure state, one can combine properties 1-3 to show $Tr\rho^2 = 1$.

In the case of mixed states, all $N$ objects of the ensemble are not in the same state. Then one defines the probability $p_i$ to find an individual system in the $|\psi_i\rangle$ by $p_i = \frac{N_i}{N}$ where $\sum_i p_i = 1$, $N_i$ denotes the number of systems in state $|\psi_i\rangle$ and $N$, the total number of objects in the ensemble. Then the mixed state can be described by the following:

$$\rho_{mix} = \sum_i p_i \rho_i = \sum_i p_i |\psi\rangle\langle\psi|. \tag{8.4}$$

Using this definition and following the same argument as in the pure state definition, the expectation value of an observable $O$ is given by,

$$\langle O\rangle = Tr(\rho_{mix} O) = \sum_i p_i \langle\psi_i|O|\psi_i\rangle. \tag{8.5}$$

This follows from the definition of the trace. Properties 2-4 are obeyed in the mixed state density matrix formalism, however property 1. is violated. Furthermore, taking the trace of

$\rho^2_{mix}$ no longer gives a value of 1 but is shown in the following to be less than 1.

Then the trace is used as a good measure for mixedness in the density matrix. For maximally mixed states, $Tr\rho^2_{mix} = \frac{1}{d} > 0$, where $d$ denoted the dimension of the system.

## 8.4 Evolution of the Density Matrix

In order to determine the equation of motion for the density matrix, one considers the time-dependent Schrodinger equation and its Hermitian conjugate.

$$\begin{aligned} i\hbar\frac{\partial}{\partial t}|\psi\rangle &= H|\psi\rangle, \\ -i\hbar\frac{\partial}{\partial t}\langle\psi| &= \langle\psi|H. \end{aligned} \tag{8.6}$$

Then, by differentiating the density matrix with respect to time and manipulating the equations in the form of the Schrodinger equation, we arrive at the von Neumann equation of motion, the quantum analogue of the classical Liouville equation:

$$i\hbar\frac{\partial\rho(t)}{\partial t} = [H, \rho]. \tag{8.7}$$

This equation holds for both the mixed state and pure state descriptions of the density matrix. The time evolution of the density matrix could alternatively be studied via the time operator $U(t, t_0) = e^{-\frac{i}{\hbar}H(t-t_0)}$, where $\rho(t) = U(t, t_0)\rho(t_0)U^\dagger(t, t_0)$ which can be used to prove the mixedness of the trace of $\rho^2$ is time-independent.

In this thesis however, we focus on the time evolution of the density matrix. Under the influences of noise, the evolution of the density matrix could be used to describe the system and its properties in its entirety via a master equation. This concept shall be built on in the following sections.

## 8.5 Appendix C: Stochastic Dynamics

### 8.5.1 Historical Note

The famous botanist, Robert Brown studied the irregular motion of pollen grains suspended in water, resulting in the concept, bearing his name, Brownian motion. Rayleigh was the first to take a statistical approach to the understanding of this behaviour, however it was not understood until 1905 when Einstein delivered a clear and elegant solution, based on

two major points: 1. the motion is caused by exceedingly frequent impacts on the pollen grain from the incessantly moving molecules in which it is suspended; 2. the motion of the molecules are so complicated, the effect can only be described probabilistically in terms of exceedingly frequent statistically independent impacts. Einstein's solution was based on a discrete time assumption which provided an approximate solution to the diffusion problem.

Langevin provided an alternative understanding to Einstein's reasoning, based on the kinetic theory of gas particles. From statistical mechanics, the mean kinetic energy of a Brownian particle in equilibrium could be expressed as the following:

$$\langle \frac{1}{2} m v^2 \rangle = \frac{1}{2} k_B T. \tag{8.8}$$

where $m$ represents the mass of the particle, $v$ the velocity, $k_B$ the Boltzmann constant and $T$ the temperature. Then there are two forces acting on the particle, viscous drag and the effective force of the incessant impacts between the molecules.

## 8.6 Langevin Equation

There is an underlying assumption in Langevin's reasoning, that the impacts are statistically independent.

Then, by Newton's second law,

$$m \frac{d^2 x}{dt^2} = -6\pi \eta_v r \frac{dx}{dt} + \chi, \tag{8.9}$$

where the left-hand side corresponds to Newton's second law, the first term on the right-hand side denoting the viscous drag, with $\eta_v$ representing the viscosity of the fluid and $r$ being the radius of the Brownian particle, and finally the last term corresponds to random fluctuations as a result of the incessant impacts due to the motion of the molecules of the fluid. This equation can be transformed into the following via integration with respect to x:

$$\frac{m}{2} \frac{d^2}{dt^2} x^2 = -3\pi \eta_v r \frac{d}{dt} x^2 + \chi x. \tag{8.10}$$

Averaging over a large number of particles,

$$\frac{m}{2}\frac{d^2}{dt^2}\langle x^2\rangle + 3\pi\eta_v r\frac{d}{dt}\langle x^2\rangle - k_B T, \tag{8.11}$$

where $\langle \chi x\rangle$ is taken to be zero due to the independency of $\chi$. The last term arises from using the equipartition theorem, where the average kinetic energy for a single particle is given by $\frac{m}{2}\langle(\frac{dx}{dt})^2\rangle = \frac{K_B T}{2}$. Under classical dissipation action, this random force must then satisfy the following,

$$\langle \chi(t)\chi(t')\rangle = \int D[\chi]\chi(t)\chi(t')e^{-\frac{1}{4k_B T}\int dt\chi^2(t)} = 2k_B T\delta(t-t'). \tag{8.12}$$

This describes a white noise term. Then the general solution is given as:

$$\frac{d}{dt}\langle x^2\rangle = \frac{k_B T}{3\pi\eta_v r} + Ce^{\frac{-6\pi\eta_v at}{m}}, \tag{8.13}$$

where $C$ is some constant. For practical approximations, one can neglect the exponential decay term and integrate the result to obtain the following:

$$\langle x^2\rangle - \langle x_0^2\rangle = \frac{k_B T}{3\pi\eta_v r}t. \tag{8.14}$$

Langevin's equation was the first stochastic differential equation. A stochastic process describes a system evolving probabilistically due to the influences of a time dependent random variable.

Since, descriptions of this nature have shifted towards continuous evolutions. These random influences can be modelled in many different ways depending on their nature[25]. The impacts of noise for these systems can vary greatly from its deterministic counterpart. A system's behaviour can be modelled in terms of slowly varying state variables and rapidly changing random forces. In order to describe stochastic dynamical equations, one must consider dynamical contributions from both the slowly changing deterministic part as well as the fast changing random part as given by Langevin's work which allows for considering the deterministic and stochastic dynamical contributions separately.

Random forces can be classified as either internal or external noise contributions. Distinguishing between these different types, depends on the boundary between the system and the external noise. External noise is considered to be imposed on a subsystem by a larger

changing environment. Often, external noise is characterised with correlation times much less than the characteristic time whereas internal noise is described with comparable correlation and characteristic times, often modelled via Langevin equations. For nonlinear systems, noise can act as a driving force.

Classical systems experience random perturbations. These arise from a multitude of factors, primarily these effects are accredited to thermal fluctuations. The trajectories of a classical bodies subject to noise can be described by the Langevin equation[58]. Consider a massless particle under the effects of a fluctuating force $\chi$. In a more general setting, the Langevin equation for this model is given by,

$$\ddot{x} = -\gamma\dot{x} - V'(x) + \chi(t), \tag{8.15}$$

where $x$ denotes the position, $V(x)$ is the potential and $\gamma$ is a scalar. This describes a Newtonian equation with a friction force $\chi(t)$ modelled as a random variable[58]. The different solutions to the Langevin equation correspond to different random trajectories[58]. Under the Langevin model, it is necessary that $\chi$ is irregular and the dynamics are independent of $\chi$, this criterion follows from the central limit theorem (detailed in Sec. 8.7.5). This equation could be rewritten as the following:

$$\frac{dx}{dt} = a(x,t) + b(x,t)\eta(t), \tag{8.16}$$

where $x$ is a variable under the influence of noise, $a(x,t)$ and $b(x,t)$ are known functions. Here, $\eta(t)$ denotes a white noise term which has strong connections in diffusion processes.

In order to obtain a considerable study of this type of equation, it is necessary to determine the properties of the random force. Often, once assumes the random force has a very small correlation time compared with the characteristic time of the system about a locally stable state, then it is justifiable to consider the random force to have zero correlation time, modelled as white noise.

In this setting, all frequencies in the power spectrum, $s(\omega)$ have equal weighting, given by the following:

$$s(\omega) = \int_{-\infty}^{\infty} \langle \xi(t)\xi(s)\rangle e^{-i\omega t} dt = 2D, \tag{8.17}$$

where $D$ is a constant. This describes white noise properties where there are several, well-

understood classes of these terms, defined by the derivative of $\xi(t)$ for stationary processes of independent increments. Beyond white noise models, consider the Ornstein - Uhlenbeck description for coloured noise.

### 8.6.1 Coloured Noise

Physically, white noise models are never exactly realised, however for systems dominated by noise, white noise models provide identical predictions to experimental results. When noise does not dominate, stochastic noise models with zero correlation time leads to stochastic realisations with non-continuous noise sample paths which are unphysical in reality. State variables are driven by white noise, have sample paths with unbounded variation which is neither continuous nor differentiable hence dynamical predictions based on these models have timescales beyond the regime of validity in the system, as such some systems benefit from more physically realistic stochastic models where noise has finite correlation time $\tau_c$[59]. As mentioned in the previous section, this corresponds to a coloured noise description, characterised by the following:

$$\langle \chi(t)\chi(s)\rangle = \frac{D}{\tau_c} e^{-\frac{|t-s|}{\tau_c}}. \tag{8.18}$$

This is referred to as an Ornstein-Uhlembeck process, describing coloured noise driven flows, where $\epsilon$ denotes the noise amplitude and $\eta$ is a white noise term.

$$d\chi = -\tau_c \chi dt + \epsilon \eta dt. \tag{8.19}$$

This description for noise is more challenging than the Markovian dynamics governing white noise models, however it is a more realistic model accounting for finite correlation times such that the noise term is differentiable. However, despite coloured noise being more realistic, white noise is still an excellent choice in modelling the combined effects of many weakly coupled environmental degrees of freedom outside critical neighbourhoods such that the noise on a system is described by the central limit theorem[26]. This states that a random variable composed of many independent random components, is Gaussian distributed as described by white noise.

In the case that $\xi(t)$ is Markovian, Doob's theorem states that $\xi(t)$ is necessarily an Ornstein-Uhlembeck process with exponential correlation function described by Eq. (8.18) with a Lorentzian power spectrum given by:

$$s(\omega) = \frac{2D}{\tau_c^2\omega^2 + 1}. \tag{8.20}$$

The absorption spectrum for coloured noise of arbitrarily long $\tau_c$, can be used to a Lorentzian spectrum in the white noise limit:

$$I_0(\omega - \omega_0) = \frac{1}{\pi}\frac{D}{(\omega - \omega_0)^2 + D^2}. \tag{8.21}$$

Another interesting class of coloured noise is when the noise term is described by, $Z(t) = a(-1)^{-n(t)}$ where

$$\langle Z(t)Z(s)\rangle = a^2 e^{-\lambda|t-s|}, \tag{8.22}$$

where $a$ and $\lambda$ are constants. This describes both telegraphic noise and dichotomous noise, particularly useful for modelling nonlinear coloured noise flows, Eq. (8.18), which provides an exact, retarded closed master equation and thus has stationary probabilities.

## 8.7 Appendix D: Master Equation

Modelling the random nature of a system via stochastic differential equations imposes the implication that the deterministic and stochastic components arise from independent origins. This is an unrealistic assumption which requires the study of fluctuation-dissipation arguments in order to rationalise an SDE model. However, measurable results can be obtained from considering the statistical properties of the random solutions. By measuring a random variable at different instances, one can form a probability distribution function over the random variable at each of the different instances it is measured hence modelling the stochastic dynamics of a system[58]. This can be explored using master equations, which encapsulate the complete description of a system. A simple example of such an equation is as follows, let $P_i(t)$ denotes the probability of a system being in a classical/quantum state $i$ at time $t$, then one can construct a simple master equation given by:

$$\frac{dP_i(t)}{dt} = \sum_j (W_{ij}P_j - W_{ji}P_i), \tag{8.23}$$

where $W_{ij} \geq 0$ for all $i, j$ and $W_{ii} = 0$, denoting the rate of transition from state $i$ to $j$. A corollary of this is that given $W_{ij} \geq 0$, then $P_i(t = 0) \geq 0$ which implies that $P_i(t) \geq 0$ for all $t \geq 0$. In the quantum sense, Eg.(8.23) corresponds to Fermi's Golden rule of states, where $W_{ij}$ takes the form,

$$W_{ij} = \frac{2\pi}{\hbar}|\langle i|V|j\rangle|^2\rho(E_j), \tag{8.24}$$

where $E_j$ denotes the eigenvalue of the system at state $|i\rangle$, $V$ represents the potential resulting in the transition and $\rho(E_j)$ is the density of states at $E_j$. the formal solution to this is determined from considering both left and right eigenvectors, $\phi_i^\alpha$ and $\psi_i^\alpha$, respectively. From this, the characteristic polynomial is used to investigate the relationship between these two given that the eigenvalues are the same. As a consequence, one arrives at the solution,

$$W_{ij} = \sum_\alpha \lambda_\alpha \phi_i^\alpha \psi_j^\alpha. \tag{8.25}$$

Then, in terms of the right eigenvectors (a similar result is found for the left eigenvectors),

$$P_i(t) = \sum_\alpha C_\alpha(t)\psi_i^\alpha. \tag{8.26}$$

Differentiating with respect to $t$, where linear independence in the eigenvalues gives $C_\alpha(t) = c_\alpha(0)e^{\lambda_\alpha t}$, then the complete form of Eq. (8.26) is as follows,

$$P_i(t) = \sum_\alpha C_\alpha(t)e^{\lambda_\alpha t}\psi_i^\alpha. \tag{8.27}$$

This dictates that $Re(\lambda_\alpha) \geq 0$, else there is negative probability. As $t \to \infty$, $P_i(t) \to P_i^{equilibrium}$, relaxing to $\lambda = 0$. In general, these dynamics are often difficult to investigate in complete form and so approximations are taken.

In considering such a description, it is necessary to realise the significance of macroscopic deterministic laws, where there is a shortcoming in the solution of any master equation approximation asymptotically in the deterministic and stochastic contributions describable by an SDE. Developing such asymptotic expansions provide developments of simpler models as given by the Fokker-Planck equation, equivalent to a master equation such that one could study an entire system simply from the Fokker-Planck equations without a master equation.

Both descriptions are highly valuable, they are advantageous for different systems. A list of such benefits however goes beyond the scope of this thesis.

### 8.7.1 Fokker-Planck Equation

The Fokker-Planck equation describes the evolution of the probability density of a particle for a certain class of stochastic differential equation;

$$dx_t = f(x_t, t)dt + g(x_t, t)dW_t, \tag{8.28}$$

where $f(x_t, t)$ denotes the drift coefficient, $g(x_t, t)$ is the diffusion coefficient and $W_t$ is Wiener process. The Fokker-Planck equation is given by the second order partial differential equation, providing an analogue of the Schrodinger equation that bridges from stochastic classical dynamics to quantum systems:

$$\frac{\partial \rho(x,t)}{\partial t} = -\frac{\partial}{\partial x}(f(x,t)\rho(x,t)) + \frac{1}{2}\frac{\partial^2}{\partial x^2}(g^2(x,t)\rho(x,t)), \tag{8.29}$$

where $\rho$ denotes the density with initial condition $\rho(x, t_0|x_0, t_0) = \delta(x - x_0)$. This describes the Fokker-Planck evolution of the probability distribution function of stochastic systems for a diffusive process under Ito regularisation, see Sec.8.7.2. Hamilton's equations for this system is given by the following:

$$\begin{aligned} \dot{\chi} &= \partial_p H(p, \chi), \\ \dot{p} &= -\partial_\chi H(p, \chi). \end{aligned} \tag{8.30}$$

It is especially suited to systems with short correlation times, providing an exact description for Gaussian white noise models. The structure of the Fokker-Planck equation is the same as that of the continuity relation. This can be demonstrated for the 1-time probability by the following;

$$p(x,t) = \int dx_0 p(x,t;x_0,t_0) = \int dx_0 p(x,t|x_0,t_0)P(x_0,t_0). \tag{8.31}$$

At $t_1$, the conditional probability at $t_1$ is then:

$$p(x_2,t_2|x_0,t_0) = \int_{-\infty}^{\infty} dx_1 p(x_2,t_2;x_1,t_1)p(x_1,t_1;x_0,t_0). \tag{8.32}$$

We note that the conditional probability $p(x_2,t_2;x_1,t_1)$ is independent of $(x_0,t_0)$, therefore the system is described by a Markov process. Then,

$$p(x,t+\delta t|x_0,t_0) = \int_{-\infty}^{\infty} dx' p(x,t+\delta t|x',t)p(x',t|x_0,t_0), \tag{8.33}$$

where

$$p(x,t+\delta t|x',t) = \delta(x-x') + A(x)\frac{d\delta(x-x')}{dx'}\delta t + \frac{1}{2}B(x)\frac{d^2\delta(x-x')}{dx'^2}\delta t. \tag{8.34}$$

Averaging over real variables and substituting into the integral for the conditional probability, dividing by $\delta t$ as $\delta t \to 0$, then one arrives at the standard Fokker-Planck equation; $\frac{\partial p(x,t)}{\partial t} = -\frac{\partial}{\partial x}(A(x,t)p(x,t)) + \frac{1}{2}\frac{\partial^2}{\partial x^2}(B(x,t)p(x,t))$.

Deriving this equation of motion for the probability density is based on finding a particle in the interval $(x;x_d x)$ and $(v,v+dv)$ at time $t$ for a single realisation of noise, $\xi(t)$. With the particle is located in the infinitesimal area $dxdv$ with probability $p(x,v,t)dxdv$. Since the particle must lie somewhere in the phase-space $-\infty < x,v < \infty$, then the following must be satisfied,

$$\int_{-\infty}^{\infty} dx \int_{-\infty}^{\infty} dv \rho(x,v,t) = 1, \tag{8.35}$$

where $\rho(x,v,t)$ denotes the probability density. Considering a finite volume, where the particle is not destroyed or changed, therefore any change must arise from changes in the probability through the surface $S_0$ surrounding initial volume, $V_0$, then:

$$\frac{d}{dt}\int\int_{V_0} dxdv\rho(x,v,t) = -\int_{S_0} \rho(x,v,t)\dot{\mathbf{x}}.\mathbf{ds}, \tag{8.36}$$

where $\mathbf{x} = (\mathbf{x},\mathbf{v})$ and $\dot{\mathbf{x}} = (\dot{\mathbf{x}},\dot{\mathbf{v}})$. Then by applying Gauss' theorem, the surface integral takes the following form:

$$\int\int_{V_0} dxdv\frac{d}{dt}\rho(x,v,t) = -\int\int_{V_0} dxdv\nabla.(\dot{\mathbf{x}}\rho(\mathbf{x},\mathbf{v},\mathbf{t})). \tag{8.37}$$

For some fixed arbitrary $V_0$, one obtains the continuity equation:

$$\frac{\partial}{\partial t}(\rho(x,v,t) = -\nabla.(\dot{\mathbf{x}}\rho(\mathbf{x},\mathbf{v},\mathbf{t})) = -\frac{\partial}{\partial \mathbf{x}}(\dot{\mathbf{x}}\rho(\mathbf{x},\mathbf{v},\mathbf{t})) - \frac{\partial}{\partial \mathbf{v}}(\dot{\mathbf{v}}\rho(\mathbf{x},\mathbf{v},\mathbf{t})). \tag{8.38}$$

This describes the continuity equation in the phase-space which states that the probability is conserved. By averaging over many realisations of noise, $p(x,v,t) = \langle\rho(x,v,t)\rangle$, where $p(x,v,t)$ macroscopic probability density of the particle. A second order differential equation that corresponds to a time dependence via the Langevin equation. It is exact for Gaussian white noise models, governing the evolution of the probability density of a Brownian particle.

For a Brownian particle, it is necessary to know the Langevin equation governing the evolution of a particle, given by the following:

$$\dot{x} = v\dot{v} = \frac{-\gamma}{m}v + \frac{1}{m}(F(x) + \xi(t)), \tag{8.39}$$

where $F(x) = V^{`}(x)$ for some potential $V$. This is used to obtain an exact description of the dynamics under the influence of noise such that the Fokker-Planck equation is then given as,

$$\begin{aligned}\frac{\partial\rho(x,v,t)}{\partial t} &= -\frac{\partial}{\partial x}(V(x)\rho(x,t)) + \frac{\gamma}{m}\frac{\partial}{\partial v}(V(x)\rho(x,v,t)) \\ &\quad -\frac{1}{m}F(x)\frac{\partial}{\partial v}\rho(x,v,t) - \frac{1}{m}\xi(t)\frac{\partial}{\partial v}\rho(x,v,t).\end{aligned} \tag{8.40}$$

Here, $\xi(t)$ is a stochastic variable, $\rho(x,v,t)$ is in principle different for each realisation of $\xi(t)$. However, in actual Brownian particles, one observes an averaging in the random nature of $\xi(t)$. The Fokker-Planck equation can be solved using a stochastic integral, for this it is neccesary to consider Ito formalism.

### 8.7.2 Ito Calculus

To solve the Fokker-Planck equation, one must define the stochastic integration procedure. Let $G(t)$ and $W(t)$ be stochastic processes and consider the following:

$$\int_{t_0}^{t} G(t')dW(t'). \tag{8.41}$$

It is challenging to compute this integral as it changes randomly due to the stochastic terms. Discretising the integral into $n$ subintervals with $t_0 \leq t_1 \leq \cdots \leq t_{n-1} \leq t$, with intermediate points $t_{i-1} \leq \tau_i \leq t_i$, the integral is then defined as the limit of partial sums $S_n$,

$$S_n = \sum_{i=1}^{n} G(\tau_i)(W(t_i) - W(t_{i-1})). \tag{8.42}$$

This limit is dependent on the choice of $\tau_i$. Taking $\tau_i = t_i$, we arrive at the Ito stochastic integral:

$$\int_{t_0}^{t} G(t')dW(t') = (meansquarelimit) - lim_{n\to\infty}\left(\sum_{i=1}^{n} G(t_{i-1})(W(t_i) - W(t_{i-1}))\right). \tag{8.43}$$

Properties of the Ito stochastic integral include the following:

a) Existence: The integral defined by Eq. (8.41) exists when $G(t')$ is continuous and nonanticipating (a process that cannot see the future) on $[t_0, t]$.

b) Integration of polynomials are given as follows:

$$\int_{t_0}^{t} W(t')^n dW(t') = \frac{1}{n+1}(W(t)^{n+1} - W(t_0)^{n+1}) - \frac{n}{2}\int_{t_0}^{t} W(t')^{n-1}dt'. \tag{8.44}$$

One arrives at this result from considering the following random process, $d(W(t))^n = (W(t) + dW(t)) - W(t)^n = \sum_{r=1}^{n} nCrW(t)^{n-r}dW(t)^r$, where $dW(t)^r \to 0$ for all $r > 2$. Consequently, $dW(t)^n = nW(t)^{n-1}dW(t) + \frac{n(n-1)}{2}W(t)^{n-2}dt$ which integrates to the above result.

c) For every $G(t)$, there exists two kinds of integrals, that described in Eq. (8.41) and $\int_{t_0}^{t} G(t')dt'$ where there is no connection between these two integrals.

d) Differentiation keeps up to the second order of $dW(t)$. Consider the general chain rule, $df(W(t), t) = \frac{\partial f}{\partial t}dt + \frac{1}{2}\frac{\partial^2 f}{\partial t^2}(dt)^2 + \frac{\partial f}{\partial W(t)}dW(t) + \frac{1}{2}\frac{\partial^2 f}{\partial W(t)}(dW(t))^2 + \frac{\partial^2 f}{\partial W(t)\partial t}(dW(t))dt + \ldots$ where, $(dt)^2 \to 0, dtdW(t) \to 0, (dW(t))^2 = dt$ and all higher orders vanish, then this chain rule takes the following form:

$$df(W(t),t) = \left(\frac{\partial f}{\partial t} + \frac{1}{2}\frac{\partial^2 f}{\partial W(t)^2}\right)dt + \frac{\partial f}{\partial W(t)}dW(t). \tag{8.45}$$

The reasoning used here applies to all other differentiation rules. Similarly, this is used to define the change of variables in Ito formalism with, $df(x(t)) = (a(x(t),t)f'(x(t)) + \frac{1}{2}b(x(t),t)^2 f''(x(t)))dt + b(x(t),t)f'(x(t))dW(t)$

e) The mean value formula, for a nonanticipating G(t) takes the form $\langle\int_{t_0}^{t} G(t')dW(t')\rangle = 0$ such that $\langle\sum_i G_{i-1}\Delta W_i\rangle = \sum_i\langle G_{i-1}\rangle\langle\Delta W_i\rangle = 0$.

f) The correlation formula for arbitrary nonanticipating functions $G(t)$ and $H(t)$;

$$\langle\int_{t_0}^{t} G(t')dW(t')\int_{t_0}^{t} H(t')dW(t')\rangle = \int_{t_0}^{t} dt'\langle G(t')H(t')\rangle. \tag{8.46}$$

Under this formalism, we see that the Langevin equation Eq. (8.16) obeys an Ito stochastic differential equation such that $dx(t) = a(x(t),t)dt + b(x(t),t)dW(t)$ if for all $t \in [t_0,t]$, $x(t) = x(t_0) + \int_{t_0}^{t} dt' a(x(t'),t') + \int_{t_0}^{t} dW(t')b(x(t'),t')$. Taking a discretised version of this with $t_0 < t_1 \ldots t_{n-1} < t_n = t$, then $x_{i+1} = x_i + a(x_i,t_i)\Delta t_i + b(x_i,t_i)\Delta W_i$ where $x_i = x(t_i), \Delta t_i = t_{i+1} - t_i, \Delta W_i = W(t_{i+1}) - W(t_i)$ then to calculate $x_{i+1}$, requires taking increments of the Weiner process, being statistically independent of $x_i$. One can determine the solution iteratively, with $x_i$ always independent of $\Delta w_j$ for all $j \geq i$.

Under Ito formula, one can obtain the the Fokker-Planck description of a stochastic system. Take the following:

$$\begin{aligned}\frac{\langle df(x(t))\rangle}{dt} &= \left\langle\frac{df(x(t))}{dt}\right\rangle \\ &= \frac{d}{dt}\langle f(x(t))\rangle \\ = \langle a(x(t),t)\frac{\partial}{\partial x}f(x(t)) &+ \frac{1}{2}b(x(t),t)^2\frac{\partial^2}{\partial x^2}f(x(t))\rangle,\end{aligned} \tag{8.47}$$

where $x(t)$ has conditional probability, $p(x,t|x_0,t_0)$, then:

$$\begin{aligned}\frac{d}{dt}\langle f(x(t))\rangle &= \int dx f(x)\frac{\partial}{\partial t}p(x,t|x_0,t_0) \\ = \int dx(a(x(t),t)\frac{\partial}{\partial x}f(x(t)) &+ \frac{1}{2}b(x(t),t)^2\frac{\partial^2}{\partial x^2}f(x(t)))p(x,t|x_0,t_0).\end{aligned} \tag{8.48}$$

Integrating by parts and disregarding surface terms,

$$\begin{aligned} &\int dx f(x(t)) \frac{\partial}{\partial t} p(x,t|x_0,t_0) \\ &= \int dx f(x(t))(-\frac{\partial}{\partial x}(a(x(t),t)p(x,t|x_0,t_0)) + \frac{1}{2}\frac{\partial^2}{\partial x^2}(b(x(t),t)^2 p(x,t|x_0,t_0)). \end{aligned} \tag{8.49}$$

Then since $f(x)$ is arbitrary, one obtains the standard Fokker-Planck equation. This is equivalent to a diffusion process defined by drift coefficient $a(x,t)$ and diffusion coefficient $b(x,t)$.

The solution of this Ito stochastic differential equation, $x(t)$ is a Markov process. Given the initial conditions $x(t_0)$, the future is uniquely determined. Then for all $t \geq t_0$, $x(t)$ is determined only from the sample path $W(t)$ and its initial value $x(t_0)$. If the stochastic differential equation depends continuously on a parameter, then the solution normally depends continuously on that parameter hence the solution depends continuously on the initial condition. This justifies the use of perturbation expansions.

This can be used to consider quantum noise. Furthermore, extending the Fokker-Planck equation to multi-variable Ito-Langevin processes[58]. In the quantum setting this equation is generalised by the Lindblad master equation, concerning the density matrix.

One can determine the statistics of a quantum system from its density matrix $\rho$ containing all measurable information of a Hamiltonian system, where the diagonal terms describe the occupation of the quantum states[13] and the off-diagonal terms correspond to the coherences.

One can describe random fluctuations using auto-correlation functions as described in the previous section. Noise can also be studied using its spectral density[25], given by:

$$S_\chi(t) = lim_{T\to\infty} \frac{\langle|\chi(t;t_0|^2\rangle}{T}. \tag{8.50}$$

Under the Wiener-Khinchin theorem which states that $2\pi\delta(t-t')S_\chi(t) = \langle\chi(t)\chi(t'\rangle$, one can describe the spectral density from the auto correlation function. This type of dynamics is relevant to the development of adiabatic quantum computers faces the same fundamental problem of impossibility of their direct simulation by classical means[1, 2, 3, 4]. This stimulates the search for alternative theoretical methods, which could provide some useful figures-of-merit describing large quantum systems out of equilibrium. A common approach to achieve quantum coherence in non-equilibrium many body dynamics is Keldysh Green function theory[30], however this approximation is limited to short time intervals where its

errors grow as a power of time[30].

### 8.7.3 Markov Processes

Consider a stochastic process continuously defined in time, $\chi_t; t \geq 0$ where $\chi_t$ is a one-parameter family of random variables. Then $\chi_t$ is a Markov process if for all time $t \geq \tau$, the distance between any $\chi_t$ against the family of variables $\chi_{s\in[0,\tau]}$ satisfies

$$Dist(\chi_t|\chi_{s\in[0,\tau]}) = Dist(\chi_t|\chi_\tau), \tag{8.51}$$

suggesting that if the conditional distribution of $\chi_t$ is conditioned on the family of events $\chi_s$ in times $s \in [0, \tau]$ is the same as being conditioned only only on the event at time $\tau$, then the process is Markovian. This implies that the state of the system at time $t$, $\chi_t$ depends only on the past between $[0, \tau]$ via the state of the system at its last past interval of $\tau$, such that all the information of the past is condensed into the previous moment. The system carries memory of its past instances, hence depends on the initial value of $\chi_0$.

The expectation of a Markov process is described through $E_x(\phi(\chi_t))$, where we let $E_x$ denote the expectation of a process starting from $x \in R^d$ or $Z^d$ and $\phi$ be the state space of the observables. Then,

$$E_x(\phi(\chi_t)) = E(\phi(\chi_t)|\chi_0 = x). \tag{8.52}$$

Markov processes are described by their generators which are operators acting on observables $\phi$. Then a Markovian generator is defined as:

$$(L\phi)(x) = \frac{d}{d\epsilon}|_{\epsilon=0} E_x\phi(\chi_\epsilon). \tag{8.53}$$

In $R^d$, a Wiener process is Markovian, with generator $L = \frac{1}{2}\Delta$. This applies to white noise models.

### 8.7.4 Wiener Processes

In order to define a Weiner process, it is first necessary to define both a continuous time process and a stochastic Gaussian process.

**Continuous time process:** A collection of uncountable many random variables where the joint probability measure on such a big space cannot be determined by finite dimensional projections.

**Stochastic Gaussian process:** given that any finite dimensional projection is a Gaussian vector-valued random variable such that for all $t_1 < t_2 < \dots t_k$, the vector $\chi_{t_1}, \dots \chi_{t_n}) \in R^d$ is a Gaussian random variable.

A continous stochastic Gaussian process $W_t = (W_t^1, \dots W_t^d) \in R^d$, where $t \geq 0$ is a d-dimensional Weiner process if it satisfies the following properties[26]:

$$\begin{aligned} W(0) &= 0, \\ E(W_t) &= 0, \\ E(W_s^a W_t^b) &= min(s,t)\delta_{ab}, \\ W(t) - W(s) &= \sqrt{t-s}N(0,1); 0 \leq s < t \leq T, \end{aligned} \tag{8.54}$$

where $N(0,1)$ denotes a normal distribution and $E(.)$ describes the expectation of a process. This determines a Weiner process uniquely, where all higher moments of $W_t$ can be determined by Wick's theorem. Moreover, this enables extending the central limit theorem to processes.

Consider the stochastic process $\chi_T^\epsilon = \sqrt{\epsilon}\sum_{i=1}^{T/\epsilon}$. The distribution for this process converges to the Weiner process; $\chi_T^\epsilon \to W_T$ as $\epsilon \to 0$. This type of process defines white noise, formulating the requirements in the application of the central limit theorem as utilised in the Brownian motion description of diffusion processes. Provided that damping effects dominate the system such that internal forces can be considered negligible, Brownian motion is a well suited model for noise. It is one of the simplest stochastic processes, arising as a limit of multiple stochastic processes such that all other diffusion processes could be described in terms of Brownian motion. Hence solutions of various mathematical problems could be expressed in terms of Brownian motion. This concept is summarised in the central limit theorem.

### 8.7.5 The Central Limit Theorem

Let $v_i$ be a sequence of independent, identically distributed random variables with zero expectation; $E(v_i) = 0$ and finite variance $E(v_i^2) = \sigma^2$, where $v_i \in R^d$ or $v_i \in Z^d$, for $d > 1$ and the variance $\sigma^2$ is a matrix, referred to as the covariance matrix such that $\sigma_{ab}^2 = E(v^a v^b)$ where $v = (v^1 \dots v^9)$.

Then, determining the location of a particle under the influence of multiple sources of noise

after $n$ steps is described as,

$$S_n = \sum_{i=1}^{n} v_i, \tag{8.55}$$

where, $E(S_n) = 0$, $E(S_n^2) = \sum_{i=1}^{n} E(v_i^2) = n\sigma^2$ and $E(v_i v_j) = 0$.

Rescaling $S_n$,

$$\chi = \frac{S_n}{\sqrt{n}} = \frac{\sum_{i=1}^{n} v_i}{\sqrt{n}}, \tag{8.56}$$

preserving the structure such that $E(\chi_n) = 0$ and $E(\chi_n^2) = \sigma^2 < \infty$. This defines a centred Gaussian process; centered because $E(\chi_n) = 0$. This has the property that all the moments of moments are determined from the covariance matrix. Then, for a centred Gaussian vector-valued random variable, higher moments can be computed via Wick's theorem;

$$E(\chi_1 \dots \chi_{2k}) = \Pi_{(i,j)\in all possible pairings} E(\chi_i \chi_j). \tag{8.57}$$

Remarkably, this distribution for the independent, identically distributed (iid) $v_i$ tends to a Gaussian distribution $\chi_n \to \chi$ where $\chi$ $N(0, \sigma^2)$ as $n \to \infty$, regardless of the initial distribution of $v_i$, defining the central limit theorem, a cornerstone of probability theory and one of the fundamental theorems of nature.

The density of this normal distribution in $R^1$ is given as follows,

$$f(x) = \frac{1}{\sqrt{2\pi}\sigma} e^{-\frac{x^2}{2\sigma^2}}. \tag{8.58}$$

This density follows the standard weak convergence of probability measures which states that a sequence of random variables $\chi_n$ converges to a random variable $\chi$ which is normally distributed, if the expectation satisfies $E(G(\chi_n)) \to E(G(\chi))$ for any continuous bounded function $G$, as such $\chi_n$ can be modelled via a white noise, justifying that random forces are uncorrelated hence reducible to Markovian white noise processes. This definition holds analogously for higher dimensions. It is under this theorem, that forms the foundations of both Einsein's and Langevin's reasoning as given in Appendix C, complemented with a summary of stochastic dynamics beyond white processes.

## 8.8 Appendix E: Integrable Dynamics

Integrable systems are exactly solvable models, however such solutions are difficult to obtain. One method to solve a problem is using quadratures which involves either solving a finite number of algebraic equations or computing a finite number of integrals. Obtaining closed form solutions however, remains a challenge.

Consider a Hamiltonian in $R^{2n}$, the associated Hamilton's equations are as follows:

$$\begin{aligned} \dot{p}_i &= -\frac{\partial H(p_i, q_i)}{\partial q_i}, \\ \dot{q}_i &= \frac{\partial H(p_i, q_i)}{\partial p_i}, \end{aligned} \tag{8.59}$$

where $i \in [1, n]$ and '.' represents derivatives taken with respect to time. These can be written in terms of Poisson brackets which can be defined by the following:

$$\{F, G\} = \sum_{i=1}^{n} \frac{\partial F}{\partial p_i}\frac{\partial G}{\partial q_i} - \frac{\partial F}{\partial q_i}\frac{\partial G}{\partial p_i}. \tag{8.60}$$

This description satisfies antisymmetric, linear and multiplicative product rule properties as well as the Jacobi identity, hence it is a Lie algebra. Then Hamilton's equations can be written as,

$$\begin{aligned} \dot{p}_i &= -\{p_i, H(p_i, q_i)\}, \\ \dot{q}_i &= \{q_i, H(p_i, q_i)\}. \end{aligned} \tag{8.61}$$

Poisson algebras can be used to determine the integrals of a Hamiltonian system. A function $F(p_i, q_i)$ on the phase space, is an integral of the Hamiltonian $H(p_i, q_i)$ if it is preserved by the flow, $\dot{F} = \{F(p_i, q_i), H(p_i, q_i)\} = 0$. Hence $F$ is a conserved quantity, that Poisson commutes with the Hamiltonian.

The Poisson theorem, further states that the Poisson bracket of 2 integrals is an integral of the same Hamiltonian. This description is used to identify integrals of motion in a given system and determine its solvability. A Hamiltonian system, $H(p_i, q_i)$ is completely integrable in the Liouville sense if there are $n$ independent functions that are mutually Poisson commuting, with $H(p_i q_i)$ being a function of these. The maximal number of Poisson commuting independent functions is $n$, however it is possible to obtain further integrals of motion of the Hamiltonian system under an algebra of integrals of motion. The harmonic

oscillator and the Calogero-Moser models are examples of such integrable systems, the latter shall be discussed further in this section.

The quadratures of complete integrable systems are often achieved through the separation of variables of the Hamilton-Jacobi equation. These can be used to investigate maximally superintegrable systems which are separable in more than one coordinate system, with all bounded orbits being closed as well as giving rise to interesting Poisson algebras with polynomial Poisson relations. Such superintegrable systems have various naturally occurring applications in physics with additional hidden symmetries. Furthermore, these systems carry interesting extensions to quantum integrable systems, however these concepts go beyond the scope of our work.

### 8.8.1 Calogero-Sutherland-Moser

The Calegero-Sutherland model (CSM) has a great range in applications from quantum field theory, condensed matter theory, statistical mechanics, collective field theory, dynamical systems, pure mathematics and chaos. It describes a1D many-body integrable system, generating the dynamics of $N$ particles interacting via a long-range potential. The corresponding Hamiltonian is given by:

$$H = \frac{1}{2}\sum_{i=1}^{N} v_i^2 + \sum_{i<j} \frac{\gamma^2}{(x_i - x_j)^2}. \tag{8.62}$$

Taking unit mass and $\gamma^2$ to denotes a positive coupling constant, describing the strengths of the interparticle pairwise repulsions. As a consequence of the coupled interactions, the CSM describes a strongly correlated system that offers insight of many-body interacting systems that is both easy to formulate as well as explicitly solvable. This description maps spectral properties to that of classical particles, which is an area of quantal systems; such that one can regard quantum systems through its eigenvalue dynamics, statistically via a classical integrable model.

Being a fully integrable model, the particles evolve in an ordered way with the following equations of motion:

$$\begin{aligned} \dot{x}_m &= v_m, \\ \dot{v}_m &= 2\sum_{m\neq n} \frac{\gamma^2}{(x_m - x_n)^3}. \end{aligned} \tag{8.63}$$

From these equations, one observes how the inverse-square potential acts as a borderline between the presence of a phase transitions (when the potential is strong) and when there are none (for weak potentials).

This allows for investigating the statistical mechanics of phase transitions which occurs when levels approach each other, reaching a minimum separation before repelling. These are known as avoided crossings or anti-crossings. At an avoided crossing, it may not be possible to distinguish between the quantum states in the event of the occurrence of a phase transition, thus is necessary to treat such events statistically. In considering large quantum systems, the probability of level (avoided) crossings become more significant. These result in transitions between states[3, 4, 24, 43]. Using the Landau-Zener model, one can approximate the changes in the occupation numbers as a consequence of level (avoided) crossings. Avoided crossings occur when levels come in the vicinity of each other with $\delta_m \neq 0$ before they repel. Landau-Zener probabilities at level (avoided) crossings describe the fundamental results of nonstationary quantum mechanics. These describe the non-adiabatic population transfer at a level (avoided) crossing for perturbed Hamiltonian systems[43, 53]. Since the discovery of the Landau-Zener formula, there has been continuous efforts in its theoretical treatment[53]. The Landau-Zener model has been profficient in the analytical description of the occupation numbers with regard to the presence of noise[43]. However, in order to gain insight on coherences and the difference found between ground state coherences and intermediate state transition probabilities, it is better to consider the description using density matrices. These such transitions could be better described under the generalised Calogero-Sutherland model; the Pechukas-Yukawa formalism, where the coupling strengths are no longer constants but dynamic variables.

## 8.9 Appendix F: Method of Lax Pairs

For two matrices $L(p_i, q_i), M(p_i, q_i)$ with their entries being functions on the phase space. If the equations of motion can be described by:

$$\dot{L} = [L, M], \tag{8.64}$$

then, $L$ and $M$ are said to be Lax pairs for the system. One crucial importance in this formalism, is that the equations of motion for $L$ expressed in Lax pairs generates conserved quantities, $F_k$;

$$F_k = Tr(L^k) \tag{8.65}$$

This follows from the equations of motion by cyclicity of the trace operator.

$$\dot{F}_k = kTr(L^{k-1}[L, M]) = 0. \tag{8.66}$$

This demonstrates that the Lax matrix $L$ is isospectral; its eigenvalues are constant. The flow given by Eq. (8.64), preserves the spectrum of $L$. Then it is possible to solve the time dependence in $L$ explicitly, following directly from the Lax equation:

$$\begin{aligned} L(t) &= g(t)L(0)g^{-1}(t), \\ M &= \dot{g}(t)g^1(t). \end{aligned} \tag{8.67}$$

This states that any isospectral deformation on $L(t)$ is described as in the above equation. Then, for any matrix $M^{'}$ such that $[L, MM^{'}] = 0$, $L, M^{'}$ also forms a Lax pair. This enables generating all constants of motion in the system.

The integrals of motion are determined from the coeffiients of the characteristic polynomial, determined from, $det(L - \lambda I)$ where $I$ denotes the identity matrix in dimension $n$ and $L$ is an $n \times n$ matrix, then the coefficients of the characteristic polynomial are given by:

$$det(L - \lambda I) = \sum_{k=0}^{n} \lambda^k I_k(p, q), \tag{8.68}$$

where $I_k$ represents the integrals of motion, used to determine the constants of motion. Furthermore, any power matrix $L^k$ also satisfies the Lax equation, hence one can determine generate all constants of motion for the system in this way.

For Lax pairs evolving parametrically through a spectral parameter $\gamma$, such that $L(\gamma) = \sum_{i=1}^{a} L_i\gamma^i$ and $M(\gamma) = \sum_{i=1}^{b} M_i\gamma^i$, then one can construct matrices such that the generated conserved quantities are determined from summing along the diagonals of the upper triangle commutator. This suggests any $\gamma$-dependent Lax pair is equivalent to an ordinary Lax pair, with greater number of conserved constants.

Moreover, using Lax formalism, it is possible to generate further integrable systems from an existing Lax pair. Consider the generalised equation of motion for Lax pairs, $L, M$:

$$\dot{L} = [L, M] + \gamma L, \tag{8.69}$$

for some constant $\gamma$. The corresponding set of equations of motion define an integrable system with first integrals $I_k = Tr(L^k)e^{k\gamma}t$. these relationships cannot be obtained naturally from the Hamiltonian, hence the Lax formalism provides further insights on the constants of motion in the system.

These concepts are explored further to investigate classical integrable models describing quantum systems, as in the case for the Calogero-Moser system as well as in our works on the Pechukas-Yukawa model.

## 8.10 Appendix G: Python Code

### 8.10.1 Investigating the Accuracy of the Factorisation Approximation

**Probability Distribution Functions**

```
Created on Sun Jun  5 12:04:46 2016
"""
import numpy as np
import time
from copy import copy
import pickle
from itertools import permutations as Perm
from math import factorial

start_time = time.time()
print("Setting up system parameters...")|

#System parameters
N = 4
Simulations = 100
dt = 0.1
timestep = np.arange(0,1,dt)
#uniformly divide interval (0,1) by increments of dt
```

```
J = np.random.randn(Simulations,1)
#creates a matrix of standard Gaussian vars with N columns, Simulations rows
J = np.hstack((J,-J,-J,J))

#define Hamiltonian and perturb matrix
h1,h2=0.01,0.02
Hb=np.matrix([[0,h2,h1,0],
              [h2,0,0,h1],
             [h1,0,0,h2],
            [0,h1,h2,0]])

XRange = ( -(3+h1+h2) , 3+h1+h2 )
VRange = ( -(h1+h2) , h1+h2)
LRange = ( -(3 + pow(h1,2) + pow(h2,2)) , (3 + pow(h1,2) + pow(h2,2)) )

print("Setting up system parameters completed", round(time.time()-start_time,2), "s\n")

print("Computing eigenvalues, velocities, momentums...")
# Creating a multi-dimensional matrix containing
# eigenvalues , X and velocities V and relative mom, L
#via a nested loop (nested so it is matrix-like)
# X entries to  read as X[timestamp][Simulation][i'th eigenvalue]
x=[[np.linalg.eigvalsh(np.diag(J[Sim, : ]) + timestep[ti]*Hb)
for Sim in range(Simulations)] for ti in range(timestep.size)]
x = np.reshape(x,((timestep.size,Simulations,N)))

#reshaping for matrix entries, seperate lines to be easier on the eyes!
v=(x[1:]-x[:-1])/dt

print("Computing eigenvalues, velocities, momentums done",
round(time.time()-start_time,2), "s\n")

data = [x,v, Hb, J]
print("Saving data...", round(time.time()-start_time,2), "s")
pickle.dump(data,open('data.pk','wb'))
print("Saving data...complete", round(time.time()-start_time,2), "s\n")
```

```
del data


#=============================================================================
#                                  build f1(t,x1,v1)
#=============================================================================
print("Building f1...")
f1=dict()
f1_normalisation_const = N*Simulations
All_x = np.reshape(x,((timestep.size,Simulations*N)))
All_v = (All_x[1:]-All_x[:-1])/dt
for ti in range(timestep.size-1):
    data = np.vstack((All_x[ti],All_v[ti]))
    hist, edges = np.histogramdd( data.transpose(), bins = 20, range = (XRange,VRange))
    f1[ti] = hist/f1_normalisation_const
    print("\tAt ti, f1 summed:" , f1[ti].sum().sum().sum().sum())
print("Building f1...complete", round(time.time()-start_time,2), "s\n")

print("Saving f1...", round(time.time()-start_time,2), "s")
pickle.dump(f1,open('f1.pk','wb'))
print("Saving f1...complete", round(time.time()-start_time,2), "s\n")
del All_x, All_v, hist, edges, data


"""                                    build f2(t,x1,v1,x2,v2)

#1) Group up data in the form Xi=[xi,Vi] and arranged in a matrix indexed as
#X[time][Sim][1]=(x1,v1)
#2) Pick up first simulation and permute it. Call this PermutedX so we have shape
#3) Pick up remaining simulations in loop and combine via stacking below.
#4) Make historam and store in dictionary
"""
print("Building f2...")
s=2
f2=dict()
PermutedXList=list()
```

```
X = dict([ (ti, [[[x[ti+1][Sim][i],v[ti][Sim][i]] for i in range(N)]
for Sim in range(Simulations)]) for ti in range(timestep.size-1)])

for ti in range(timestep.size-1):
    PermutedX = np.vstack( np.array(list(Perm(X[ti][Sim])))
    for Sim in range(Simulations))

    PermutedX = PermutedX[:,:s,:].reshape((Simulations*factorial(N),2*s))

    PermutedXList.append(PermutedX) #added for building F2
    Hist,edges=np.histogramdd(PermutedX,bins = 20, range= (XRange,VRange,XRange,VRange)
    f2[ti]=Hist/(Simulations*factorial(N)),edges
    print("...completed ",str(ti+1), " out of " , timestep.size-1, "timesteps",
    round(time.time()-start_time,2), "s")

    print("\tAt ti, f2 summed:" , f2[ti][0].sum().sum().sum().sum())
del PermutedX, Hist
print("Building f2...complete", round(time.time()-start_time,2), "s\n")

print("Saving f2...", round(time.time()-start_time,2), "s")
pickle.dump(f2,open('f2.pk','wb'))
print("Saving f2...complete", round(time.time()-start_time,2), "s\n")
del f2


"""

                                        build h2(t,lmn,lnm)
h2[time] := h2(lmn,lnm)
Lmn[time] = [lmn of all simulations at t=time]
"""
#Getting the L matrix as a list of numbers
print("Building h2...", round(time.time()-start_time,2), "s")
h2=dict()
L=dict([ (ti,[[(x[ti][Sim][m]-x[ti][Sim][n])*Hb[m,n]
for n in range(N) for m in range(N)]
```

```
for Sim in range(Simulations)]) for ti in range(timestep.size)])

#L[time][simulation] = [12 lmn values]
[L[ti][Sim].pop(pow(N-i,2)-1) for i in range(N)
for Sim in range(Simulations) for ti in range(timestep.size)]

#removing diagonal entries [zero based recall] and
#going backwards due to the nature of "pop" (for each time and simulation)

PermutedLList = list() #using for F2

for ti in range(timestep.size):
    L12List = list()
    L21List = list()
    for Sim in range(Simulations):
        for l12 in L[ti][Sim]:
            TempList = copy(L[ti][Sim])
            TempList.pop(TempList.index(l12))
            for l21 in TempList:
                L12List.append(l12)
                L21List.append(l21)
    L12 = np.array(L12List).reshape(132*Simulations,1)
    #132 = 12*11 = (N^2 - N)!/(N^2 - N-s)!
    L21 = np.array(L21List).reshape(132*Simulations,1)
    L12_L21 =  np.hstack((L12,L21))
    hist,edges = np.histogramdd(L12_L21, bins = 20, range = (LRange,LRange) )
    h2[ti] = hist/(132*Simulations),edges
    print("\tAt ti, h2 summed:" , h2[ti][0].sum().sum().sum().sum())
    PermutedLList.append(L12_L21)

del hist, L12_L21, L12, L21, L12List, L21List, TempList
print("Building h2...completed", round(time.time()-start_time,2), "s\n")

print("Saving h2...", round(time.time()-start_time,2), "s")
pickle.dump(h2,open('h2.pk','wb'))
print("Saving h2...complete", round(time.time()-start_time,2), "s\n")
```

```
del h2

"""

                                        build F2(t,x1,v2,x2,v2,l12,l21)
-Will need PermutedXList!
-Idea: for each existing line of (X1,V1,X2,V2) "attach" on each 2-permutation of L's
"""
print("Building F2...")
F2=dict()
F2_Normalising_Const = Simulations *  factorial(N) * 12 * 11
for ti in range(timestep.size-1):
    print("Processing timestep " , str(ti+1) , "...")
    H = np.empty((20,20,20,20,20,20))
    for Sim in range(Simulations):
        XVL = np.empty((0,6)) # 6 because 2 x's, 2 v's and 2 'ls
        for Xline in PermutedXList[ti][Sim*24:(Sim+1)*24]:
            XVL_part = [np.hstack((Xline,Lline)) for Lline in PermutedLList[ti]
            [Sim*132:(Sim+1)*132]]

            XVL = np.vstack((XVL,XVL_part))
        hist , edges = np.histogramdd(XVL, bins = 20,
        range= (XRange,VRange,XRange,VRange,LRange,LRange) )

        H += hist

        if ((Sim+1)%25) == 0:
            print("\tProcessed " , str(Sim+1) , " simulations out of ",
            Simulations,"at", round(time.time()-start_time,2), "s")

    F2[ti] = H/F2_Normalising_Const , edges
    print("\tAt ti, F2 summed = ",
    H.sum().sum().sum().sum().sum().sum()/F2_Normalising_Const)

    del H, hist
```

```
    print("completed ",str(ti+1), " out of " ,
    timestep.size-1 , "timesteps", round(time.time()-start_time,2), "s")

del XVL, XVL_part, Xline, ti,
print("Building F2...completed", round(time.time()-start_time,2), "s\n")

print("Saving F2...", round(time.time()-start_time,2), "s")
for key in F2.keys():
    pickle.dump(F2[key],open('F2_'+str(key)+'.pk','wb'))
del F2
print("Saving F2...complete", round(time.time()-start_time,2), "s\n")


end_time = time.time()
TotalDuration = end_time - start_time
print("Total duration: " , str(TotalDuration))
print("Average runtime per simulation : " , str(TotalDuration/Simulations))
```

### Factorisation Error

```
Created on Thu Jun  9 13:43:23 2016

import time
import pickle
import numpy as np

start_time = time.time()
#System parameters
N = 4
Simulations = 100
dt = 0.1
timestep = np.arange(0,1,dt) #uniformly divide interval (0,1) by increments of dt


#============================================================================
# Check factorisation
```

```
#=============================================================================
Error = dict()
F2 = dict()
def ComputeError():
    f1 = pickle.load( open( "f1.pk", "rb" ) )
    h2 = pickle.load( open( "h2.pk", "rb" ) )
    for ti in range(timestep.size-1):
        nonzero_terms = 0
        try:
            F2[ti] = pickle.load( open( "F2_"+str(ti)+".pk", "rb" ) )
            print("Loaded F2 for timestep"+str(ti))
        except:
            print("Unable to load F2 for timestep"+str(ti))

        print("Processing timestep ", str(ti+1),
        round(time.time()-start_time,2), "s")

        error_ti = np.zeros((20,20,20,20,20,20))
        for x1 in range(20):
#            print("Processing x1 = ", x1, "...at" ,
round(time.time()-start_time,2), "s")

            for x2 in range(20):
                for v1 in range(20):
                    for v2 in range(20):
                        for l12 in range(20):
                            for l21 in range(20):
                                F2_point = F2[ti][0][x1][x2][v1][v2][l12][l21]
                                factorisation = f1[ti][x1][v1]*f1[ti][x2][v2]
                                *h2[ti][0][l12][l21]

                                if F2_point and factorisation:
                                    nonzero_terms += 1
#                                    print("x1,x2,v1,v2,l12,l21 = " ,
x1,x2,v1,v2,l12,l21)
#                                    print("F2 = ", F2_point)
```

```
#                                       print("Factorisation = ",
f1[ti][x1][v1]*f1[ti][x2][v2]*h2[ti][0][l12][l21])
#                                       print("\tf1[ti][x1][v1]= ", f1[ti][x1][v1])
#                                       print("\tf1[ti][x2][v2]= ", f1[ti][x2][v2])
#                                       print("\th2[ti][0][l12][l21]= ",
h2[ti][0][l12][l21])

                                      error_ti[x1,x2,v1,v2,l12,l21] =
                                      (F2_point- factorisation)/F2_point
#                                       print("RE = ", error_ti[x1,x2,v1,v2,l12,l21],"\n")
                                  else:
                                      error_ti[x1,x2,v1,v2,l12,l21] = 0
#         Error[ti] = error_ti #store error at time ti into memory
#         print("Saving error at time", ti ,round(time.time()-start_time,2), "s")
#         pickle.dump(error_ti,open('error_'+str(ti)+'.pk','wb'))
#         print("Saving error at time"+str(ti)+"_complete",
round(time.time()-start_time,2), "s\n")

        SumOfError = error_ti.sum().sum().sum().sum().sum().sum()
        print("Average error for timestep " + str(ti) +" " +
        str(SumOfError/nonzero_terms))
        print("Standard dev for timestep " + str(ti) +" " + str(error_ti.std()) + "\n")


#def ComputeAverageError():
#    NC = pow(20,6)
#    for ti in range(timestep.size-1):
#        error = pickle.load( open( "error_"+str(ti)+".pk", "rb" ) )
#        print("Loading up error #" + str(ti) + " computing total error")
#        SumOfError = error.sum().sum().sum().sum().sum().sum()
#        print("Average error for timestep " + str(ti) +" " + str(SumOfError/NC))
#        print("Standard dev for timestep " + str(ti) +" " + str(error.std()) + "\n")
```

### 8.10.2 Investigating Numerical Solutions for the Evolution of the Eigenstate Expansion Coefficients

**Set up for Pechukas Functions**

```
import numpy as np

"""PECHUKAS FUNCTIONS"""

"""Matrix and other generic maths functions"""
def MatrixExpList(ListofMatrices):
    def MExp2(matrix):
        #Exponentiate a matrix by change of basis
        eigenvalues, eigenvectors = np.linalg.eig(matrix)
        ExpD = np.diag(np.exp(eigenvalues))
        BasisChange = np.matrix(eigenvectors)
        return BasisChange*ExpD*BasisChange.I

    return map(MExp2, ListofMatrices)

def Comm(A,B):
    A , B = np.matrix(A), np.matrix(B)
    return (A*B - B*A)

def MinDist(ListofNumbers):
    #Gives the minimum distance between two numbers in a list
    return np.min(np.ediff1d(np.sort(ListofNumbers)))


"""Integration functions"""
def CumulativeTrapezium(A, ds):
    # A(s) being a list of matrix say along s. ds can be a list
    or a (uniform) scalar for integration
    #Suppose we discrete integration space s0 < s1 < ... < sn then, CumulativeTrapz
    #Then Trapezium integration to s0 is zero is zero
    then adding incrementing via trapeziums
```

```
    if type(ds) == 'float':
        ds = len(A)*[ds] #if sclar, treat uniform ds along the axis

    CumTrapList = [ 0*A[0] ] #integral upto time 0 is zero (matrix)
    for ti in range( len(A) -1 ):
        CumTrapList.append( CumTrapList[-1] + 0.5*ds*( A[ti] + A[ti+1]) )
    return CumTrapList

"""Statistical functions"""
def RelError(MatrixPair): #or vectors
    RealMatrix , FakeMatrix = MatrixPair[0], MatrixPair[1]
    return np.linalg.norm( np.matrix(RealMatrix) - np.matrix(FakeMatrix) )
    / np.linalg.norm(RealMatrix)

#Fake = Approximation
def RelErrorList(RealMatrixList, FakeMatrixList):
return np.array( map(RelError, zip(RealMatrixList, FakeMatrixList)) )
def RelErrorList_base10Log(RealMatrixList, FakeMatrixList):
return np.array( map(np.log10, RelErrorList(RealMatrixList,FakeMatrixList) ) )
logresult = np.vectorize(np.log10)

"""Functions for initial conditions"""
def GenerateRandomInitialConditions(low = 0, high = 1, N = 5):
    while True:
        vector = np.random.uniform(low, high , N)
        s = set( entry for entry in vector )
        if s.__len__() == N : #unique only if same number of entries!
            return(vector)

def GenerateGaussianVector(mean = 0, sigma = 1, N = 5):
    #This part generates a N-dimensional Guassian vector
    with unique entries (as precaution!) distributed N(mean,sigma)
    #we use a set as this is quickest to check uniqueness.
    If unique, break. Else, repeat.

    if sigma == 0:   sigma = 1e-5 #to avoid zero variance
```

```
    while True:
        vector = np.random.normal(mean,sigma,N)
        s = set(entry for entry in vector)
        if s.__len__() == N : #unique only if same number of entries!
            return(vector)

def GenerateRandomL0(low = 0, high = 1, N = 5, imaginary = "y"):
    R = np.random.uniform(low, high, N**2).reshape(N,N)
    if imaginary == "y":
        I = np.random.uniform(low,high,N**2).reshape(N,N)
        I = I - np.diag(np.diag(I)) #zero-out the diagonal entries!
        return (R-R.T) + 0.5*(I+I.T)*1j
    else:
        return (R-R.T)

#Denote the following space of matrices BoldL
(although need not be normal distributed)

def GenerateGaussianHermitianMatrixZeroDiagonal(mean = 0 ,
sigma = 1, imaginary="y", N = 5):

    #Idea: create 2 Gaussian distribted N(mean,sigma) matrices for real matrix R
    and imaginary matrix I
    #Using property that R+R.T is symmetric while I-I.T is conjugate symmetrix
    then adding them yields a scaled complex-valued Hermitian matrix

    if sigma == 0:   sigma = 1e-5 #to avoid zero variance
    R = np.random.normal(mean,sigma,N**2).reshape(N,N)
    if imaginary=="y":
        I = np.random.normal(mean,sigma,N**2).reshape(N,N)
        I = I - np.diag(np.diag(I)) #zero-out the diagonal entries!
        return((R-R.T)+0.5*(I+I.T)*1j)
    else:
        return(R-R.T)

def GenerateRandomPointInBall(radius = 1, N = 5, centre = 0 ): #uniform sampling!
```

```
    #Idea: generate uniform distribution ON a sphere then scale by a uniform radius
    #See http://mathworld.wolfram.com/SpherePointPicking.html eqn (16) for ON
    #Centre can be an number or a vector
    x = GenerateGaussianVector(0,1,N)
    x = x / np.linalg.norm(x)
    SampleRadius = np.random.uniform(low = 0, high = radius) #sample radius uniformly
    return SampleRadius*x + centre

def GenerateBoldLMatrixInBall(radius = 1, N = 5, centre = 0 ):
#may not be uniform in this space!
    L = GenerateGaussianHermitianMatrixZeroDiagonal(N = N)
    L = L / np.linalg.norm(L)
    SampleRadius = np.random.uniform(low = 0, high = radius) #sample radius uniformly
    return SampleRadius*L + centre

def GenerateInitialXConditions(x_radius,N, epsilon = 0.05):
    counter = 0
    while True:
        counter += 1
        X0 = GenerateRandomPointInBall(x_radius,N)
        dist = [abs(X0[i] - X0[j]) for j in range(N) for i in range(j)]
        if min(dist) > epsilon:
            return X0

        if counter > 500:
            print("Computer says no, the epsilon is too big, innit")
            break

def GeneratePechukasInitialConditions(N = 5,
x_radius = 1, v_radius = 1, l_radius = 1, epsilon = 0.05 ):

    if epsilon:
        return GenerateInitialXConditions(x_radius,N, epsilon) ,
        GenerateRandomPointInBall(v_radius,N),  GenerateBoldLMatrixInBall(l_radius,N)
    else:
        return GenerateRandomPointInBall(x_radius,N) ,
```

```
        GenerateRandomPointInBall(v_radius,N),  GenerateBoldLMatrixInBall(l_radius,N)

"""Pechukas Eqns and Euler Method"""
def EulerRoutine(X0 ,V0 ,L0 , dLambda, N = 5):
    N = X0.size
    X, V, L = [X0], [V0] ,[L0]

    def Vdot(i): #Computes Vdot for each time t_i, returning Vdot as a vector
        def Vdot_component(m): #function to calculuate the m'th component of Vdot
            vdot_m = 0
            for n in range(N):
                if n != m:
                    vdot_m += (pow(abs(L[i][m,n]),2)/pow(X[i][m]-X[i][n],3))
            return(vdot_m)
        #returns the vector gluing all the components together, returning a vector
        return(2*np.array([Vdot_component(m) for m in range(N)]))

    def Ldot(i): #Computes Ldot for each time t_i, returning Ldot as a matrix
        def Ldot_component(m,n):
        #function to calculate the (m,n)'th matrix entry of Ldot
            ldot_lmn = 0
            for k in range(N):
                if (k != m and k != n):
                    ldot_lmn += L[i][m,k]*L[0][k,n]*(pow(X[i][m]-X[i][k],-2)
                    - pow(X[i][k]-X[i][n],-2))

            return(ldot_lmn)

        def Ldot_row(m): #for each fixed m, compute Ldot_m,n and combine into a row
            return(np.array([Ldot_component(m,n) for n in range(N)]))
        #glue up each row to produce the required matrix
        return(np.array([Ldot_row(m) for m in range(N)]))

    #Euler routine here
    for i in range(len(dLambda)-1):
        X.append(X[i] + dLambda[i]*V[i])
```

```
        V.append(V[i] + dLambda[i]*Vdot(i))
        L.append(L[i] + dLambda[i]*Ldot(i))

    return X, V , L


"""Building XMatrix and PMatrix for solving differential eqn for C"""
def BuildXMatix( X ):   return map(np.diag, X )
#    return [np.diag(X[i]) for i in range(len(X))]

def BuildPMatrix(X ,L):
    N = len(X[0])
    PMatrices = []
    for ti in range(len(X)):
        P = np.zeros((N,N)) + 1j*np.zeros((N,N))
        for i in range(N):
            for j in range(i):
                P[i][j] = L[ti][i][j] / ((X[ti][i] - X[ti][j]) ** 2)
        PMatrices.append(P - (P.conj()).T)
    return PMatrices

"""Piecewise routine"""
def PWC_Propagator(A,dt):
    IntAdt = CumulativeTrapezium(A,dt)
    PropagatorList = MatrixExpList(IntAdt)
    return PropagatorList

"""Integrating Xdt with no P terms"""
def NoLambdaPropagator(XMatrix,dt): #Ignoring P terms essentially, adibatic theorem
    IntXdt = CumulativeTrapezium(XMatrix,dt)
    iIntXdt = [-1j*intxdt for intxdt in IntXdt]
    PropagatorList = MatrixExpList(iIntXdt)
    return PropagatorList #gibb returning IntXdt

"""Magnus to the second order routine"""
def Magnus_SecondOrder(A,dt):
```

```
    Omega1 = CumulativeTrapezium(A,dt)
    #left hand side approx (partly by nature of commutator)
    Omega2_InnerInteg = [ sum([Comm(A[tj],A[ti])*dt for tj in range(ti)])
    for ti in range(1,len(A))]

    Omega2 = [np.zeros(A[0].shape)] +  CumulativeTrapezium(Omega2_InnerInteg,dt)
    OmegaTotal = [ Omega1[i] + 0.5*Omega2[i] for i in range(len(Omega1)) ]

    return MatrixExpList(OmegaTotal)

"""Iterative method"""
def CIterative(C0 , NoLambdaPropagator , LambdaDotP , dt, power = 10):
#Build CIterative for one initial conditions
    C_0 = [NLProp*C0 for NLProp in NoLambdaPropagator]
    #solving the homogeneous solution via propagator
    C_All = [C_0]

    C_i = C_0 #starting with initial homogeneous solution
    for dummy in range(1,power):
        integrand = [LambdaDotP[ti]*C_i[ti] for ti in range(len(LambdaDotP))]
        #add zero vector as same with adding zero matrix in above methods
        C_i = CumulativeTrapezium(integrand,dt)
        C_All.append(C_i)

    #Conversion to array allowing us to sum up C_i to give required perturbation
    C_Series = [ np.array(C_All[0]) ]
    for i in range(1,len(C_All)):
        C_Series.append( C_Series[-1] + np.array(C_All[i]) )

    return C_Series

def SimulateCIt(PiecewiseProp, NoLambdaProp, LambdaDotP, dt, C_Simulations = 1000 ,
N = 5, power = 10): #Ran many sims
    #Simulate CIt and get error average over simulations
    RelErrorC, PWCC = [] , []
    n = N
```

```
    for csim in range(C_Simulations):
        C0 = GenerateGaussianVector(N = n)
        C0 = np.matrix(C0.reshape((n,1))) / np.linalg.norm(C0)
        #turn into unit vector/matrix

        CIter = CIterative(C0 , NoLambdaProp , LambdaDotP, dt , power = 10)
        #CIter[n][t] = C_n(t) = n'th iterate at time t

        """Collecting up results"""
        PWCC = [PiecewiseProp[ti]*C0 for ti in range(len(PiecewiseProp))]
        RelErrorC.append( RelErrorList( PWCC, CIter[-1]) )
    AvgRelErrorC = np.average(RelErrorC, axis = 0)
    return AvgRelErrorC
```

### Set Up for Pechukas Objects

```
import numpy as np
import PechukasFunctions as PF
import matplotlib.pyplot as plt

class PechukasTrajectory(object):
    def __init__(self, x0 = np.array([-0.2,0.3]) , v0 = np.array([-0.6,0.8]) ,
    l0 = np.array( [[0,1.5],[1.5,0]] ), t_0 = 0, t_end = 1, steps = 100,
    Lambda = lambda ti: 0.01*ti, c_simulations = 10):
        #initial conditions
        self.x0 = x0
        self.v0 = v0
        self.l0 = l0
        self.N = x0.size

        #Euler paramters
        self.t_0 = t_0
        self.t_end = t_end
        self.steps = steps
        self.t = np.linspace(t_0 ,t_end ,steps+1)
        self.dt = float((t_end - t_0))/steps
#        self.Lambda = Lambda
```

```
### Uncommenting this line will break the multiprocessing!###
        self.dLambda = np.append( np.diff(np.vectorize(Lambda)(self.t)) ,
        Lambda(self.t[-1]+self.dt) - Lambda(self.t[-1]))

        #Trajectory and data
        self.X, self.V, self.L = PF.EulerRoutine(self.x0 ,self.v0 , self.l0,
        self.dLambda)

        self.XMatrix , self.PMatrix = PF.BuildXMatix(self.X) ,
        PF.BuildPMatrix(self.X,self.L)

        self.A = [-1 *(1j * self.XMatrix[ti] + (self.dLambda[ti]/self.dt)
        * self.PMatrix[ti]) for ti in range(len(self.dLambda))]

        #note that this has one less entry than X (say)
        because we took len(dlambda) is one less.
        Given N points, there are (N-1) spacings...

#        #Build Propagators
        self.PiecewiseProp = np.array( PF.PWC_Propagator(self.A,self.dt) )
        self.NoLambdaProp = PF.NoLambdaPropagator(self.XMatrix,self.dt)
        self.MagnusProp = PF.Magnus_SecondOrder(self.A,self.dt)
#
#        #Cit
        self.c_simulations = c_simulations
        self.LambdaDotP = [self.dLambda[i]*self.PMatrix[i]
        for i in range(len(self.PMatrix))]

#
#        #Results/Errors
        self.Errors = {}
        self.Errors['Magnus'] = PF.RelErrorList(self.PiecewiseProp, self.MagnusProp)
        self.Errors['NoLambdaProp'] = PF.RelErrorList(self.PiecewiseProp,
        self.NoLambdaProp)

        self.Errors['CIT'] = PF.SimulateCIt(self.PiecewiseProp, self.NoLambdaProp,
```

```
        self.LambdaDotP, self.dt, self.c_simulations, self.N, power = 2)
#
        self.LogErrors = {}
        self.LogErrors['Magnus'] = PF.logresult(self.Errors['Magnus'])
        self.LogErrors['NoLambdaProp'] = PF.logresult(self.Errors['NoLambdaProp'])
        self.LogErrors['CIT'] = PF.logresult( self.Errors['CIT'] )

        #Level-crosings...



class PechukasEnsemble(object):
    def __init__(self, Ensemble):
        self.EnsembleData = Ensemble

        #System/Simulation parameters
        self.functions = Ensemble.keys()
        self.t = Ensemble[Ensemble.keys()[0]][0].t #pick out the time space
        self.methods = Ensemble[Ensemble.keys()[0]][0].Errors.keys()
        self.Simulations = len(Ensemble[Ensemble.keys()[0]])
        self.N = Ensemble[Ensemble.keys()[0]][0].N

        self.LoggedErrors = self.GenerateErrors() #LoggedErrors[method][function]

    def GenerateErrors(self):
        LoggedErrors = dict()
        for method in self.methods:
            LoggedErrors[method] = {}
            for function in self.functions:
                LoggedErrors[method][function] =
                PF.logresult( self.AverageErrorsOverSimulations(method,
                self.EnsembleData[function]) )

        return LoggedErrors

    def AverageErrorsOverSimulations(self, method, ListofTrajectories):
```

```
        return (1./self.Simulations)*np.sum( ListofTrajectories[i].Errors[method]
        for i in range(len(ListofTrajectories)))

    def Plot_Method(self, method):
        plt.figure()
        for function in self.functions:
            plt.plot(self.t, self.LoggedErrors[method][function], label = function)
        plt.xlabel(r'$t$')
        plt.ylabel("Log Rel Error(t)")
        plt.title(method)
        plt.legend()
        plt.show()
        savename = " ".join([method, "N=", str(self.N), str(self.Simulations),
        "simulations"])

        plt.savefig( savename + '.jpeg')

    def Plot_AllMethods(self):
        for method in self.methods:
            self.Plot_Method(method)

    def Plot_Function(self, function):
        method_crisscross = {'Magnus': 'b--', 'CIT': 'rx', 'NoLambdaProp': 'k'}
        plt.figure()
        for method in self.methods:
            plt.plot(self.t, self.LoggedErrors[method][function],
            method_crisscross[method] , label = method)

        plt.xlabel(r'$t$')
        plt.ylabel("Log Rel Error(t)")
        plt.title(function)
        #plt.legend()
        plt.show()
        savename = " ".join([function, "N=", str(self.N), str(self.Simulations),
        "simulations"])
```

```
        plt.savefig( savename + '.jpeg')

    def Plot_AllFunction(self):
        for function in self.functions:
            self.Plot_Function(function)
```

### Comparing approximation Schemes

```
Multiprocessing Pechkuas Trajectories

"""
import time
import multiprocessing
import PechukasObject
import PechukasFunctions as PF
import numpy as np

def worker(parameters, CPUi ,OutQueue):
    """ This is a mulitprocessing "worker" function
    Define a set of Lambda functions, creates a dictionary that's pushed to a queue.
    The following creates dictionary keyed by function name
     to a list of simulations/trajectory
    """
    Lambdas = {'Linear': lambda ti: 0.001*ti,\
               'Cubic': lambda ti: 0.001*(ti**3 + ti**2 + ti),\
               'Exp': lambda ti: 0.001*np.exp(-ti)}

    batchsize = int(parameters['Simulations']/parameters['nprocs'])
    TrajectoryDict = {function: [] for function in Lambdas.keys()}

    for sim in range(batchsize):
        output = "CPU " + str(CPUi) + ": I am still Running " + str(sim) +
        " simulation of batch size " +  str(batchsize) + " @" + str(time.ctime())
        print(output)

        x0, v0, l0 = PF.GeneratePechukasInitialConditions(N = parameters['N'],
        x_radius = parameters['xradius'], v_radius = parameters['vradius'],
```

```
         l_radius = parameters['lradius'], epsilon = 0.01)

        for function in Lambdas.keys():
            TrajectoryDict[function].append( PechkuasObject.PechukasTrajectory
            (x0, v0, l0, t_0 = parameters['t_0'], t_end = parameters['t_end'],
            steps = parameters['steps'], Lambda = Lambdas[function],
             c_simulations = parameters['c_simulations']) )

    OutQueue.put(TrajectoryDict)

def RandomPechkuasEnsemble(parameters):
    OutQueue = multiprocessing.Queue() #create the multiprocessing queue
    procs = []

    for i in range(parameters['nprocs']):
        p = multiprocessing.Process(target=worker, args=(parameters, i , OutQueue) )
        procs.append(p)
        p.start()

    # Collect eacb batch of ensemble into one big ensemble
    EnsembleList = list()
    for i in range(parameters['nprocs']):
        EnsembleList.append( OutQueue.get()) #"peeling off" results from OutQueue

    #Merging into one (dictionary) big ensemble (keyed by function),
    probably memory-exhaustive
    EnsembleDict = EnsembleList[0]
    for ensemble in EnsembleList[1:]:
        for function in EnsembleDict.keys():
            EnsembleDict[function] += ensemble[function]

    # Wait for all worker processes to finish
    for p in procs:
        p.join()
    return EnsembleDict
```

```
if __name__ == '__main__':

    print("I is actually started and running")
    start_time = time.time()

    parameters = {'Simulations': 8*125, \
                  'N': 3, \
                  't_0': 0, \
                  't_end': 100, \
                  'steps': 1000, \
                  'xradius': np.pi/6, \
                  'vradius': np.pi/6, \
                  'lradius': np.pi/6, \
                  'c_simulations': 10,\
                  'nprocs': 8}

    EnsembleDict = RandomPechkuasEnsemble(parameters)
    Ensemble = PechkuasObject.PechukasEnsemble(EnsembleDict)
    elapsed_time = round(time.time() - start_time,2)
    print("Finished in ", elapsed_time)
#    Ensemble.Plot_AllMethods()
    Ensemble.Plot_AllFunction()
```

### 3 Sat Occupation Dynamics

```
import numpy as np
from numpy import linalg as la
import matplotlib.pyplot as plt
import time
import math
import PechkuasObject
import PechkuasFunctions as PF

print("Running")
start = time.time()
f = lambda ti: 0.01*math.exp(-ti)
t0, t_end, steps = 0 , 1, 100
```

```
t = np. linspace (t0 ,t_end ,steps+1)
dt = float((t_end - t0))/steps

I = np.matrix([[1, 0], [0, 1]])
SigX = np.matrix([[0, 1], [1, 0]])
SigY = np.matrix([[0, -1j], [1j, 0]])
SigZ = np.matrix([[1, 0], [0, -1]])

Count=2
A=Count*(np.kron(I,I)-np.kron(I,SigZ)-np.kron(SigZ,I)+np.kron(SigZ,SigZ))
B=(np.kron(I,I)-0.5*np.kron(I,SigX)-0.5*np.kron(SigX,I))-
Count*(np.kron(I,I)-np.kron(I,SigZ)-np.kron(SigZ,I)+np.kron(SigZ,SigZ))

i = 0
Lambda1 = []
Lambda2 = []
Lambda = []
H = []
X = []
V = []
L = np.zeros((4, 4))
#print(t0)
while i < t_end+dt:
    Lambda.append(f(i))
    H.append(A+Lambda[-1]*B)
    X.append( np.linalg.eigvals(H[-1]))
    i = i + dt

def BuildL(X,B):
    L = np.zeros(B.shape)
    for i in range(4):
        for j in range(4):
            L[i,j] = (X[i] - X[j])*B[i,j]
    return L

k = 0
```

```
j = 0
L = []
Density = []
while k < t_end+dt:
    if(j < 100):
        V.append((X[j+1]-X[j])/(Lambda[j+1]-Lambda[j]))
        j = j + 1
        L.append( BuildL(X[j],B) )
#         Density.append(np.kron(c0*P.MagnusProp[-1], c0*P.MagnusProp[-1]))
     #L.append(X[j][m]-X[j][n])B[m][n]
    k = k + dt

P = PechkuasObject.PechukasTrajectory(X[0], V[0], L[0], t_0 = 0, t_end = 1, steps = 100,
Methods = {'Magnus':'b--', 'CIT':'k', 'NoLambdaProp':'rx'}
for method in Methods.keys():
    plt.plot(P.t, P.LogErrors[method], Methods[method])
    plt.xlabel(r'$t$')
    plt.ylabel("Log Rel Error(t)")
c0 = PF.GenerateGaussianVector(N=4)
c0 = np.matrix(c0)/np.linalg.norm(c0) #unit 1xN vector (i.e. covector)
Ct = [P.MagnusProp[z]*c0.T for z in range(len(P.MagnusProp))]

Density = [np.kron(c,c.H) for c in Ct]
Density_diagonal = [d.diagonal() for d in Density]

plt.figure()
for x in range(Density_diagonal[0].size):
    den =[Density_diagonal[z][0,x] for z in range(len(Density_diagonal))]
    plt.plot(P.t, den, label = str(x+1))
    plt.xlabel(r'$t$')
    plt.ylabel('Occupation Number')
    plt.legend()
```

# Bibliography


[1] E. Fahri et al., Science **292**, 472 (2001).

[2] R Requist, J Schliemann, AG Abanov, D Loss, Physical Review B **71**, 115315 (2005).

[3] A. M. Zagoskin, S. Savel'ev and F. Nori, Phys. Rev. Lett. **98**, 120503 (2007).

[4] A.M. Zagoskin, E. Il'ichev, M. Grajcar, J.J. Betouras and F. Nori, Front. Physics **2**, 33 (2014).

[5] R. D. Wilson, A. M. Zagoskin and S. Savel'ev, Phys. Rev. A **82**, 052328 (2010).

[6] Y. Manin, *Computable and Uncomputable*, Sovetskoye Radio, Moscow (1980).

[7] R. P. Feynman, International Journal of Theoretical Physics, 21 6/7, (1982).

[8] H. Weinfurter, Europhys. Lett. **25**, 8 (1994).

[9] M. A. Qureshi, J. Zhong, J. J. Betouras, A. M. Zagoskin, Phys. Rev. A 95, 032126 (2017).

[10] A. M. Childs, E. Farhi, J. Preskill, Phys. Rev. A **65**, 012322 (2001).

[11] M. Sarovar, K. C. Young, New Journal of Physics, **15** 125032 (2013).

[12] R. Di Candia, B. Mejia, H. Castillo, J. S. Pedernales, J. Casanova and E. Solano, Phys. Rev. Lett. **111**, 240502 (2013).

[13] M. A. Qureshi, J. Zhong, Z. Qureshi, P. Mason, J. J. Betouras, A. M. Zagoskin, Phys. Rev. A **97**, 032117 (2018).

[14] M. Amin, Phys. Rev. Lett. **102**, 220401 (2009).

[15] P. Pechukas, Phys. Rev. Lett. **51**, 943 (1983).

[16] T. Yukawa, Phys. Rev. Lett. **54**, 1883 (1985).

[17] T. Yukawa, Phys. Lett. **116A**, 227 (1986).

[18] T. Yukawa and T. Ishikawa, Prog. Theor. Phys. Suppl. **98**, 157 (1989).

[19] F. Haake, *Quantum Signitures of Chaos*, Ch. 6 (Springer, Berlin, 2001).

[20] T. Yukawa, Phys. Lett. A, **116**, 5 (1986).

[21] W. H. Steeb and A. J. van Tonder, Z. Naturforschung **42a**, 819 (1987).

[22] J. Yvon, *La Theorie Statistque des Fluids et L'equation d'Etat*, Act. Scient. et ind. No. 203 (Hermann, Paris, 1935).

[23] R. Balescu, *Equilibrium and Nonequilibrium Statistical Mechanics*, Vols 1/2 (Wiley, New York, 1975).

[24] R. D. Wilson, A. M. Zagoskin, S. Savel'ev, M. J. Everitt and F. Nori, Phys. Rev. A **86**, 052306 (2012).

[25] A. M. Zagoskin, *Quantum Theory of Many-Body Systems*, Ch. 5 (Springer, 2014)

[26] C. W. Gardiner, *Handbook of Stochastic Methods for Physics, Chemistry and the Natural Sciences* Third Edition, Ch. 7, (Springer, 2009)

[27] H. J. Stockmann, *Eigenvalue Dynamics in Quantum Chaos An Introduction*, (Cambridge Press, 1999).

[28] B. V. Alexeev, *Generalized Boltzmann Physical Kinetics* (Elsevier, 2004).

[29] S. Suzuki, J. Phys.: Conf. Ser. **302**, 012046 (2011).

[30] R. Requist, Phys. Rev. A **86** (2), 022117 (2012).

[31] R Requist, O Pankratov, Physical Review A **81**, 042519 (2010).

[32] S. Savel'ev, F. Marchesoni and F. Nori, Phys. Rev. E **70**, 061107 (2004).

[33] G. Schaller, S. Mostame, R. Schutzhold, Phys. Rev. A **73**, 062307 (2006).

[34] T. Kato, Journal of the Physical Society of Japan. **5** (6): 435439 (1950).

[35] M. Baake and U. Schlegel, no.arXiv:1011.1775v2, (2016).

[36] W. Magnus. Comm. Pure and Appl. Math., **7**, 639 (1954).

[37] S. Blanes, F. Casas, J. A. Oteo and J. Ros, Eur. J. Phys. **31**, 907 (2010).

[38] F. R. Gantmacher. The theory of matrices. Chelsea Publishing Co., New York, 1959. Two volumes. Translated by K. A. Hirsch.

[39] S. Klarsfeld and J. A. Oteo. J. Phys. A, **22**, 4565 (1989).

[40] P. Pechukas and J. C. Light. J. Chem. Phys., **7**, 3897 (1966).

[41] S. Wojciechowski, Phys. Lett. **111A**, 3 (1985).

[42] Ghatak A., Lokanathan S. (2004) Time Dependent Perturbation Theory. In: Quantum Mechanics: Theory and Applications. Fundamental Theories of Physics (An International Book Series on The Fundamental Theories of Physics: Their Clarification, Development and Application), vol 137. Springer, Dordrecht

[43] M. A. Qureshi, J. Zhong, P. Mason, J. J. Betouras, A. M. Zagoskin, Phys. Rev. A **98**, 012128 (2018).

[44] D. E. Knuth, Fundamental Algorithms, Ch. 1.2 (Addison-Wesley, 1973).

[45] H. Wang, L.Wu, Nature, Sci. Rep. **6**, 22307 (2016).

[46] S. Boixo, T. F. Rnnow, S. V. Isakov, Z. Wang, D. Wecker, D. A. Lidar, J. M. Martinis and M. Troyer, Nature. Physics **10**, 218-224 (2014).

[47] N. V. Vitanov and B. M. Garraway, Phys. Rev. A **53**, 4288 (1996).

[48] J. R. Rubbmark, M. M. Kash, M. G. Littman and D. Kleppner, Phys. Rev. A **23**, (6) 3107 (1981).

[49] M. Wilkinson, J. Phys. A: Math. Gen. 21, 4021-4037 (1988).

[50] M. Wilkinson, J. Phys. A: Math. Gen. **22**, 2795-2805 (1989).

[51] J. Zakrzewski, D. Delande, M. Kus, Phys. Rev. E **47**, (3) 1665 (1993).

[52] M. H. S. Amin, D. V. Averin and J. A. Nesteroff, Phys. Rev. A **79**, 022107 (2009).

[53] V. L. Pokrovsky, N. A. Sinitsyn, Phys. Rev. B 67, 144303 (2003).

[54] M. B. Kenmoe, H. N. Phien, M. N. Kiselev and L. C. Fai, Phys. Rev. B **87**, 224301 (2013).

[55] Z. X. Luo and M. E. Raikh, Phys. Rev. B **95**, 064305 (2017).

[56] P. Cejnar, J. Jolie, Prog. Part. Nucl. Phys. **62**, 210-256 (2009)

[57] G. E. Astrakharchik, D. M. Gangardt, Yu. E. Lozovik, I. A. Sorokin, Phys. Rev. E **74**, 021105 (2006)

[58] A. Kamenev, *Field Theory of Non-Equilibrium Systems*, Ch. 5 (Cambridge Press, 2011).

[59] P. Hanggi, P. Jung, *Colored noise in dynamical systems*, Ch. 3 (John Wiley and Sons, 1995).